GRANT NAG2-88
IN-04
63005-CR
105 p.

WEATHER RADAR APPROACH SYSTEM (WRAPS)

PROGRESS REPORTS No. 1, 2, 3

PERIOD COVERED: AUGUST 1 - NOVEMBER 30, 1980

PREPARED BY

DAVE ANDERSON/JOHN BULL
AMES RESEARCH CENTER
NATIONAL AERONAUTICS AND
SPACE ADMINISTRATION
MOFFETT FIELD, CA

JOHN CHISHOLM
ATMOSPHERIC SCIENCES CENTER
DESERT RESEARCH INSTITUTE
UNIVERSITY OF NEVADA SYSTEM
RENO, NV

NASA-AMES COOPERATIVE AGREEMENT
No. NCC 2-88

AND

DRI ACR No. 1-6-220-6909-001

FEBRUARY 1981

(NASA-CR-180271) WEATHER RADAR APPROACH SYSTEM (WRAPS) Progress Report, 1 Aug. - 30 Nov. 1980 (NASA) 105 p

N87-70353
63005

Unclas
00/04 45003

ABSTRACT

This report includes the three Progress Reports, 1, 2, and 3 prepared under NASA-Ames Cooperative Agreement No. NCC 2-88 and DRI ACR No. 1-6-220-6909-001. Progress Report No. 3 also includes a summary of work done to date, with recommendations for further efforts.

In brief, the effort has been successful, in that the program has demonstrated that a conventional airborne weather radar can detect passive ground-based reflectors in a clutter environment representative of a municipal type airport. The Abstract in Progress Report No. 3 elaborates on this topic.

PROGRESS REPORT NO. 1

Period Covered: August 1 - September 1, 1980

Weather Radar Approach System
(WRAPS)

Prepared by

Dave Anderson/John Bull
Ames Research Center
National Aeronautics and
Space Administration
Moffett Field, CA

John Chisholm/Paul Lage/
Harold Faretto
Atmospheric Sciences Center
Desert Research Institute
Reno, NV

NASA-Ames Cooperative Agreement
No. NCC 2-88

September 1980

Introduction

The WRAPS program is a cooperative effort between Ames Research Center, NASA, and the Atmospheric Sciences Center, Desert Research Institute, University of Nevada System. The purpose of the program is to explore the possibility of using passive radar reflectors of the corner reflector type, in conjunction with an airborne weather radar, as a helicopter navigational aid.

This concept has been explored many times in the past for fixed-wing aircraft with uniformly disappointing results. The present program is based on the belief that previous programs have not been successful because the multipath phenomena, i.e., ground bounce, was not taken into account, and that once this factor is accounted for, a successful navigational aid will evolve.

This first progress report on the WRAPS program is divided into three sections. The first section discusses the data collection system; the second section considers the radar system; and the third section discusses work during the next period. In general, results to date are encouraging.

SECTION I. DATA COLLECTION SYSTEM

In the original program outline, two possible data collection systems were discussed, those of Fig. 1.1 (Fig. 4.4 of the program outline) and Fig. 1.2 (Fig. 4.6 of the program outline). The Fig. 1.1 system utilized a multiple DME positioning system; the Fig. 1.2 system merely records DME range to a beacon located with the reflectors. The Fig. 1.2 system was proposed because of time and monetary limitations.

The system actually being fabricated is that shown in Fig. 1.3. It utilizes the multiple DME system of Fig. 1.1 and a new method of recording raw radar data. The system operation is as follows:

System operation is controlled by the 11/23 microcomputer. Inputted into the 11/23 is antenna angle data (stepping motor signal). At the extremes of the antenna scan this data is used by the 11/23 to switch the multiple DME range data into the cycler/tracker. The C/T outputs range data to multiple beacons during this antenna scan interval. When the antenna is scanning the $\pm$ 40° dead ahead region, the 11/23 switches the output of the pulse pair decoder to the C/T. The output of the pulse pair decoder contains a decoded signal from the installed corner reflectors. In this manner, precision range data for ground range and ground speed computation is provided.

The output of the pulse pair decoder may also contain "decoded" signals from ground clutter targets. This subject is considered in Section II.

The raw radar data is recorded as follows. The radar data is first inputted into an analogue storage device. This analogue register

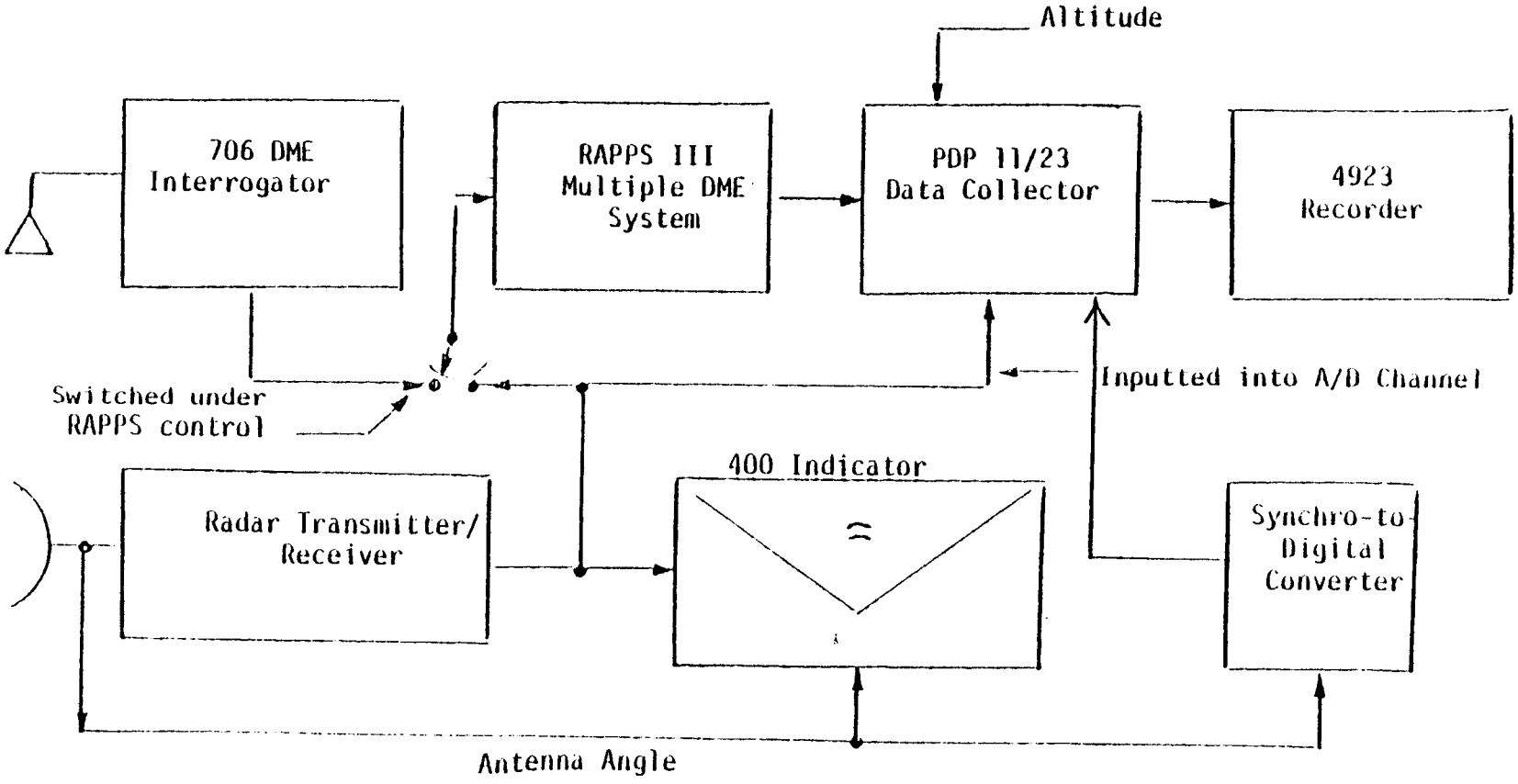

Figure 1.1. Suggested Possible Data Collection System for Ames Test Aircraft.

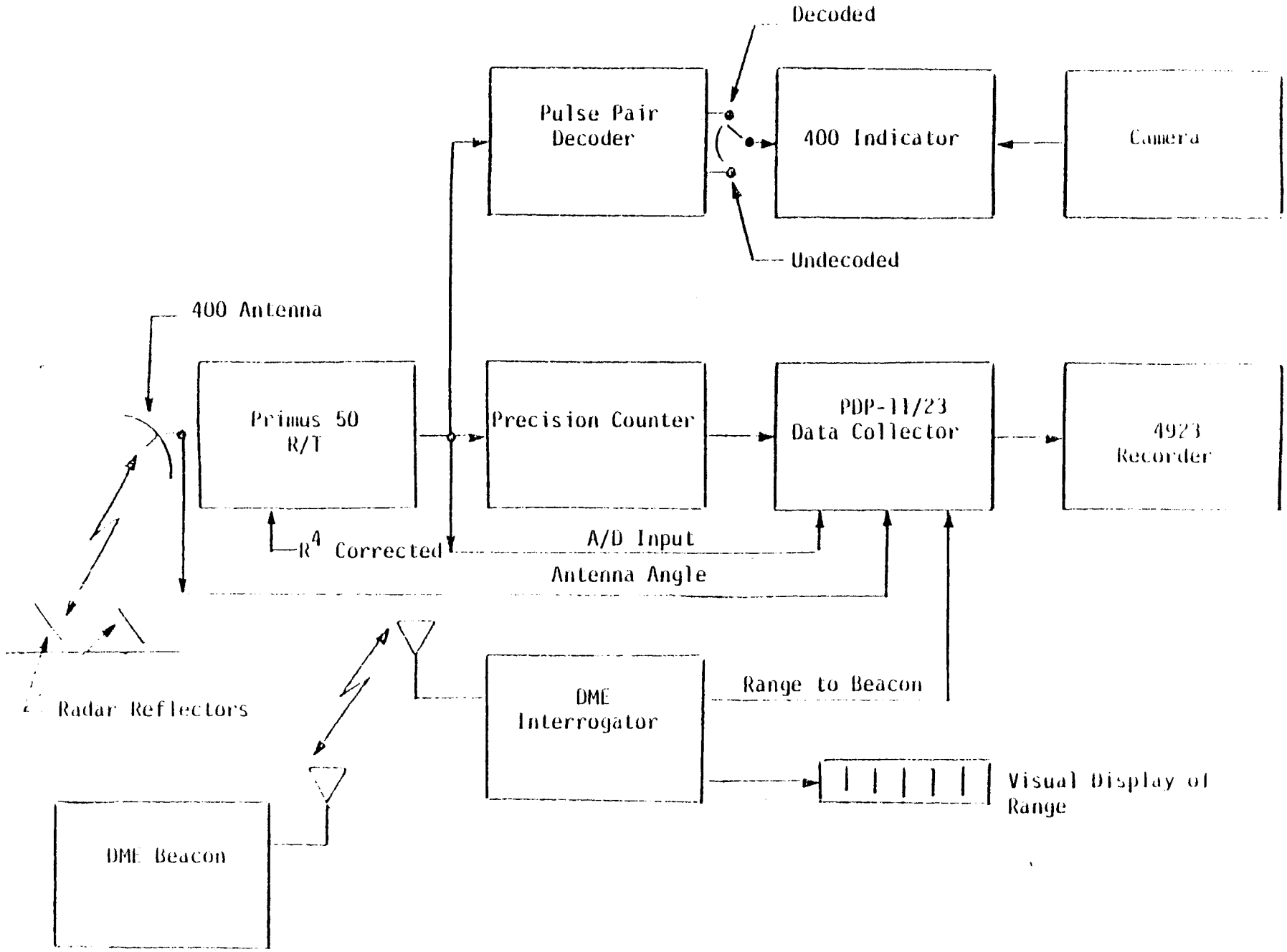

Figure 1.2. Proposed Data Collection System

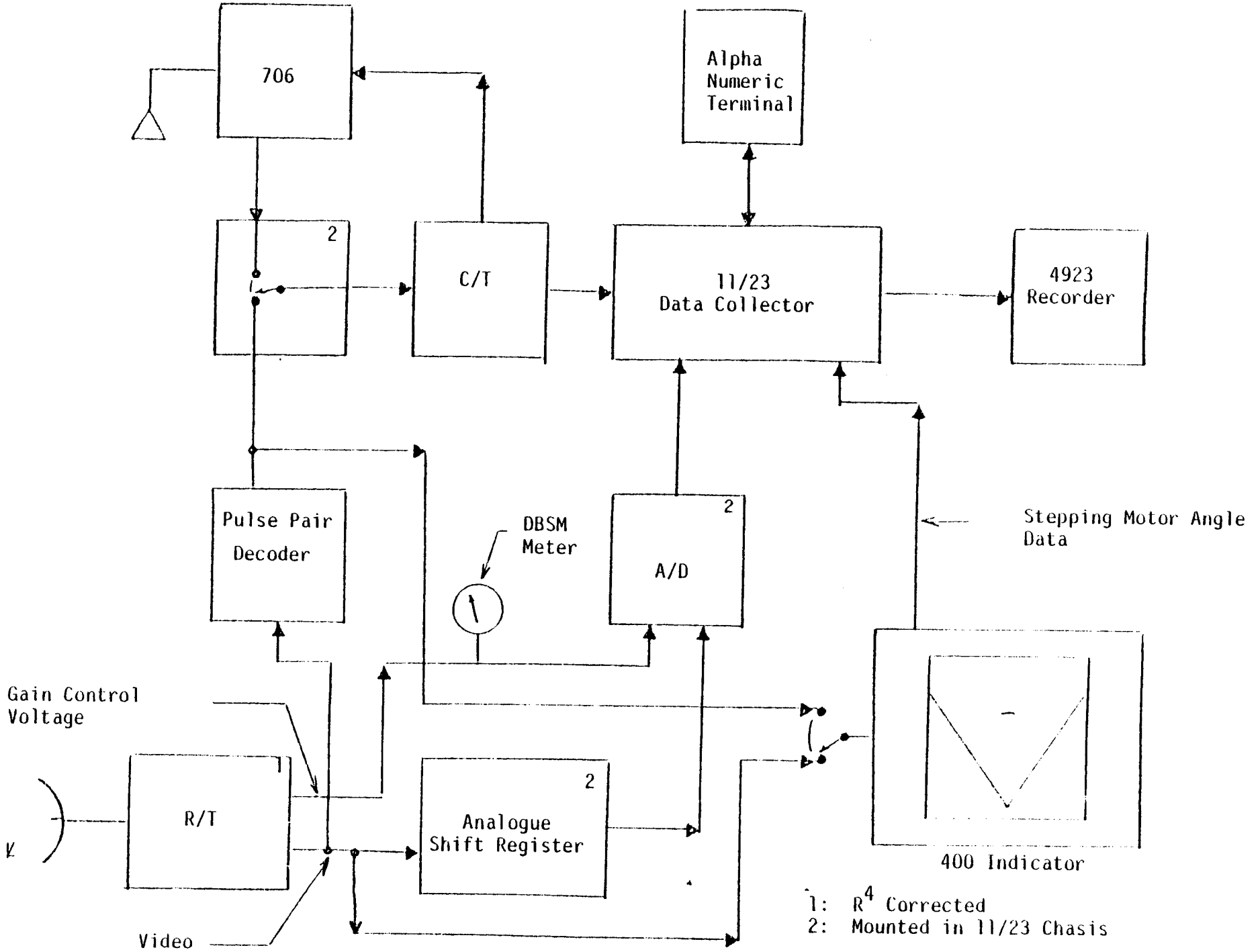

Figure 1.3. Data Collection System being Fabricated for Ames Test Aircraft

(termed a bucket brigade) is based on using a charge coupled device. Basically, the input signal is sampled at a high rate and this sampled data is stored in the form of an electric charge. This electric charge is sequentially transferred from one storage element to another until all storage elements are filled. The stored data can then be transferred out at a much slower rate.

In the unit employed, there are some 450 storage elements. While the data can be sampled and inputted at a 20 MHz rate, a nominal rate of about 3 MHz is being used due to the limitations of the 4923 recorder being used. The three MHz rate corresponds to a range resolution of about 150 ft. thus providing several samples during the 0.6 microsecond pulse return from a point target, i.e., corner reflector.

At the 3 MHz rate, the 450 storage elements correspond to a range of about 11 miles. At the end of this 11 miles, which corresponds to about 135 microseconds, the data in the "bucket brigade" is shifted into the 11/23 A/D converter at a 100 KHz rate, which is the operating rate of the standard 8-bit A/D converter installed in the 11/23. This transfer takes about 4.5 milliseconds. The output of the A/D converter is then stored in the 11/23. Fig 1.4 is a printout from the 11/23 of a 100 KHz square wave inputted into the bucket brigade. Fig. 1.5 is an 11/23 printout of two 0.6 microsecond pulses, separated by two microseconds, inputted into the bucket brigade. Data also stored, for every target above a preset dbsm threshold, as determined by the receiver gain control signal, is the angle at which data is obtained, the clockwise or counter-clockwise rotation of the antenna, and the range at which it is obtained.

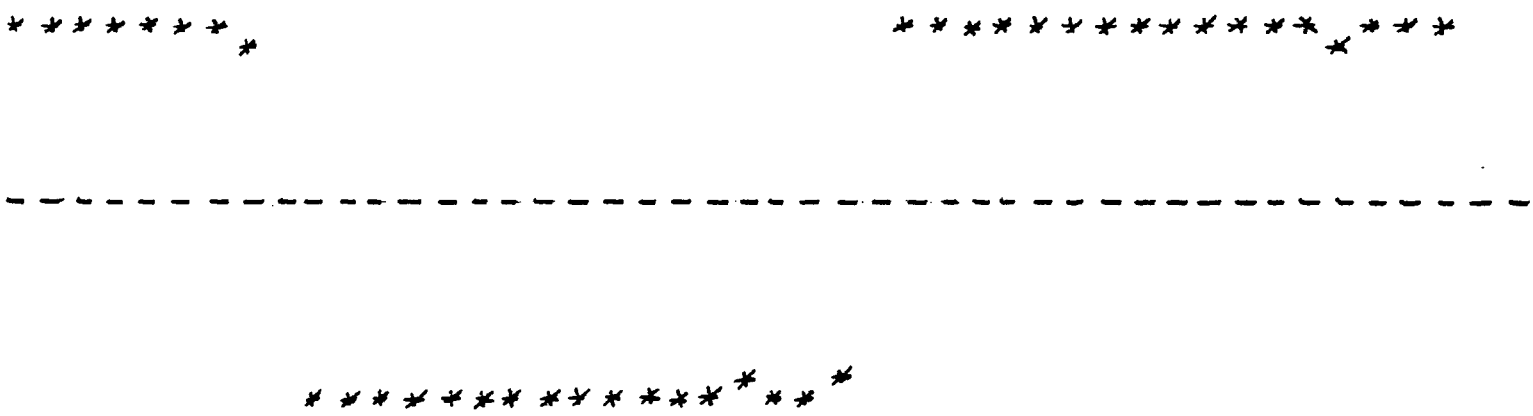

Figure 1.4. PDP 11/23 Printout of 100 KHz Square Wave Inputted into "Bucket Brigade".

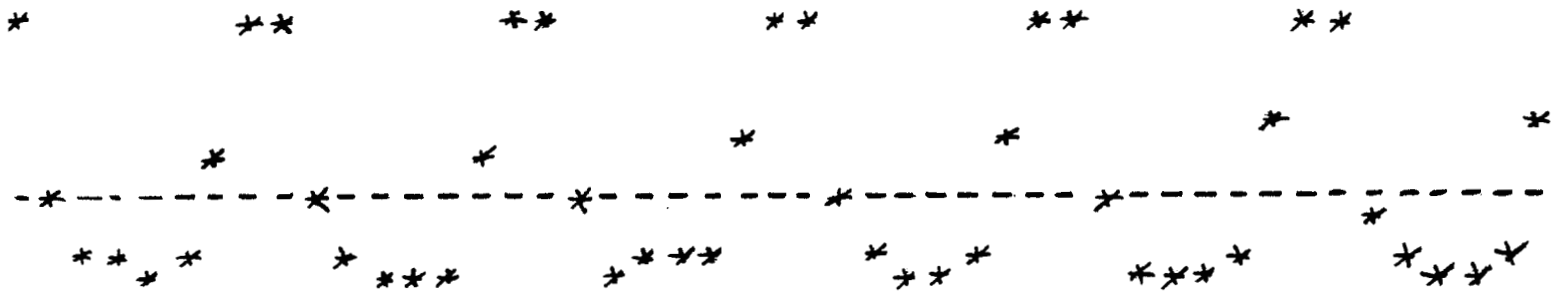

Figure 1.5. PDP 11/23 Printout of 0.6 Microsecond Pulses Separated by 2 Microseconds Inputted into "Bucket Brigade".

As the antenna is stepped, additional radar data is generated and stored in the 11/23. This data is examined within the 11/23 to determine if a return is being obtained at a similar range and angle as previous data. If this is the case, the 11/23 records the number of times this occurs. At the end of such an occurrence, a record is established and read out to the recorder. This record permits, via post-flight analysis, the display of the "beam-split" center of such targets. It may also permit the elimination of extended targets, i.e., distributed ground clutter, if such targets have more than the nominal number of returns per beam passage. The nominal number of returns per beam passage for a point target, i.e., a corner reflector, is determined as follows:

Antenna Scan Rate	$\approx 60°$/sec
Beam Width	$\approx 6°$
Beam Passage over a point target	$\approx$ 0.1 second
PRF	$\approx$ 120 pps
Pulses Per Beam Passage	$\approx$ 12

It should be noted that an aircraft, traveling at a nominal 200 ft/sec, moves 20 ft. during such beam passage.

In addition to recording raw radar data during passage of the antenna over the $\pm$ dead-ahead region, there is also recorded the range to any targets that are "decoded" by the pulse pair decoder. The number of such targets are, hopefully, much less than raw radar targets.

The net result is a record as shown in Fig. 1.6. It includes antenna direction, antenna angle at which the radar target drops below

threshold, the number of times above threshold, the sum of the intensities above threshold and the range. Also recorded are the ranges of targets decoded by the pulse pair decoder. The multiple DME data collected and time and date, etc. information is also part of the information outputted to the recorder. Time is inputted to the 11/23 at the start of each flight by means of a compact (hand-held) alpha-numeric keyboard.

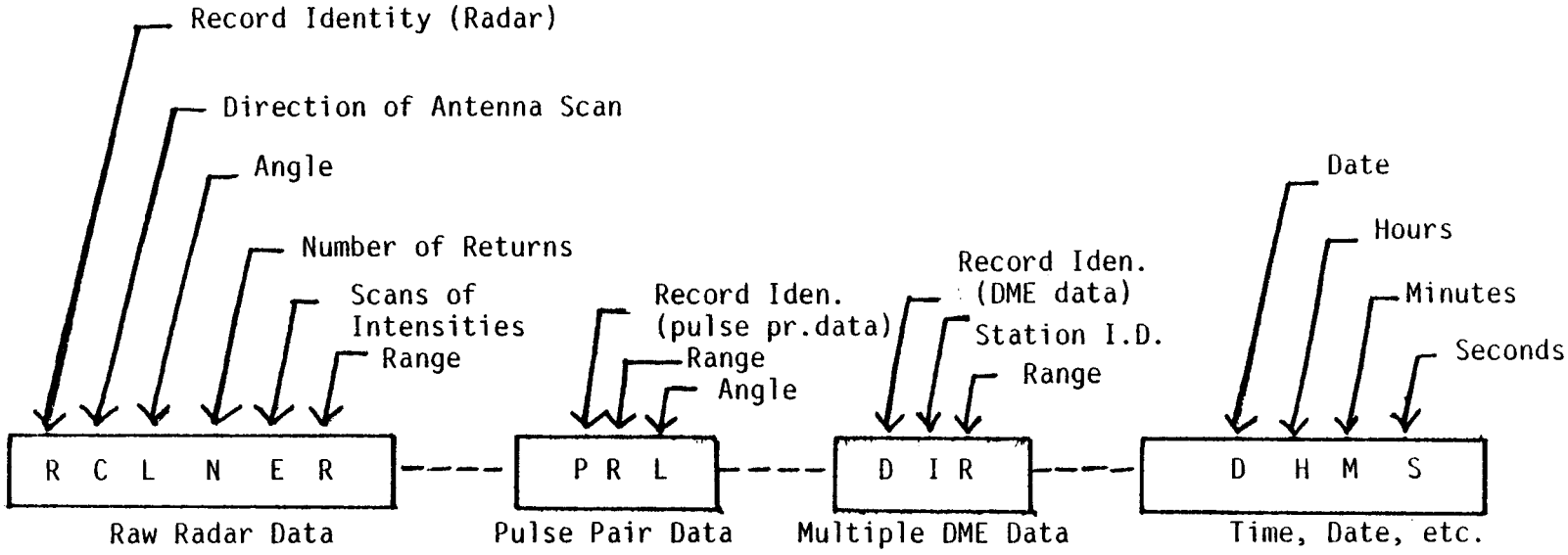

Figure 1.6. Format of Data Recorded

SECTION II. RADAR SYSTEM

In parallel with work on the data collector, effort has also been expended on the radar system as discussed below.

A. Range Correction

To properly measure and display the size of spectral targets independent of range, it is necessary to have the radar video corrected by R^4, instead of the conventional R^2 correction. R^2 correction is appropriate for volume targets such as rain where the target volume observed increases by R^2. Conversations with RCA personnel indicated that R^4 correction might be accomplished by means of existing adjustments. This was tried and it worked. The present range correction is shown in Fig. 2.1, showing R^4 correction out to about a range of five miles that is accurate to within the desired $\pm$ 3 db.

B. Gain Control

In order to display only targets above a desired dbsm level, it is necessary to have an operator-adjustable calibrated level control. It has been decided to do this by means of the existing gain control which control biases the IF amplifier. Fig. 2.2 indicates dbsm level displayed as a function of the gain control voltage. This voltage is displayed to the operator and also recorded as shown in Fig. 1.3. The operator can set the control by reference to Fig. 2.2. In order to ensure that the calibration is stable from flight to flight, the gain control can be periodically placed in the preset position and the voltage noted. This "preset" voltage is automatically adjusted by means of automatic gain control circuits (AGC) with respect to a standard "noise" generator internal to the radar.

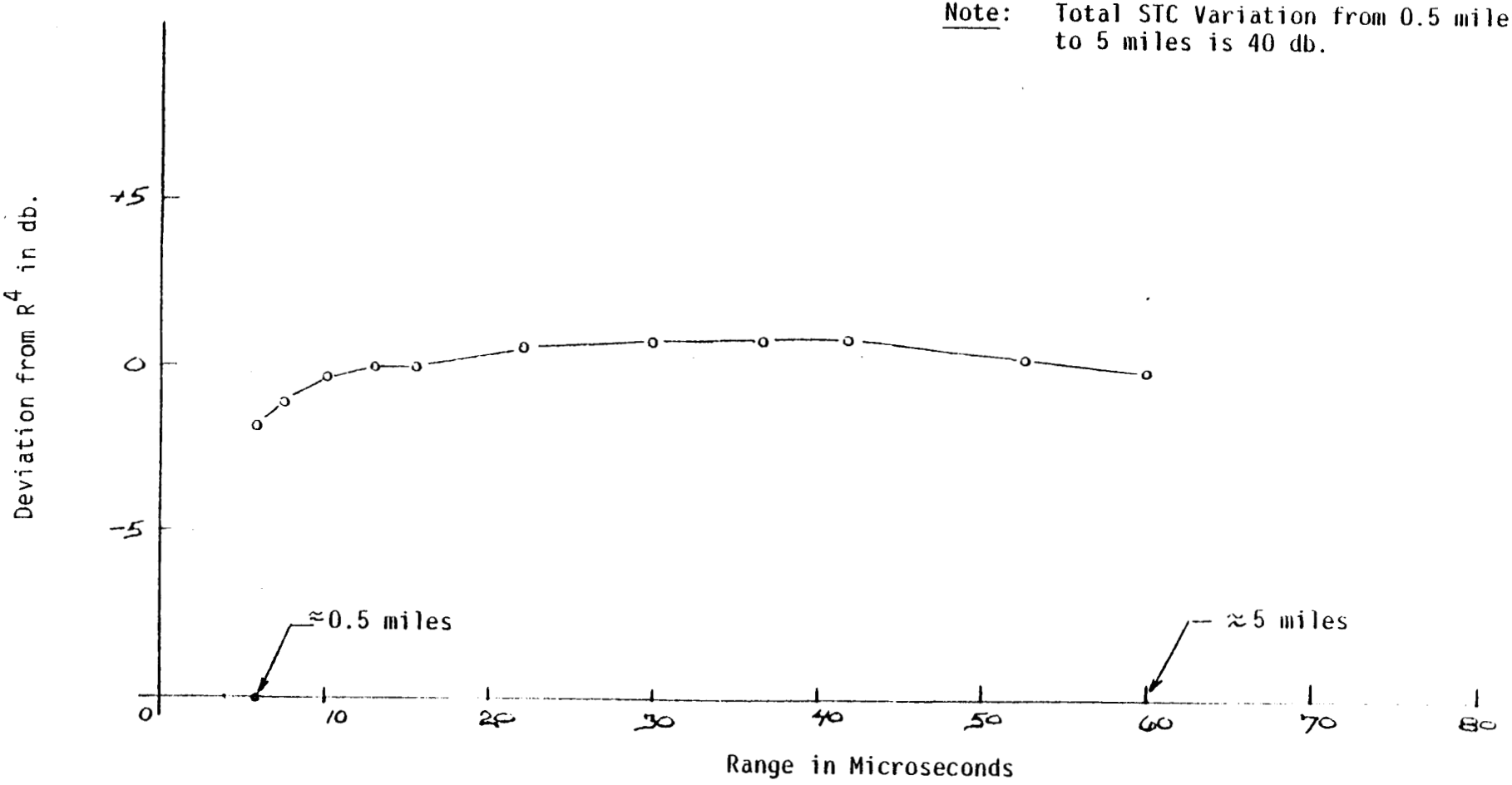

Figure 2.1. Deviation of Sensitivity Time Control From R^4 from 0.5 miles to 5 miles.

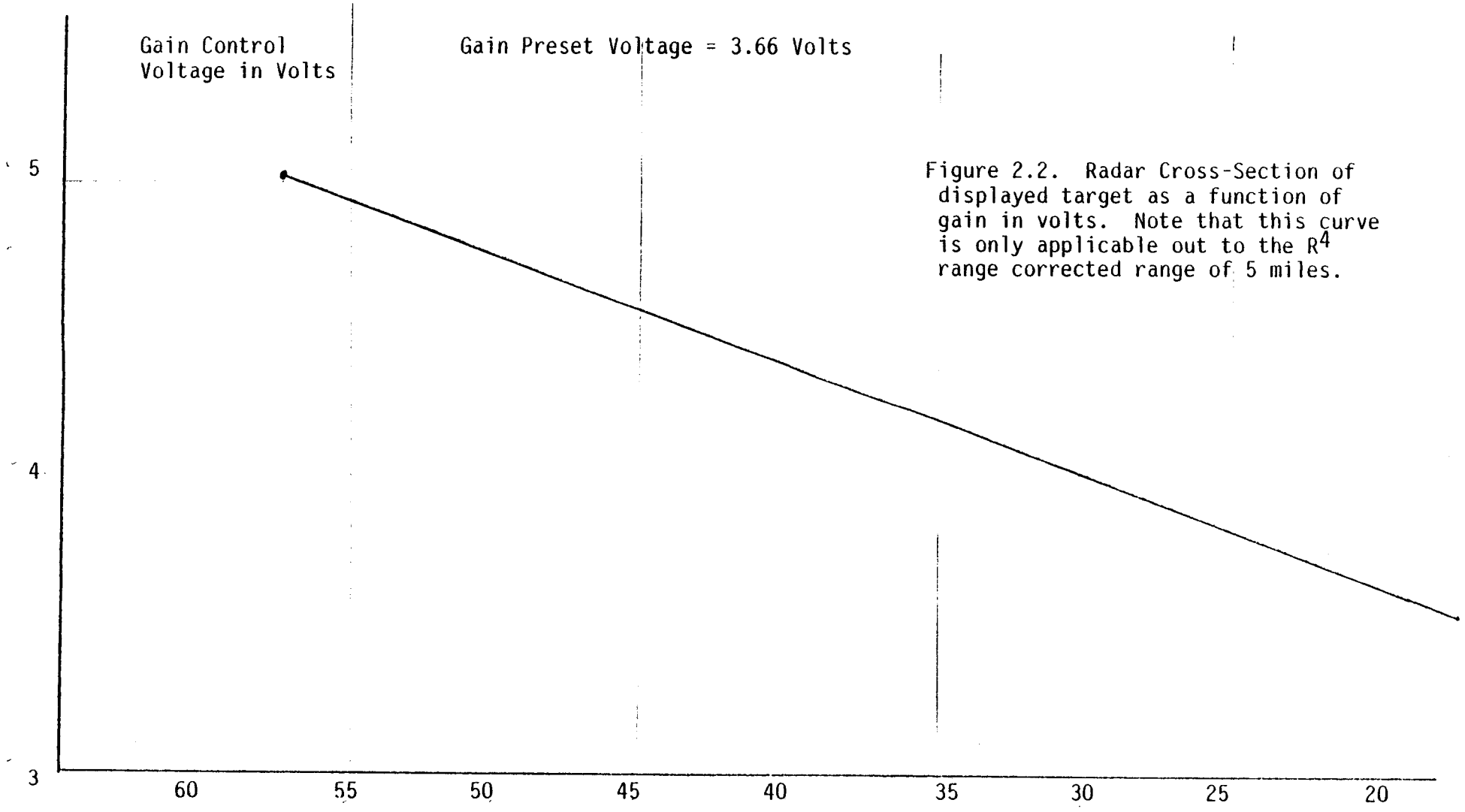

Figure 2.2. Radar Cross-Section of displayed target as a function of gain in volts. Note that this curve is only applicable out to the R^4 range corrected range of 5 miles.

Since the R^4 range correction has only been applied out to a range of about five miles, Fig. 2.3 can be used to interpret displays out to five miles and beyond.

C. Pulse Pair Decoder

A pulse pair decoder has been obtained and tested. The unit was fabricated by Vega Precision and loaned to the project because of their interest in this program. Vega manufacturers beacons for use with the Primus 50 radar. The unit consists of a pulse detector and a pulse pair decoder.

The pulse detector is designed to sample the leading edge of the incoming pulse at a consistent level, independent of pulse amplitude. This is desirable for purposes of precision radar range measurement. It does this by detecting the peak of the incoming signal and comparing this detected level with the signal delayed by a delay network as shown in Fig. 2.4. The detection level should be relatively independent of input signal.

The decoding circuit operates as follows (see Fig. 2.4). The output of the level comparator, U-1, from the first pulse triggers a pulse shaper. This shaped pulse triggers a 2 microsecond delay multivibrator. At the end of two microseconds, a decoding gate opens for 0.5 microseconds. The comparator output from the second pulse of the pulse pair also generates a shaped pulse. This second pulse, if it appears in the 0.5 microsecond window of the decoding gate, provides an output signal indicating a valid pulse pair.

D. Receiver Overloading

In the process of implementing the R^4 range correction and dbsm level control circuits, it was determined that, at the minimum gain

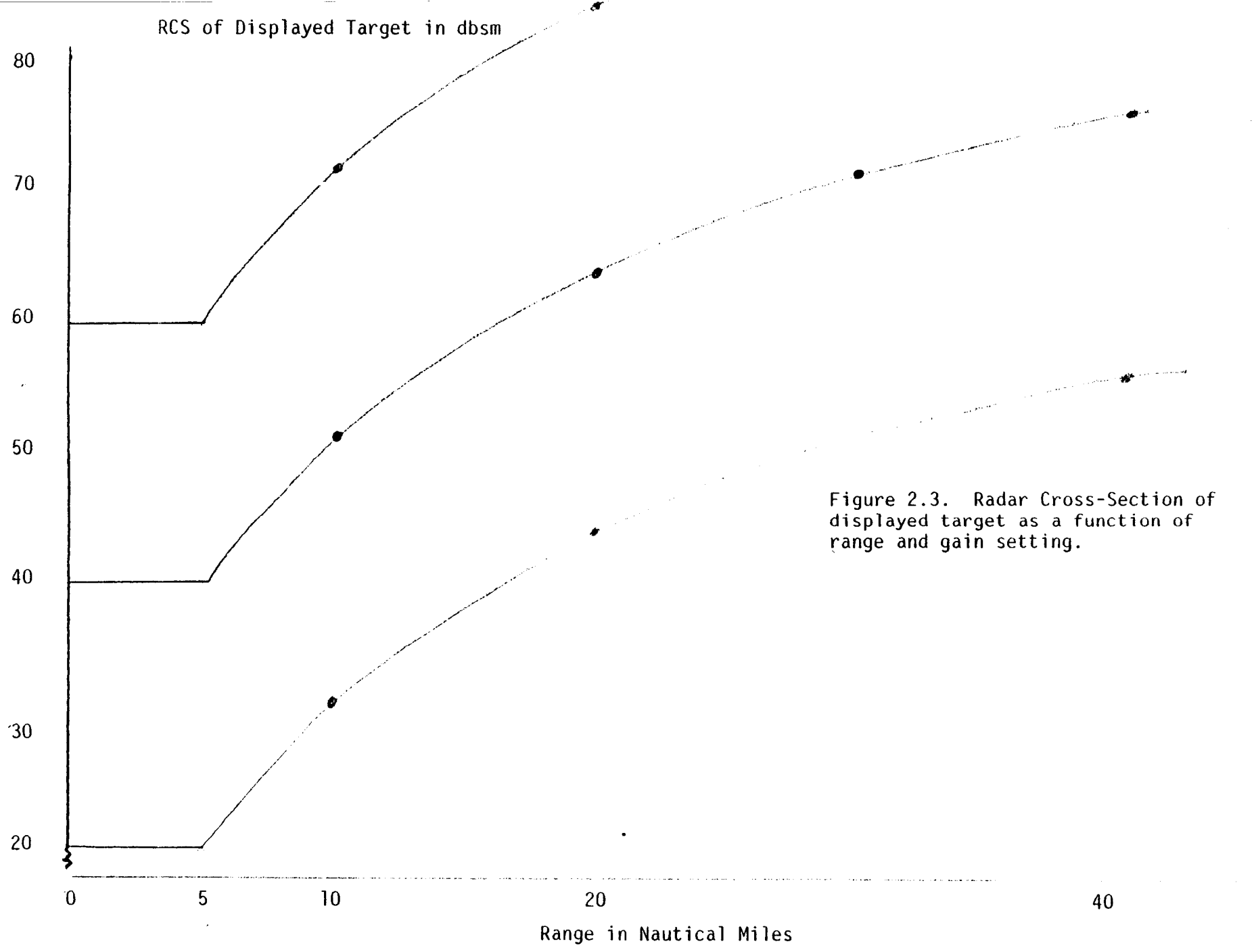

Figure 2.3. Radar Cross-Section of displayed target as a function of range and gain setting.

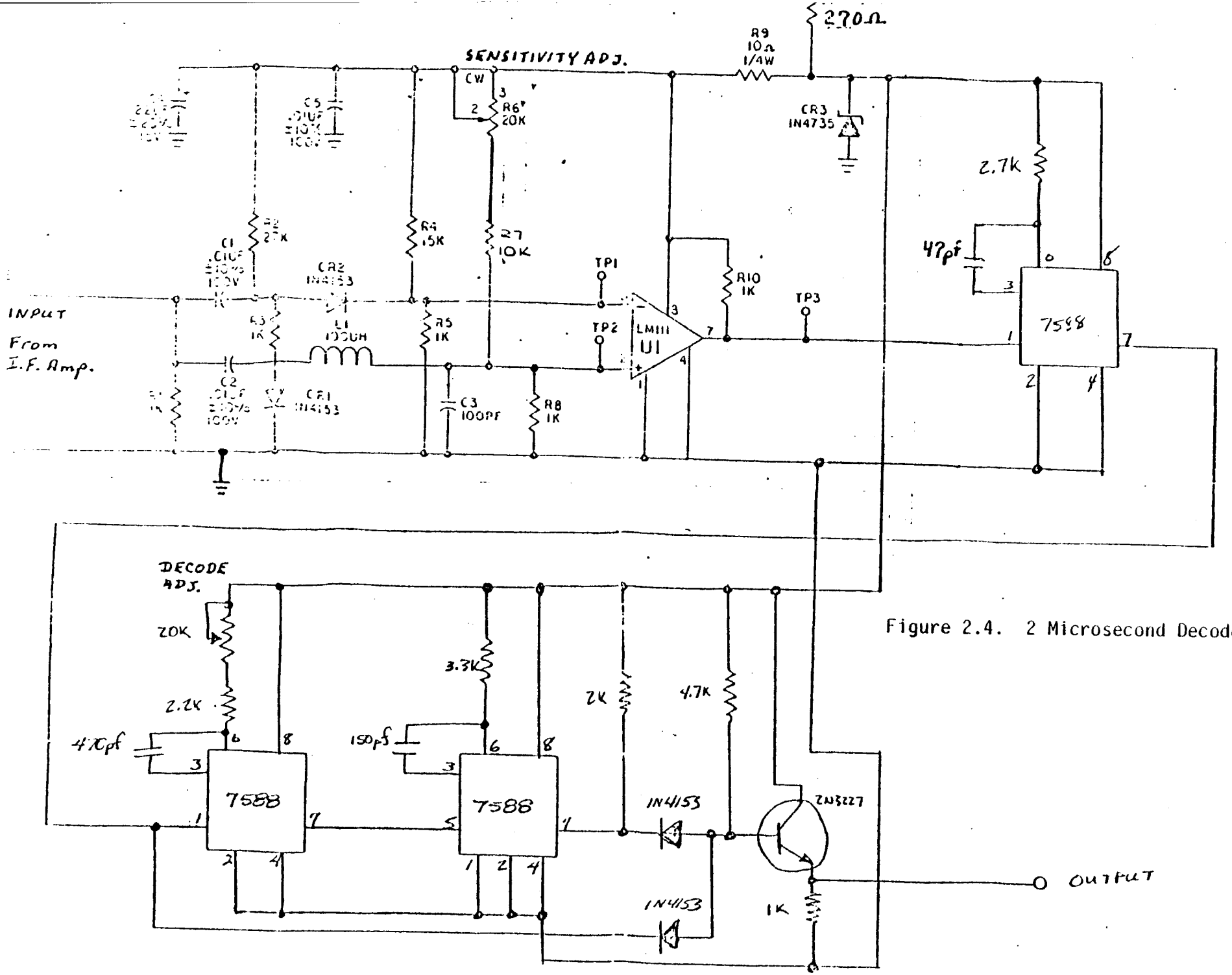

Figure 2.4. 2 Microsecond Decoder

control possible with the unmodified radar, all targets above 30 dbsm would be displayed, i.e., it was not possible to reduce the gain sufficiently to display only targets comparable to the 46 dbsm corner reflectors. This limitation, unless corrected, makes it very difficult, if not impossible, to recognize 46 dbsm reflectors, i.e., they would always be displayed with more numerous and much weaker targets.

This problem was solved by inserting an 8 db attenuator (16 db two-way) between the R/T unit and the antenna as shown in Fig. 2.5. In this manner, the minimum gain control would permit the display of only targets of 46 dbsm and greater, i.e., the corner reflectors and larger targets. The calibration curve of Fig. 2-3 is taken with the attenuator inserted.

E. Field Testing

Preliminary field testing has been conducted in the area shown in Fig. 2.6. The most significant data was obtained by placing a single dihedral reflector on the top of Peavine at the Location A noted in Fig. 2.6, with the radar located (B) at the DRI building. Fig. 2.7 provides a vertical profile of the test site.

As a first step, the reflector was tilted in the vertical with the results shown in Fig. 2.8. The angle of maximum return corresponds to the computed angle of Fig. 2.7.

With the radar pointed at the reflector, the only target visible on the display at minimum gain was the reflector as shown in Fig. 2.9. The measured and computed value of the radar cross-section of the reflector was within the probable $\pm$ 3 db measurement accuracy. Table 2-1 provides a computation of the computed and measured signal return.

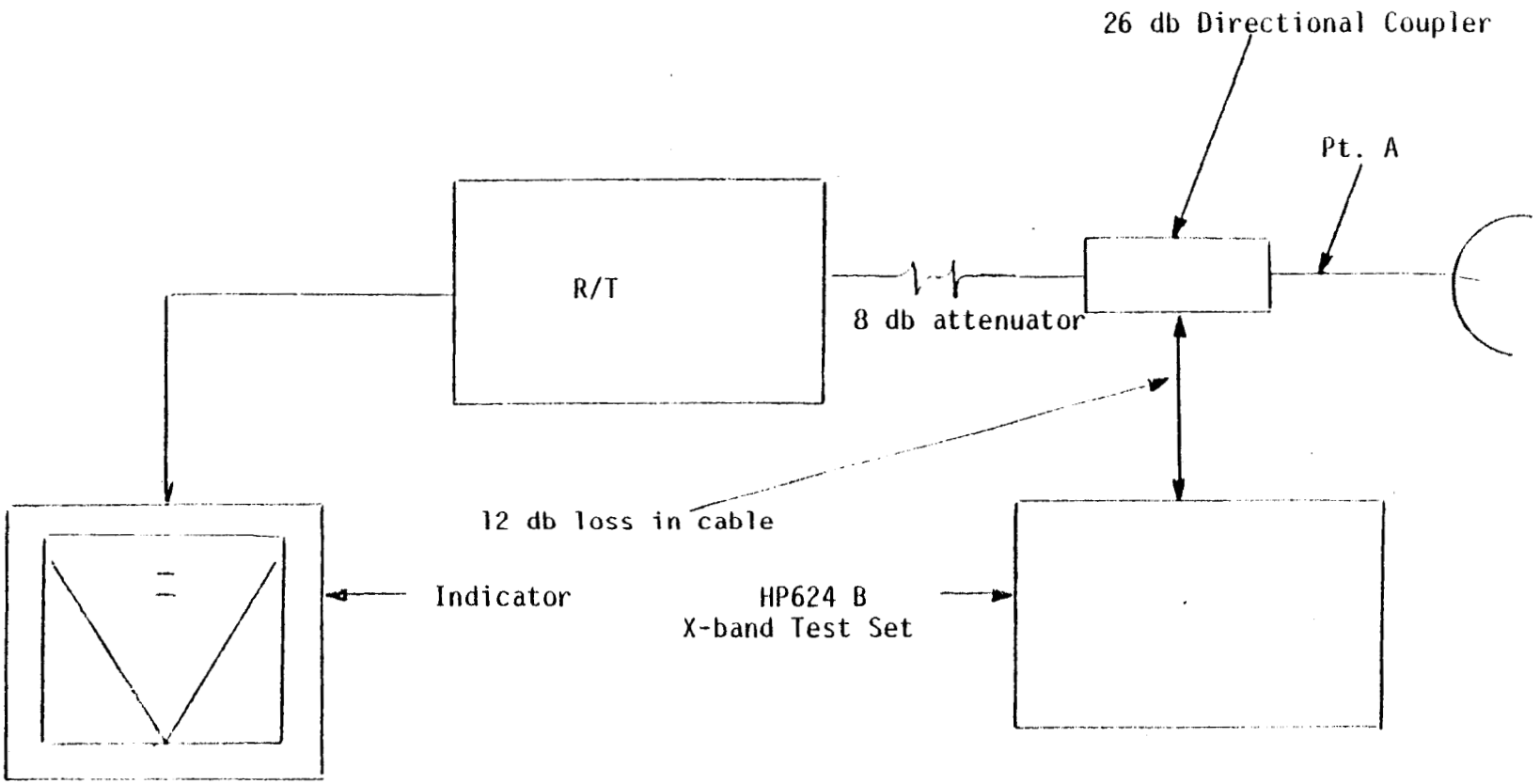

Figure 2.5. Block Diagram of Test Setup.

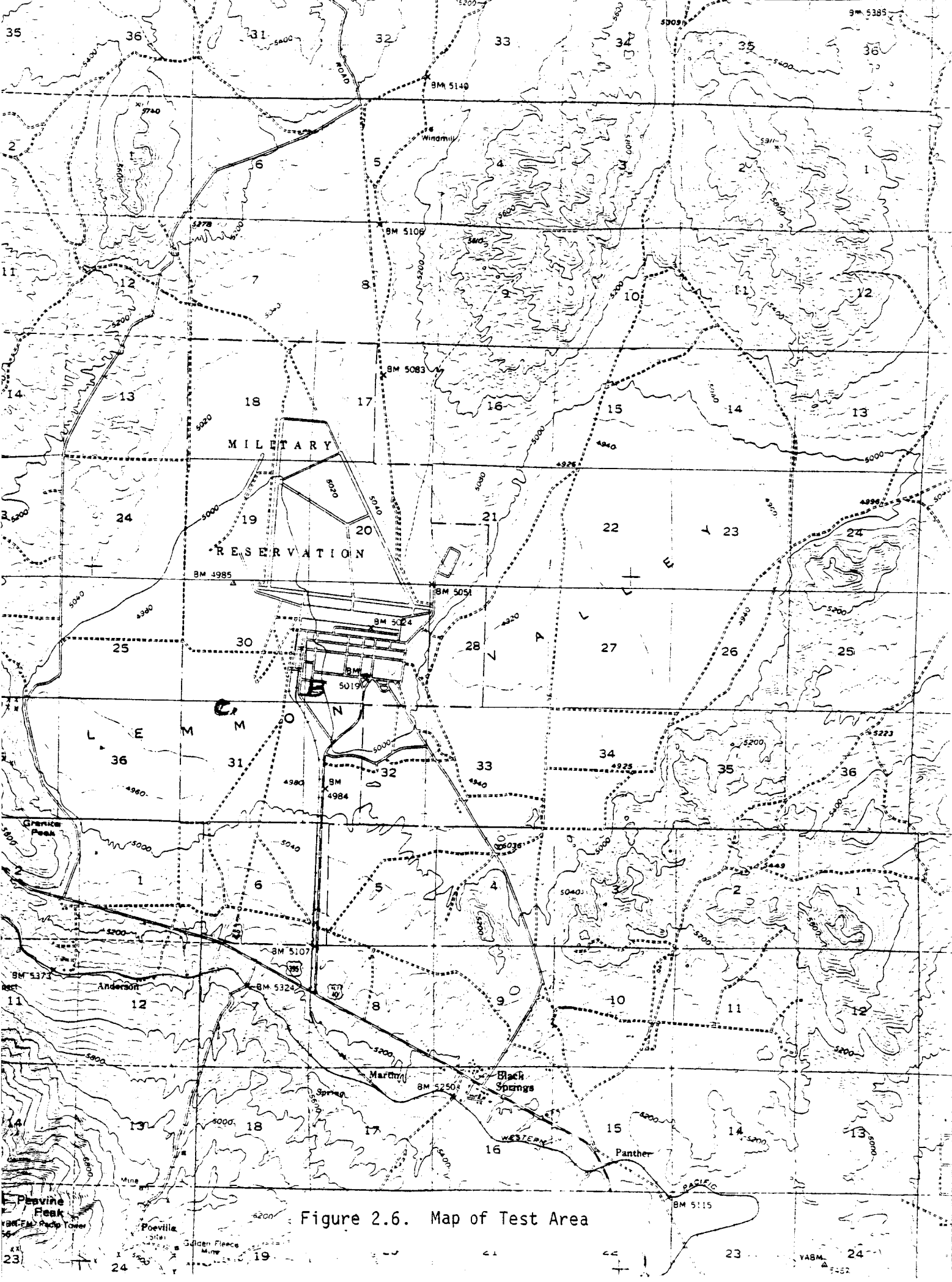

Figure 2.6. Map of Test Area

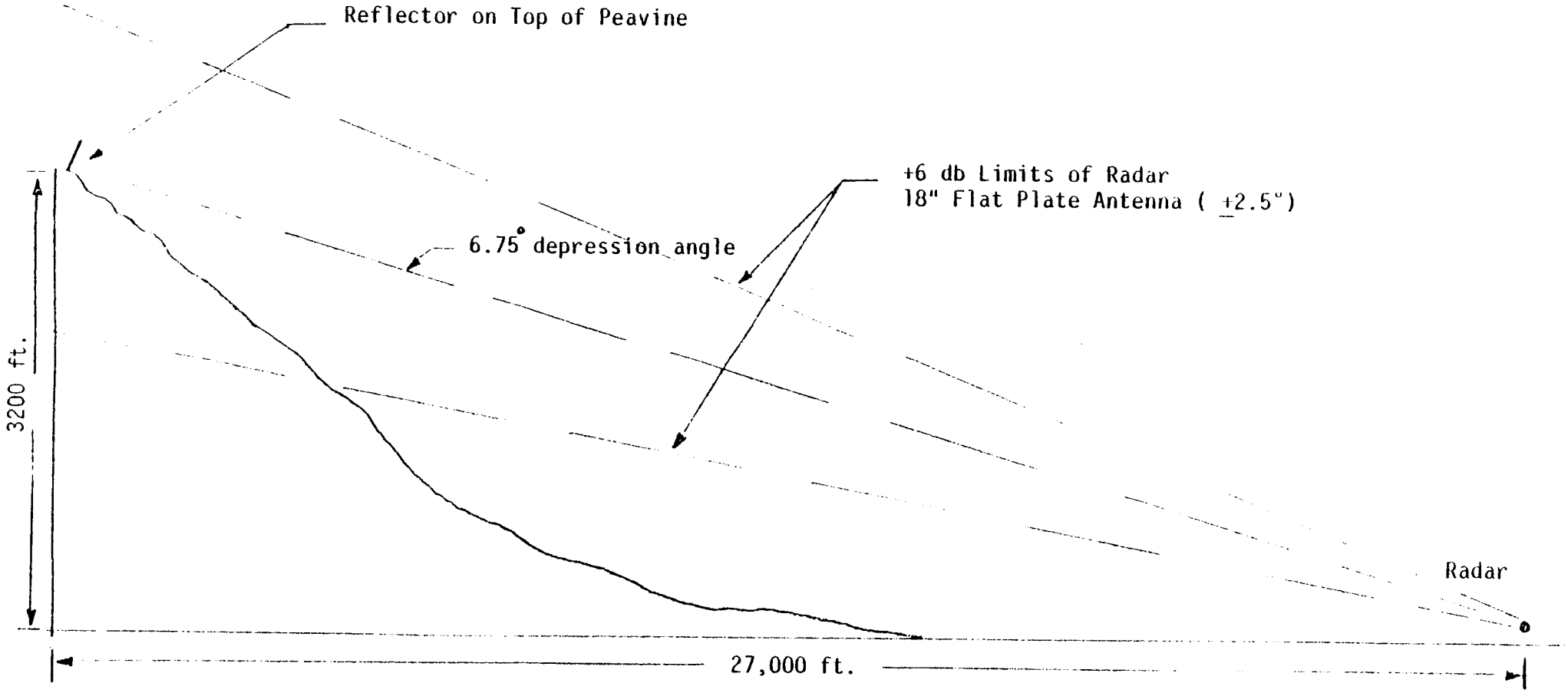

Figure 2.7 Profile of Peavine Test Arrangement

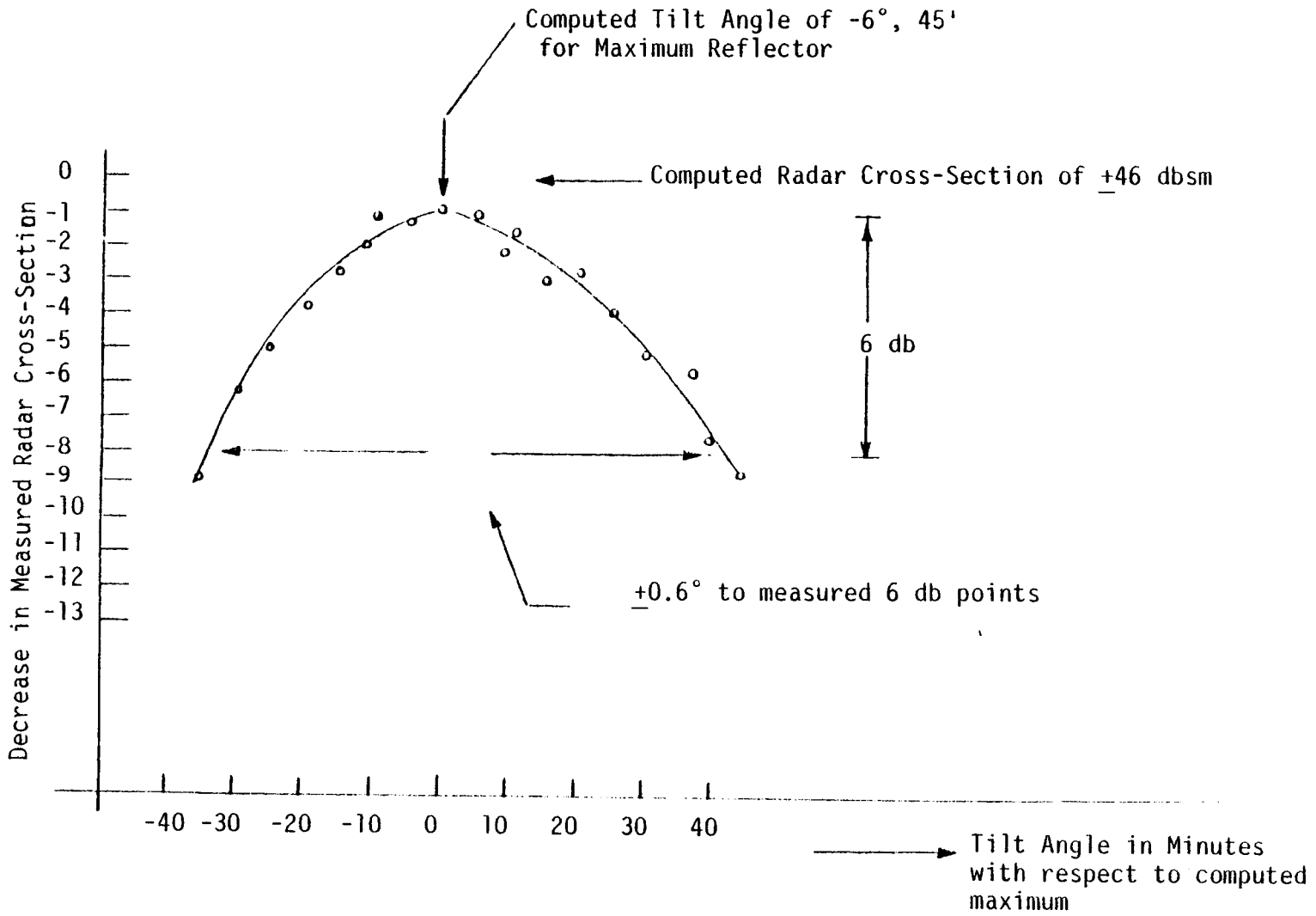

Figure 2.8. Measured Radar Cross-Section of Dihedral Reflector on Peavine as a Function of Tilt Angle.

TABLE 2-1. COMPUTATION OF SIGNAL FROM REFLECTOR ON PEAVINE

Reflector Gain = $G = \frac{4\pi A}{\lambda^2}$

A = 4 ft. high x 5.64 ft. (open face)

= 1.22 meter x 1.72 meter

= 2.10 sq. meter

$G = \frac{4 \times 3.14 \times 2.10}{(3.2 \times 10^{-2})^2} = 25{,}800$

G 43 db

Reflector Cross-Section = 43 db above 2.10 sq. meters

≈ 46 dbsm

Power Out (8 kw - 8db)	= +61 dbm (Point A)		
Path Loss (4.3 miles)	≈130 db x 2	= -260 db	
Ant. Gain	≈ 30.5 db x 2	= 61 db	
Reflector Gain	≈ 43 db x 2	= 86	
Received Signal	≈	= -52 dbm	

This received signal is at Point A of Fig. 2.6. The output signal from the signal generator to match the signal from the reflector at Point A was -14 dbm, which is within ±3 db of the computed value of Table 2-1, based upon the 26 db directional coupler and 13 db cable loss to the signal generator.

As a next step, the signal generator was used to insert a signal equal to the reflector return but two microseconds further out in

range. This continuous signal which appears as a "range ring" is shown in Fig. 2.10.

When the antenna scanned the reflector on Peavine, this continuous signal would simulate a second reflector 1000 ft. behind the installed unit. If the decoder output was displayed on the CRT, the display then appeared as in Fig. 2.11.

As a next step, the radar antenna was tilted towards the horizon to pick up ground clutter and the radar video displayed with minimum gain, i.e., only 46 dbsm targets and above were displayed. Fig. 2.12 shows two such targets. The close-in target is a very large warehouse (Pennys). The further-out target is probably a large water tank. When the display was switched to decode, no decodes could be detected.

As a next step, the gain was increased to display 40 dbsm targets as in Fig. 2.13. Again, no decodes were observed. The gain was further increased to show 36 dbsm targets as in Fig. 2.14. Decodes corresponding to this display are shown in Fig. 2.15.

From the above, it can be observed that the reflector is of the correct magnitude and that clutter targets are similar in magnitude to that expected from data provided in the program outline. The "protection" provided by the decoder used was not as great as hoped for however. In this connection, it appeared that the false decodes were coming from "distributed" targets of about 35/40 dbsm rather than the larger 46 dbsm spectral targets.

Another test of interest was the measurement of the radar cross-section of the dihedral reflectors at a range of about 0.66 miles and at a depression angle of about 1° from the radar at the DRI. (Location C of Fig. 2.6).

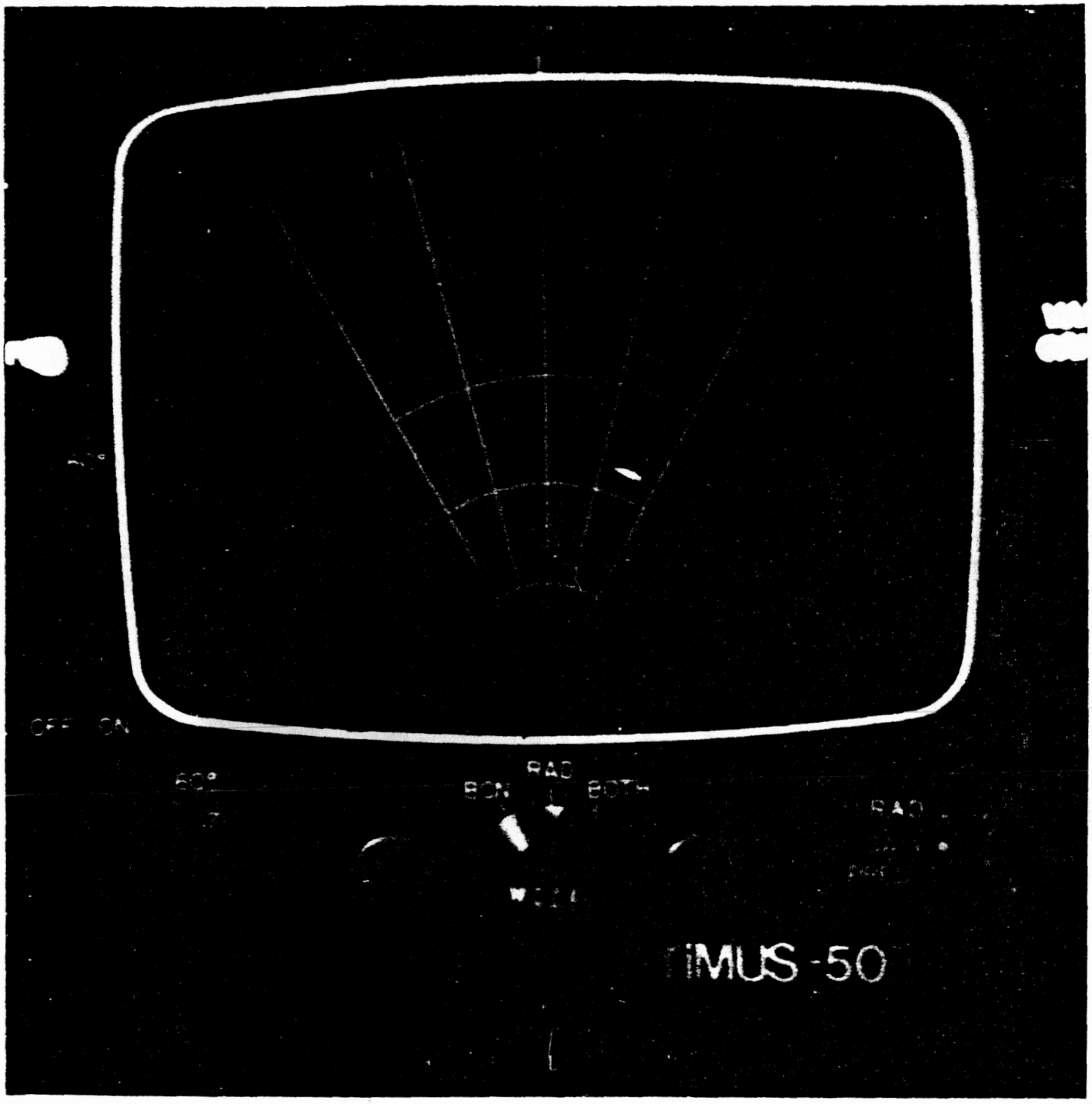

Figure 2.9. Display of Radar Video. Manual gain set to display targets of 46 dbsm and greater. Radar antenna tilted up 7° to aim at 46 dbsm reflector on top of Peavine. Note that the reflector is the only target visible. Range marks are two miles.

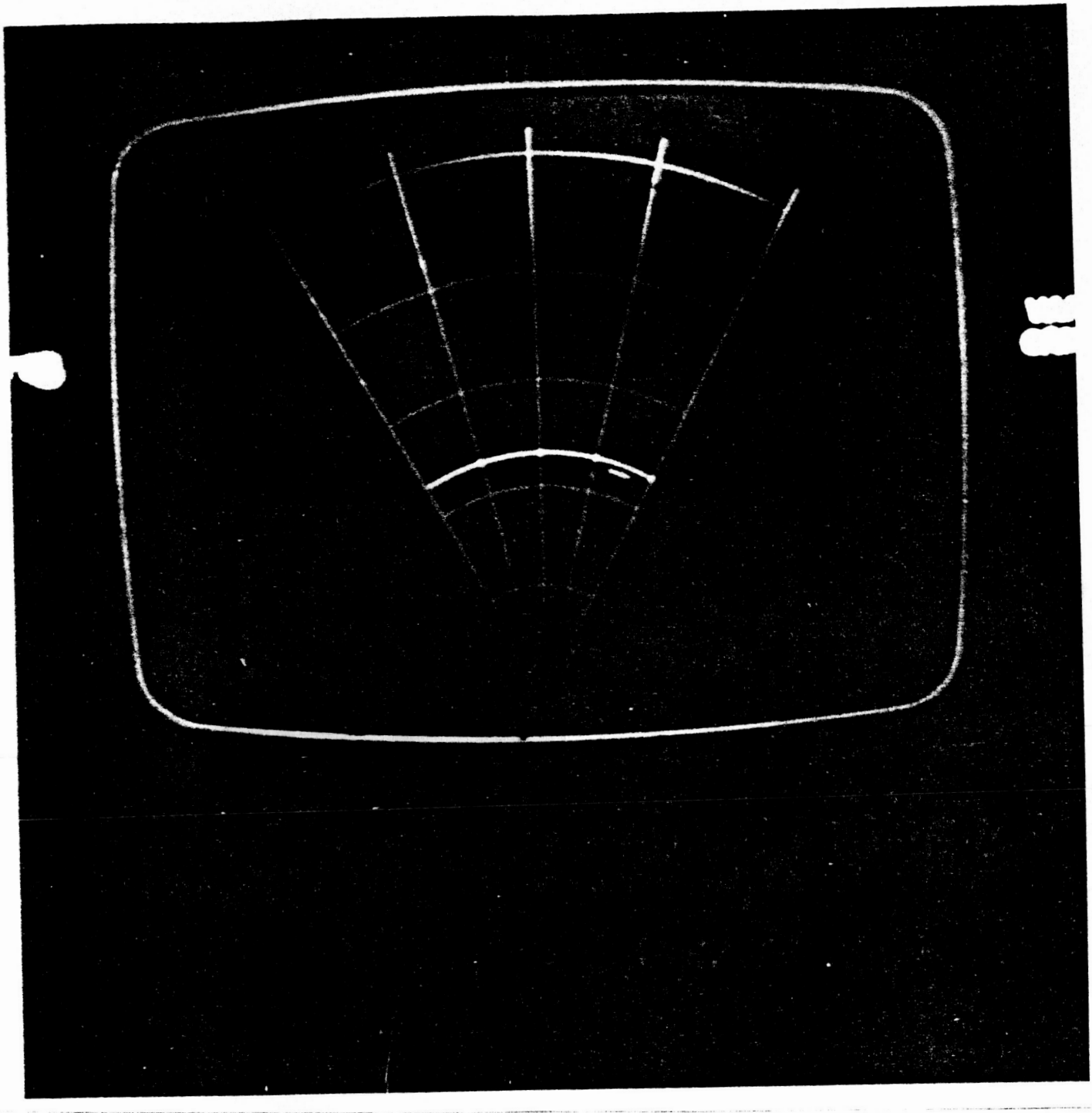

Figure 2.10. Display of radar video as in Fig. 2.9 except that signal generator provides a "continuous" target some two micro-seconds (1000 ft.) further out in range.

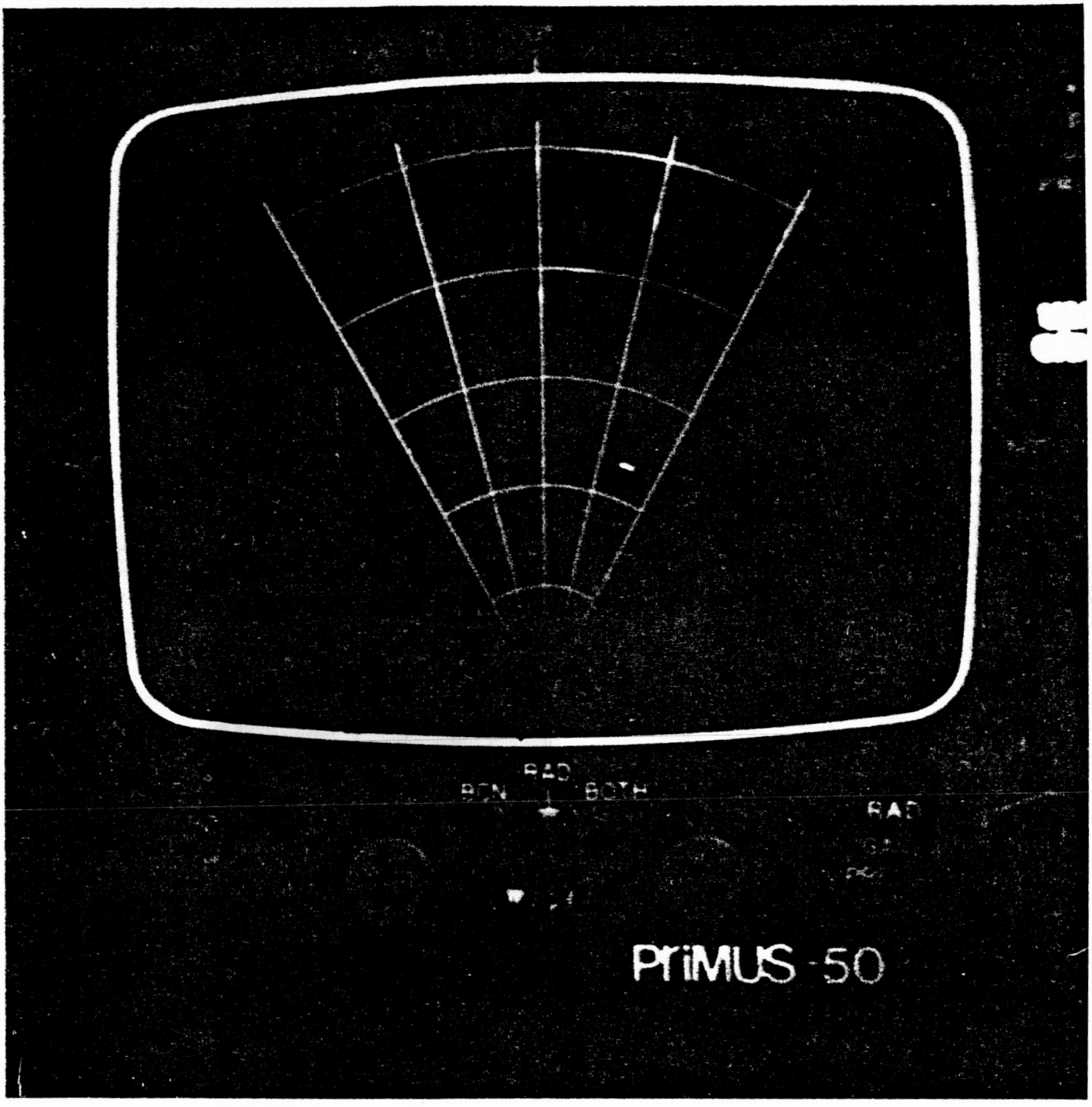

Figure 2.11. Display of output of pulse pair decoder. Radar antenna oriented as in Fig. 2.9 and 2.10. Input to decoder radar video which in this case is echo from reflector on Peavine and signal generator pulse of Fig. 2.10.

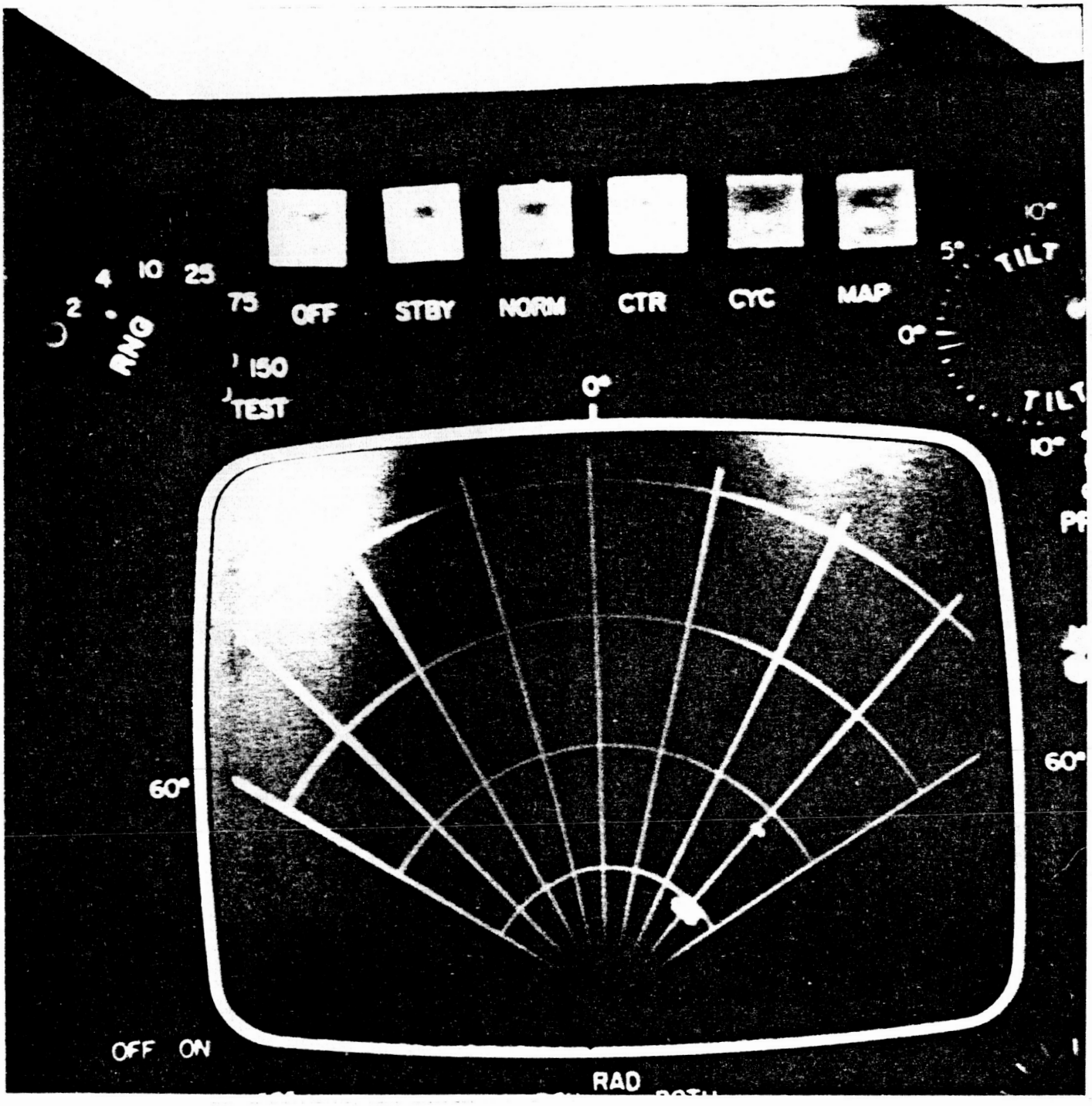

Figure 2.12. Display of Radar Video. Gain setting as in Fig. 2.9 and 2.10, i.e., set to display targets of 46 dbsm and greater. Antenna tilted horizontally to pick up clutter. Note the two targets, one of which is a very large warehouse. Range markers are one mile.

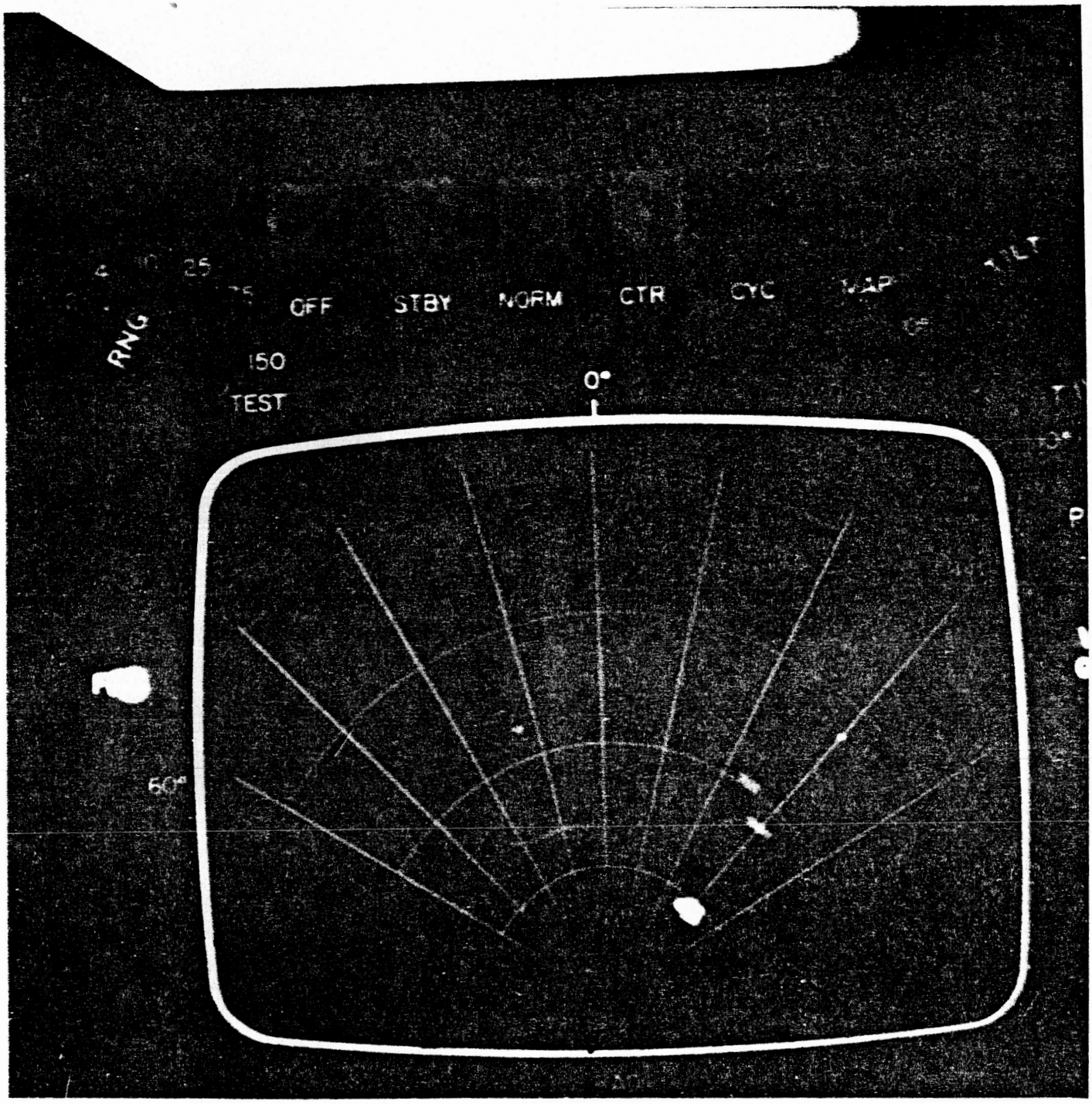

Figure 2.13. Display of Radar Video. Gain increased by 6 db over Fig. 2.12 to display targets of +40 dbsm and greater. No false decodes were noted for this gain setting.

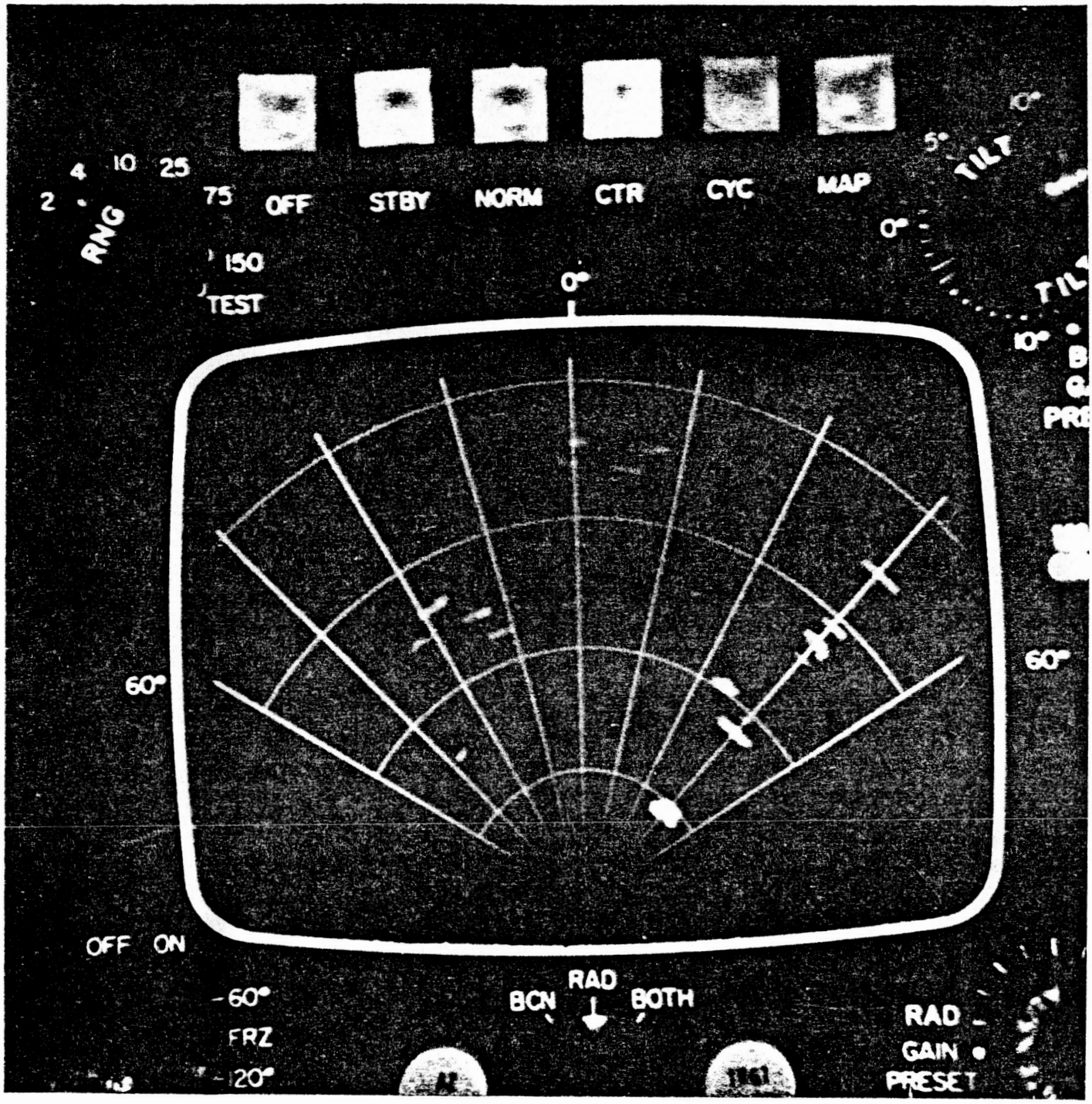

Figure 2.14. Display of Radar Video. Gain increased by 10 db over Fig. 2.9 to display targets of +36 dbsm or greater.

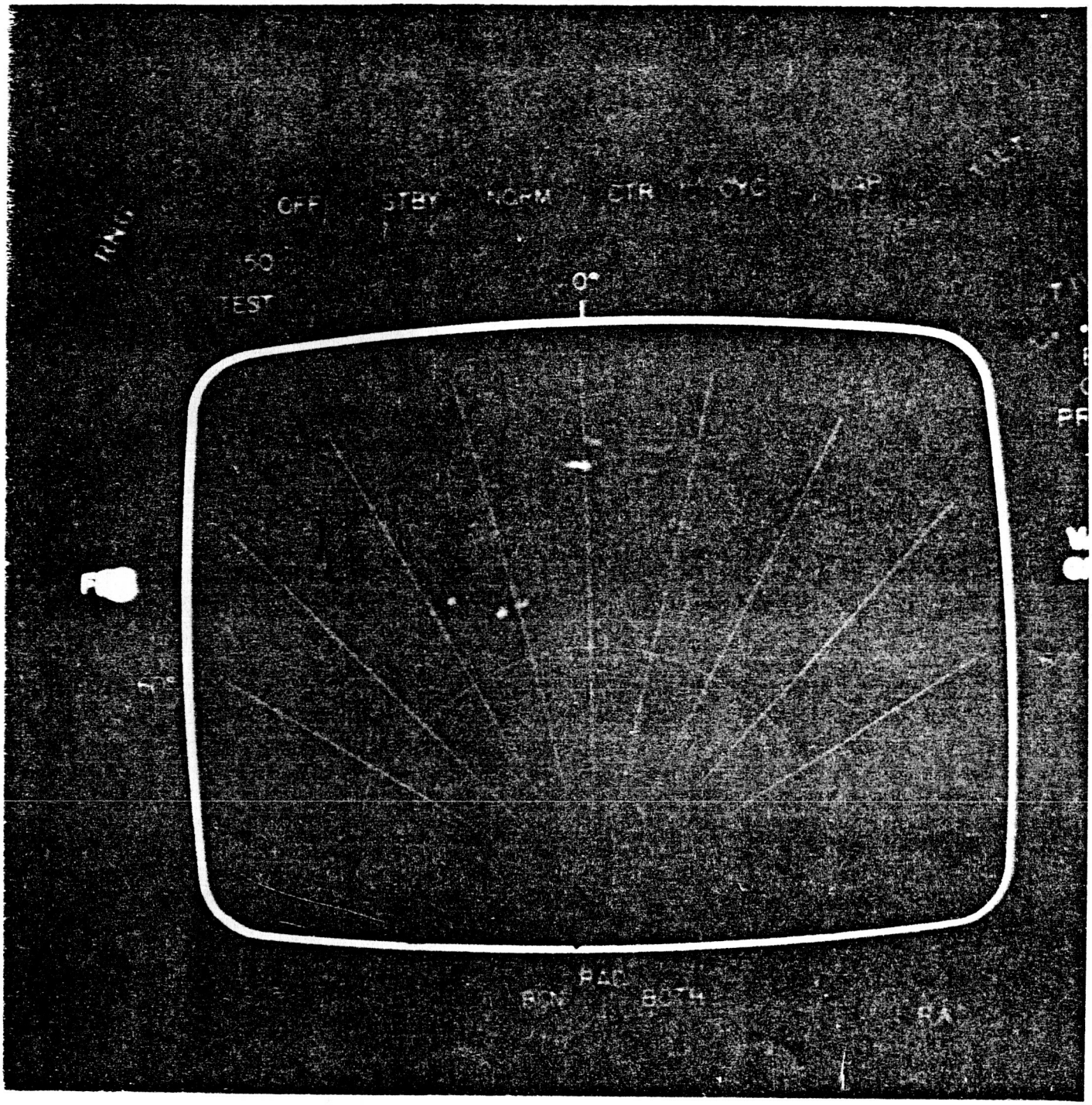

Figure 2.15. False decodes for gain setting of Fig. 2.14. Decodes appear to be coming from distributed clutter rather than the large spectral targets of Fig. 2.13.

The purpose of this test was to determine if the dihedral would become a multipath immune trihedral (MIT) when orientated vertically to a flat, dry lakebed. This phenomenon had been observed several years ago in preliminary testing.

In the initial portion of the tests, the wind was calm and the observer at the reflector was readily able to measure tilt angle data as noted in Fig. 2.16. The wind then became severe, however, and the dashed data is estimated, based on tilting the reflector up and down many times. It does indicate, however, that the dihedral reflector does indeed act as expected, i.e., it is a dehedral at +1° - a trihedral (MIT) at 0°, using the earth as the third side, and a dihedral at -1° using the earth as a mirror.

F. Distributed Clutter

Prior to the Peavine tests, the belief has been that spectral clutter, i.e., point targets such as buildings, etc. would be the major concern, and that distributed targets, i.e., rocks, trees, etc. would be of minor concern.

Based on the Peavine data, distributed clutter appears to cause decodes with the single decoder used, even when such clutter was 10 db below spectral targets that did not cause decodes.

Examination of the distributed clutter return provides a clue in this regard in that the return from distributed clutter tends to be "noisy" and of extended area, i.e., the noise extends over many micro-seconds. This type of signal can readily cause decodes in contrast to a very strong uniform signal of limited extent, i.e., range, with the simple decoder used.

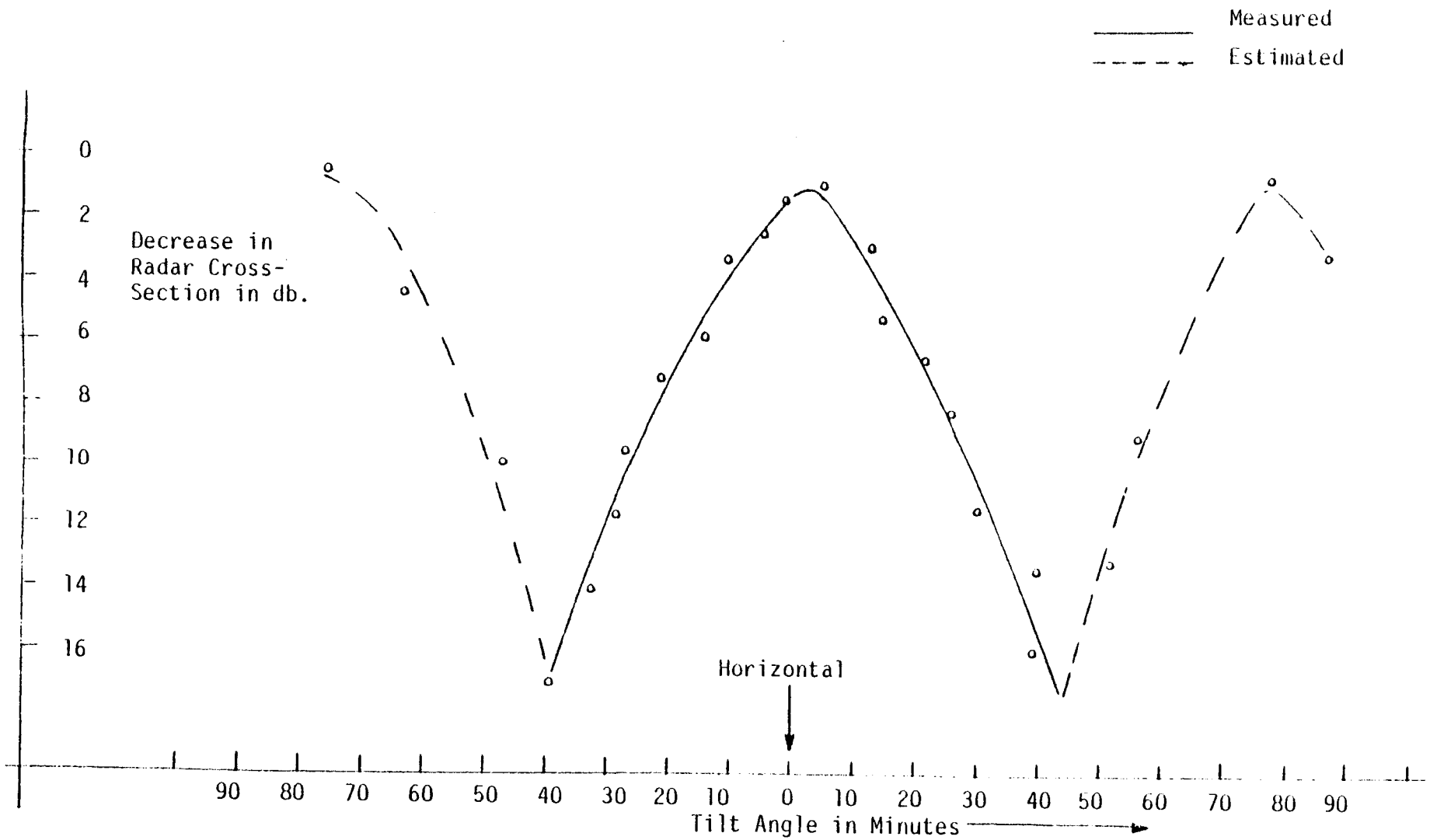

Figure 2.16. Measured Radar Cross-Section of Dehedral Reflectors on Dry Lake.

In this connection, it is interesting to further consider distributed clutter. Distributed clutter arises from many individual returns from targets within the area illuminated by the pulse. In general, distributed clutter is described in terms of the area illuminated by the pulse multiplied by the coefficient of reflectivity of the area.

The area illuminated by the 0.6 microsecond radar pulse at 4 miles is given by:

$$\text{Area Illuminated} = \frac{\text{Pulse Length} \times \text{Beam Width}}{2}$$

$$= \frac{600 \text{ ft.}}{2} \times \frac{5^\circ}{57^\circ} \times 4 \times 6000 \text{ ft.}$$

$$= 6.3 \times 10^5 \text{ sq. ft.}$$

$$\approx 5.7 \times 10^4 \text{ sq. meters} \approx 47 \text{ dbsm}$$

Now some of the distributed clutter targets on Peavine area are of the order of 37 dbsm or so. This implies a coefficient of reflectivity of -10 db, i.e., the 47 dbsm area illuminated reduced by 10 db.

Data pertaining to distributed clutter targets is given in Figs. 2.17, 2.18, and 2.19. From Figs. 2.18 and 2.19 it would appear that a coefficient of reflectivity of -10 db is rare although it does occur. In this connection, Fig. 2.18 indicates that only 16% of the target cells have a reflection coefficient greater than -20 db for wooded hills and 14 db for cities. But it should be noted that there are lots of "target" cells, i.e., 16% of a lot is a lot.

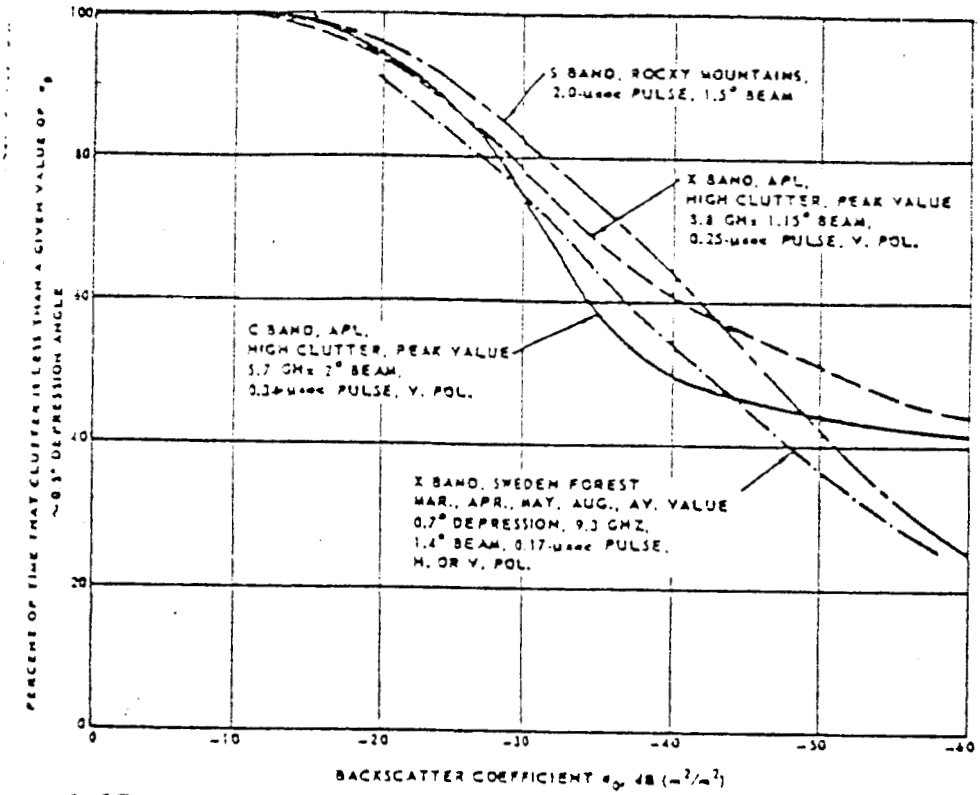

Figure 2.17 *Land clutter backscatter distributions from surface radars.*

Figure 2.18 Land Clutter Reflectivity (0 to 1.0° Incident Angle)

Terrain type	Reflectivity, dB, below 1 m^2/m^2 at indicated carrier frequency, GHz						
	UHF 0.5	L 1.2	S 3.0	C 5.6	X 9.3	K_u 17	K_a 35
	σ_m, σ_{84}	σ_m, σ_{84}	σ_m, σ_{84}	σ_m, σ_{84}	σ_m, σ_{84}	σ_m, σ_{84}	σ_m, σ_{84}
Desert		45,35	-,31		38,30		
Cultivated land	30,- 28,-	32V,-		38,30	36,30		23H, 15H 18V, 10V
Open woods		34H,-	33,26		30,22		
Wooded hills	24,18 34,-	35,20 45,27	32,24 47,29	-,27	30,20 36,28		21H, 13H 13V, 8V
Small house Districts			35,26	35,26	30,24,		
Cities	22,- 30,-	30,20			36,- 24,14		

Average of both polarizations except where noted.
σ_m = median backscatter coefficient in decibels below 1 m^2/m^2
σ_{84} = coefficient that 84 percent of the cells are below
τ = pulse length = 1 μsec
θ_3 = beamwidth = 2°

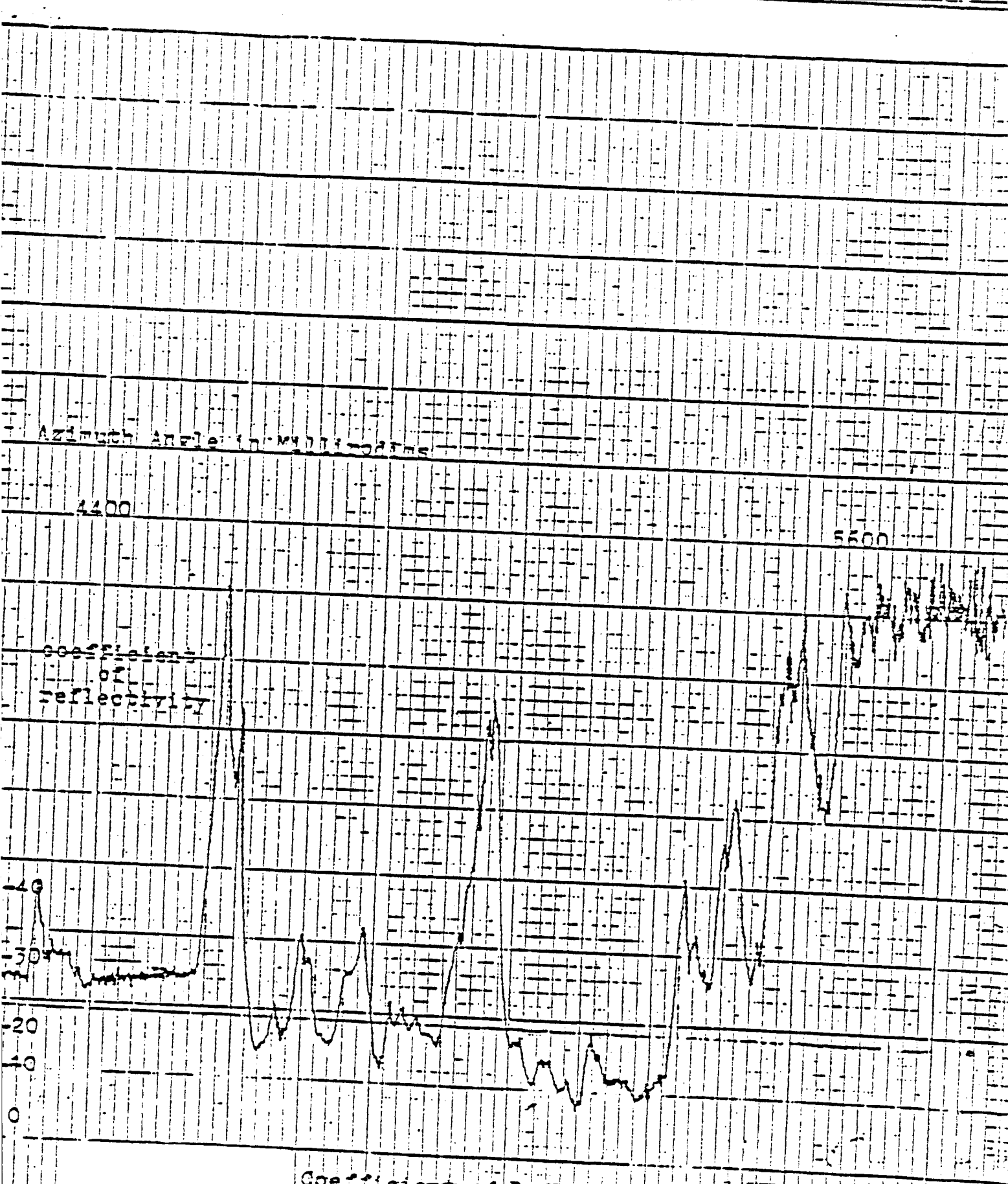

Figure 2.19 Coefficient of Reflectivity looking into side of mountain at 8000 yards. (Dyna)

Fig. 2.19 is very appropriate to the Peavine tests. It is a measure of the coefficient of reflectivity looking into Peavine taken with an X-band radar some 4 years ago when the subject of corner reflector detectability was being initially studied. It shows a measured coefficient of -10 db. Fig. 2.19 is included in the original proposal to FAA on this subject.

Subsequent to the Peavine tests, conversations with personnel who had made X-band measurements on similar mountainous terrain around China Lake, CA, indicated that -10 db was not unexpected when looking at steeply rising portions of a mountain.

In any event, distributed clutter is now considered to be as significant a problem as spectral clutter. Fig. 2.20, which depicts the coefficient of reflectivity of the ocean as a function of sea state, is included for reference.

G. Potential for Improvement

There are certain avenues that can be followed to improve the current "margin" of performance (which is 6 db at the Peavine site). They are as follows:

(1) Increase the reflector size. This can readily be accomplished by clamping 4x8 plates to the existing units. An improvement of 6 db can be expected.

(2) Decrease the pulse length. Current marine navigational radars use a 0.06 microsecond pulse. Bendix has provided the Coast Guard with a 0.1 microsecond version of their RDR-1400. A decrease of 10 db to 7 db can therefore be expected in distributed clutter if readily available short pulse R/T units are used.

σ_o (dB Below 1 m^2/m^2)

SEA STATE / ψ	0.1°		0.3°		1.0°		3.0°		10°		30°	
	HOR.	VERT	HOR.	VERT	HOR.	VERT	HOR.	VERT	HOR.	VERT	HOR.	VERT
1	71*	65*	66*	58	51	50	48	45	51	42	-	39
2	61*	56	56*	52	46	44	42	41	43	36	44*	32
3	53*	51	46	45	40	39	39	38	37	32	34	28
4	48	48	42	43	36	37	35	35	34	31	33	24
5	42*	44	39	39	33	33	32	31	31	26	24	20*

*5 dB error not unlikely

MEDIAN BACK SCATTER

Table 1

Hydrographic Sea State	1	2	3	4	5
Wave Height (ft.) (Crest to Trough)	< 2	2-3	3-5	5-7.5	7.5-12

HYDROGRAPHIC SEA STATES

Table 2

Figure 2.20. Coefficient of Reflectivity for Different Sea States.

(3) Pulse Pair Decoder. The present pulse pair decoder is relatively unsophisticated. An improvement of at least 6 db should be expected with a more sophisticated decoder.

In this connection, there are several avenues to follow in decreasing false decodes due to distributed clutter. A first avenue is to use a pulse width discriminator on the individual returns. This apparently is a very powerful tool, based on conversations with personnel who have used it to detect point targets, i.e., low-flying aircraft in ground clutter. The technique is based on the fact that a return from a point target, such as a reflector is 0.6 microseconds, i.e., the pulse width, whereas by definition, the return from distributed clutter is greater than the pulse width.

Another technique is to require a certain amount of signal decrease between pulses. Another is to have a very small decoding tolerance.

SECTION III. WORK FOR THE NEXT PERIOD

As a result of a meeting at Ames in August, 1980, in which the above was discussed, effort for the next several weeks will focus on:

1. A MIT unit will be installed on a dry lakebed and its RCS measured by the radar from Peavine. If successful, this test will establish that a wide angle-high gain reflector is practical in at least certain terrain.

2. Clutter data on Reno Airport and Reno will be obtained.

3. The 8x4 reflector will be configured and tested.

4. The Ames trihedrals will be installed adjacent to the MIT units and tested for multipath.

5. A pulse width discriminator will be installed on the radar and tested on distributed clutter.

6. Radar reflectivity data will be recorded by the bucket brigade technique of Section I and various decoding schemes may be tried in software on the 11/23.

At the end of the period, the following data/conclusions should be available:

(a) Is the MIT a practical wide-angle coverage reflector?

(b) Can a 52 dbsm reflector be easily built?

(c) What size wide-angle reflector is obviously identifiable to an unmodified radar?

(d) What size wide-angle coverage reflectors are obviously identifiable to a radar with a state-of-the-art pulse width, pulse decoder system?

PROGRESS REPORT NO. 2

Period Covered: September 1 - October 1, 1980

Weather Radar Approach System
(WRAPS)

Prepared by

Dave Anderson/John Bull
Ames Research Center
National Aeronautics and
Space Administration
Moffett Field, CA

John Chisholm/Larry Baker/
Stan MacDonald
Atmospheric Sciences Center
Desert Research Institute
Reno, NV

NASA-Ames Cooperative Agreement
No. NCC 2-88

and

DRI ACR No. 1-6-220-6909-001

October 1980

INTRODUCTION

Effort during this reporting period has focused on improving the system performance, i.e., the ability to detect the coded reflectors in clutter. This effort has been directed along two avenues; one has been improving the ability to distinguish the individual reflectors from clutter, and the other has been improving the return from the reflectors themselves, both in intensity and angular coverage. Results are quite encouraging in that the problem of distributed clutter generating false decodes appears to have been greatly reduced.

SECTION I. DETECTION OF A POINT TARGET IN CLUTTER

In the previous report, it was noted that the return from a point target such as a corner reflector should be different from the return from distributed clutter in that a point target should reproduce the radiated pulse, i.e., be of the same pulse width, whereas the return from distributed targets should, by definition, be "distributed", i.e., extend longer than the pulse width since more than one "reflector", i.e., trees, rocks, etc., spread out over a region, will be simultaneously radiating back.

Three parallel approaches have been followed in order to distinguish these "elongated" distributed clutter returns from the returns from point targets.

All approaches focused on the same concept, that of using some form of pulse width discrimination. Two of the approaches employed hardware, the other was to be based on software in the PDP-11/23.

The first approach was to use the conventional pulse width discriminator of Fig. 1-1. This discriminator was originally developed by Vega Precision to permit a radar beacon to distinguish between interrogating pulses from the Primus 50 weather radar and undesired pulses from other X-band radars, such as marine radars, that could also trigger the beacon.

This pulse width discriminator did appear to provide some protection, say, of the order of 3 db or so; that is, distributed clutter targets some 10 db below the reflector would trigger the decoder, instead of targets 7 db below the reflector as was the case without the pulse width discriminator. This improvement was not considered ade-

Figure 1.1. Pulse Width Discriminator Initially Used.

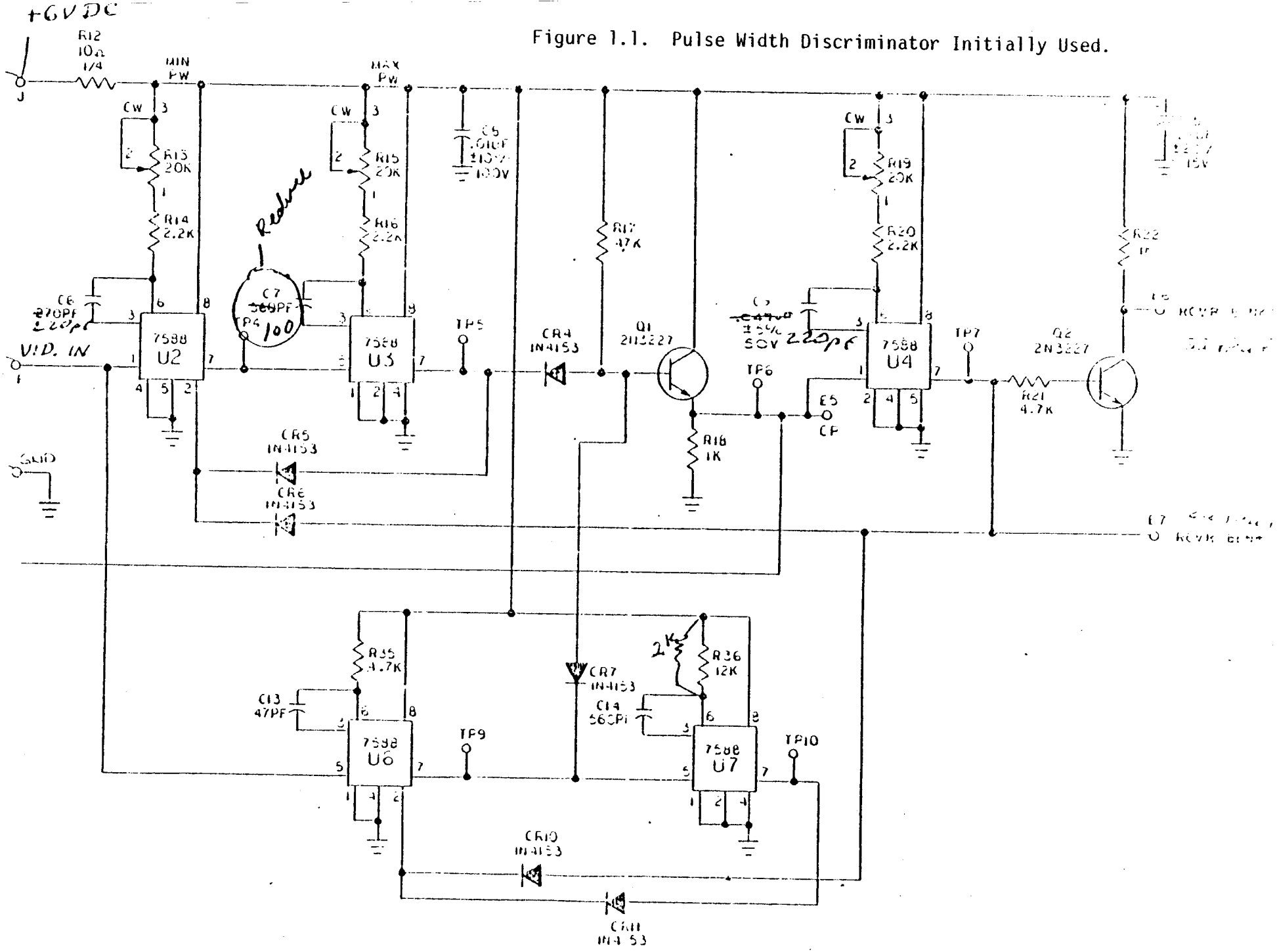

quate. It is believed that its limitations stem from the "non-linearities" in the half-amplitude detection process employed. This process would generate a signal with proper timing on the leading edge of a received echo but not on the trailing edge, i.e., the "pulse width" was not being measured properly.

Attention was therefore focused on a system that would detect both the leading and trailing edges of a pulse properly and then would use this data to suppress the undesired, or stretched pulses.

The technique utilized was quite simple and conventional. It consisted of two detectors, one of which measured the leading edge of the pulse and one of which measured the trailing edge. The reference level for detection was the same in both cases. It consisted of a delayed version of the input pulse.

The time between the leading and trailing edges was then measured and if it exceeded a prescribed amount, the echo was not validated. The tolerance used, for the data discussed later in this report, was approximately 0.3 μs, i.e., if the transmitted 0.6 μs pulse generated an echo greater than 0.9 μs, then that echo was not validated. This circuit was assembled and tested on the radar. It appeared to eliminate a great amount of the clutter.

As a next step the output of the pulse width discriminator was fed into the pulse pair decoder as shown in Fig. 1.2 and the radar was used to detect a 4'x5' dihedral reflector on the top of Peavine. A signal generator was used to simulate a second reflector as noted in Progress Report No. 1. It appeared that the combination of the pulse width discriminator and pulse pair decoder effectively eliminated all signals except that from the "coded" reflector.

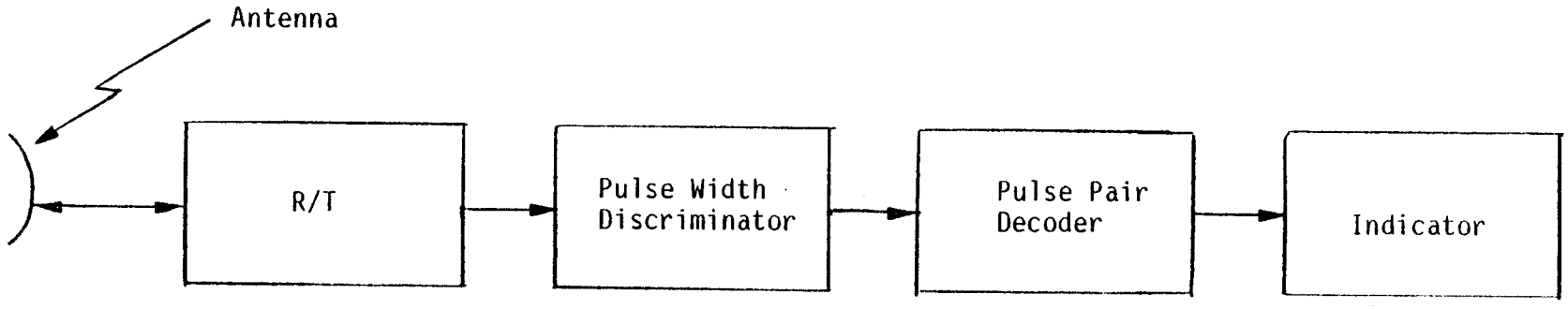

Figure 1.2. Block Diagram of Radar System Showing Addition of Pulse Width Discriminator and Pulse Pair Decoder.

It was possible to obtain false "decodes" at certain settings of the gain control, etc. These decodes, however, were "unstable" in that they were not consistent, i.e., similar from scan to scan, or equal to the beamwidth, but rather were shorter in angle. This later phenomena is probably because a target that breaks through the pulse width discriminator is a small target such as a truck, etc. and that as the beam scans such a target it is only briefly that adjacent clutter does not extend it in range, and hence prevent it from getting through the pulse width discriminator.

Based on the results of the above tests, the effort on the software pulse width discrimination effort was dropped. This effort had progressed to the point where the raw radar data had been inputted into the computer at a 10 MHz sampling rate. It was intended to use this data in the computer to implement, via software, a pulse width discriminator and associated pulse pair decoder.

As a next step, the radar was installed on the top of Peavine and two dihedral reflectors were installed at the locations B and C, noted in Fig. 1.3. This subject is discussed in the next section.

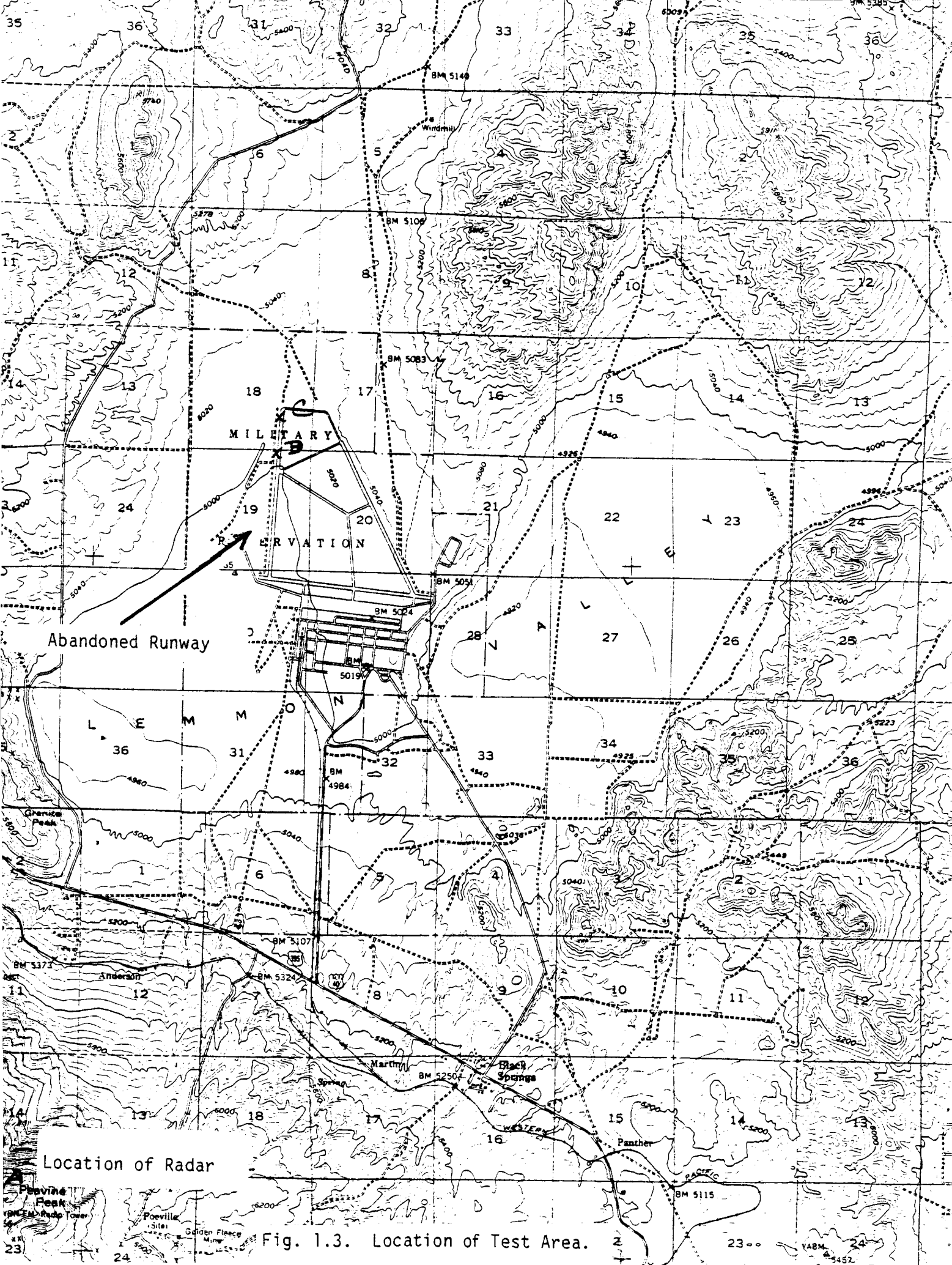

Fig. 1.3. Location of Test Area.

SECTION II. IMPROVED RADAR REFLECTORS

This effort has two parts. One is to increase the radar cross-section of the existing dihedral reflector 6 db, by installing 4'x8' plates on the 4'x4' plates of the unit. This has not yet been done for reasons noted later.

The next objective was to obtain data on the MIT (Multipath Immune Trihedral,) also called MER (Mother Earth Reflector). This was basically a determination of how smooth the ground must be in front of the two dihedral plates in order to result in a satisfactory trihedral reflector.

As part of this effort, a 4'x5' dihedral was installed at Location B of Fig. 1.3 The ground in front of the reflector was the asphalt pavement of the abandoned runway of Fig. 1.3. The results are as shown in Fig. 2.1 indicating that the reflector operated as hoped, i.e, the pavement was usable as the third plate of the reflector. Fig. 2.1 indicates that the reflector acted as a dihedral at an elevation angle of 5.1°. This is correct, based on the range of 6 miles (36,000 ft.) and the altitude of the radar of 3260 ft. above the reflector.

The dihedral became a trihedral at an elevation angle of 0°. The second reflector at location C some 2,000 ft. away, was within a db or so of the same RCS when positioned at 0° elevation.

It should be noted that the RCS at an elevation angle of 5.1° is some 46 dbsm and at 0° it becomes 49 dbsm, some 3 db greater. This is because the mirror image of the reflector effectively doubles the vertical dimensions of the unit thus increasing its RCS by 6 db.

The reflection coefficient of the earth however is not unity but varies as a function of polarization, grazing angle and surface as noted in Fig.2.2.

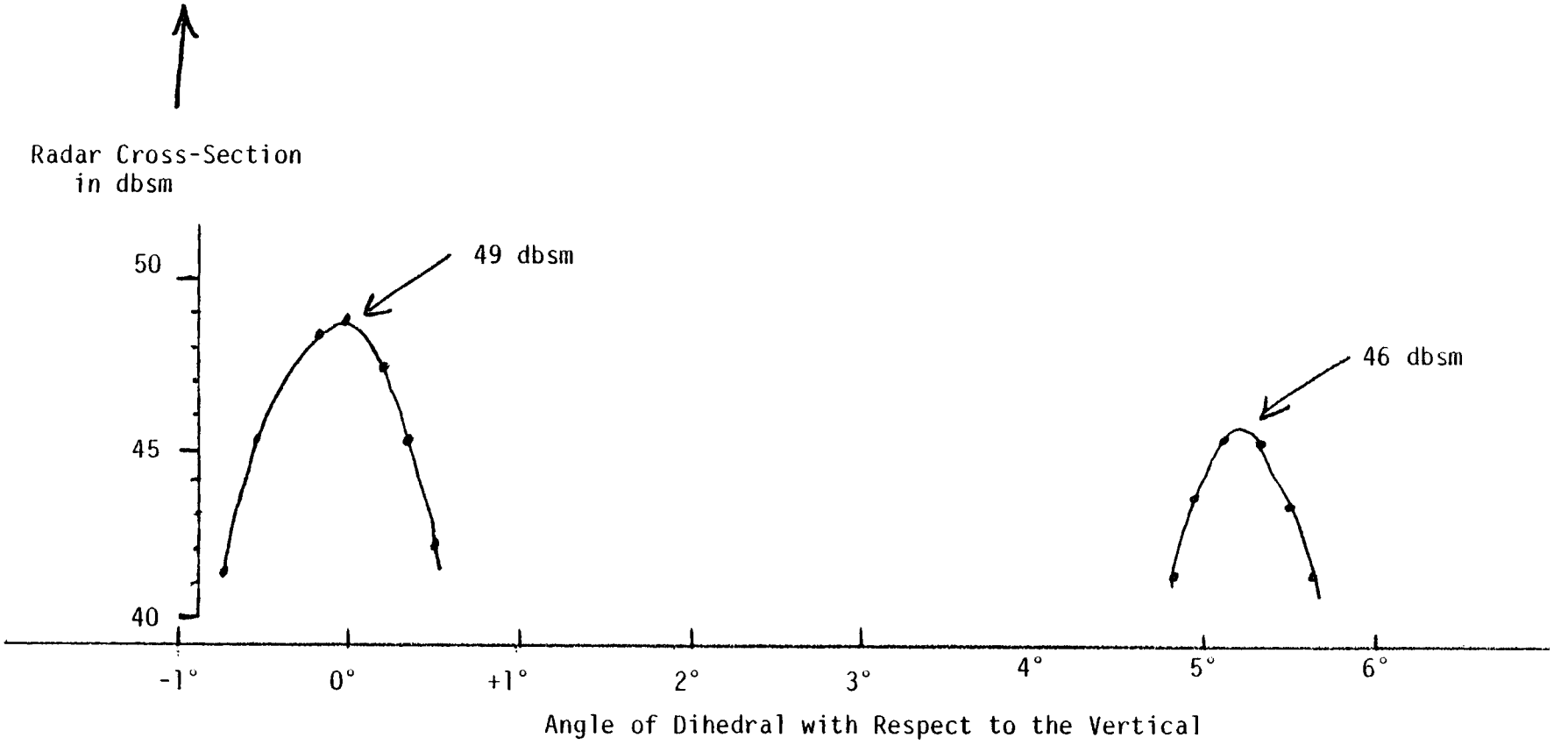

Figure 2.1. Measured Radar Cross-Section of Dihedral as a Function of Angle.

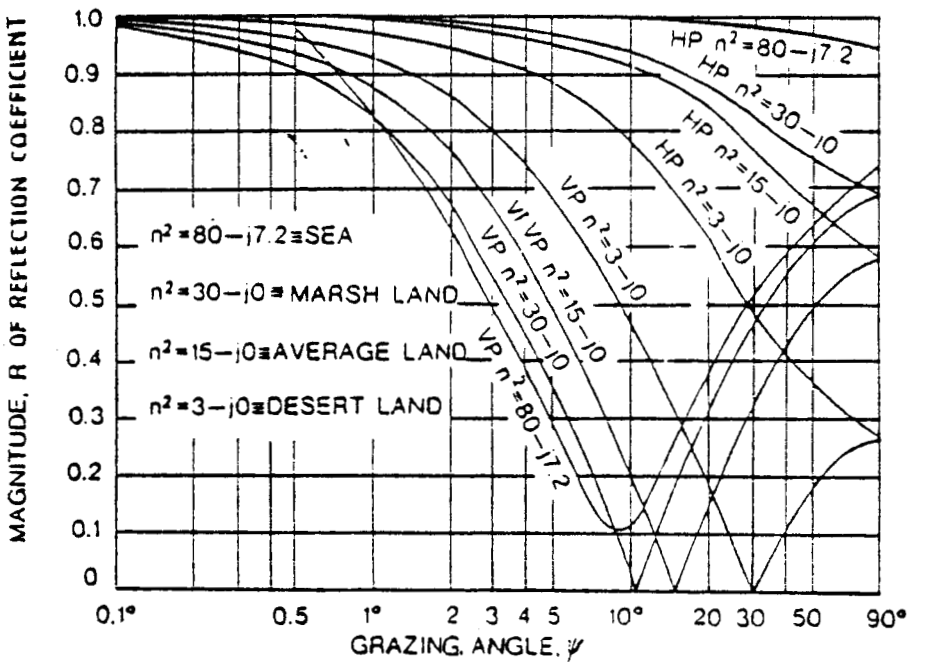

Figure 2.2(a) Reflection Coefficient as a Function of Grazing Angle and Surface.

Within the limits of experimental measurement, it appears that the reflection coefficient of the asphalt pavement for the horizontal polarization used is similar to that of the desert land of Fig. 2.2(a) and at 5°, is probably -3 db, i.e., it decreases the radar cross-section from 52 dbsm to 49 dbsm. In effect, therefore, the RCS of the dihedral reflectors have been increased 3 db without adding the larger plates.

Fig. 2.2(b) has been prepared to indicate the vertical coverage to be expected of the dihedral for the two angular settings of Fig. 2.1 where data was obtained.

When the dihedral is set at 5.1° it should provide narrow vertical coverage, i.e., it acts as a 4 ft. flat plate reflector in the vertical. This is the type of vertical coverage that is useful for providing glideslope data. Specifically, one such reflectivity pattern would be orientated above the desired glideslope and a second orientated below the desired glideslope. When the dihedral is set at 0° it becomes a trihedral with wide vertical coverage, i.e., an MIT (or MER). This is the type of coverage that is desired for locating the landing area, prior to making a precision approach. The MIT RCS, as a function of vertical angle, should be determined by the combination of the variation in coefficient of reflectivity of the horizontal asphalt surface as a function of grazing angle, which appears to act like dry desert soil and corner reflector behavior. There is one experimental point available, that at the 5.1° viewing angle from the top of Peavine. The rest of the curve is "guesstimated" based on assuming the coefficient reflectivity of desert soil of Fig. 2.2(a) for horizontal polarization. At 0° viewing angle, the coefficient of reflectivity should be 100% and the RCS should be 52 dbsm. At 45° the RCS should go to about 46 dbsm as the coefficient of reflectivity goes to 50%. Based on these assumptions, a

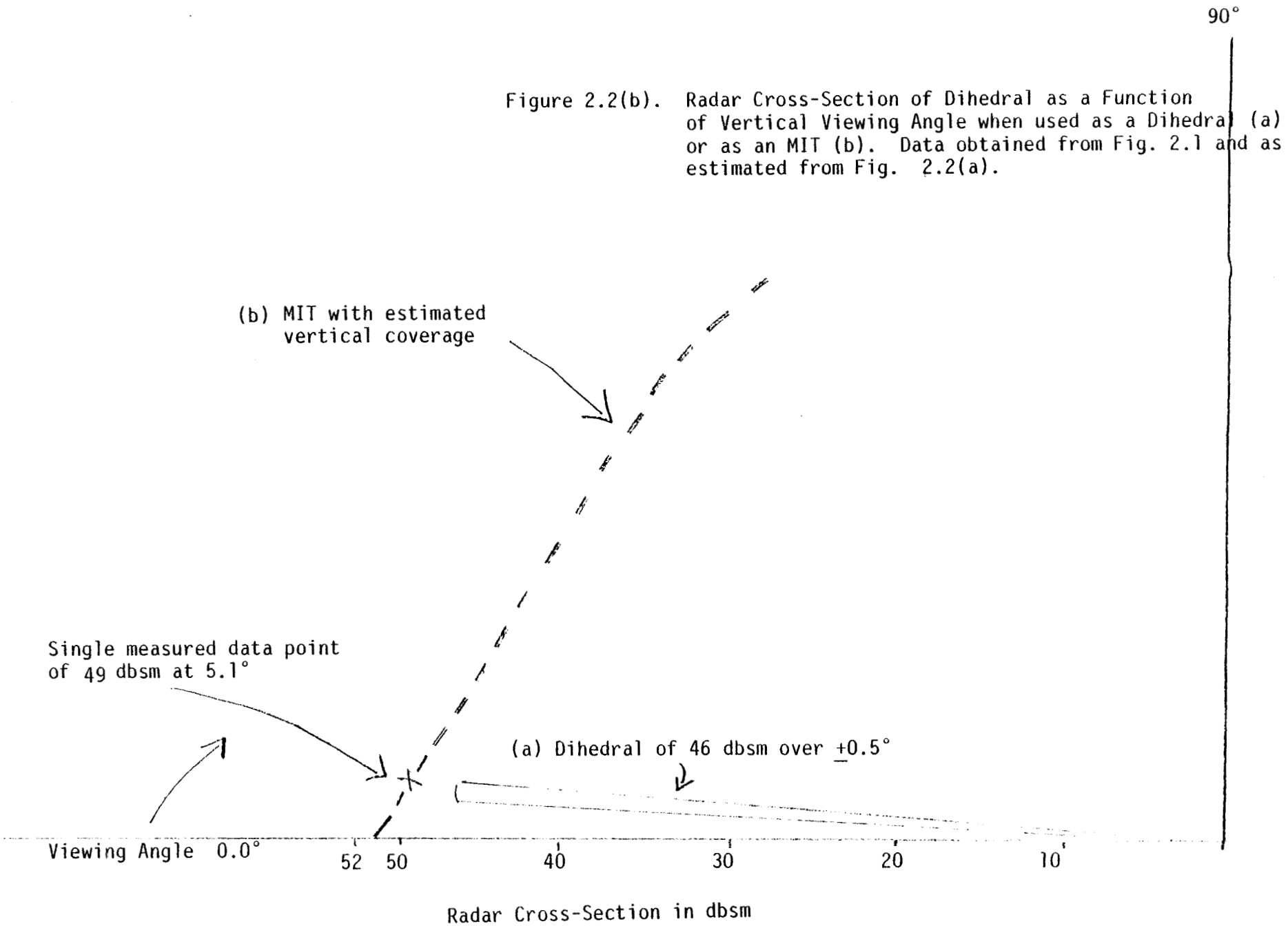

Figure 2.2(b). Radar Cross-Section of Dihedral as a Function of Vertical Viewing Angle when used as a Dihedral (a) or as an MIT (b). Data obtained from Fig. 2.1 and as estimated from Fig. 2.2(a).

"guesstimate" of the reflectivity curve is provided up to a viewing angle of 45°. In practice a viewing angle of greater than this should not be of practical interest.

Figs. 2.3(a) and (b) is a compilation of various measurements made on the dihedral at different times and locations, and a measurement made of the 18" radar antenna pattern, using the return from the dihedral on Peavine. This data is included for reference. It should be noted that the measurement procedure was rather crude, involving the use of a tiltmeter on reflectors that were positioned in vertical angle by the use of rocks, etc., sometimes in windy conditions. Communication was via a two-way radio between the radar operator, where the signal strength measurements were made and the reflector site.

A question of interest is why relatively rough pavement acts satisfactorily as one side of a trihedral reflector, when normally one tends to believe that the surface of reflectors must be held to very close tolerances, i.e., a fraction of a wavelength.

Previous test data on the multipath phenomena, such as that of Fig. 2.4, showing the variation in radar cross-section as a reflector was raised and lowered over asphalt and sagebrush, indicates that this is not necessarily the case, i.e., the "fresnel" zone for surface reflections need not be extremely smooth.

The ITT Handbook, "Reference Data for Radio Engineers," 4th Edition, 1956, p. 810-811, contains data pertinent to this topic. This reference is extracted below. It discusses a surface-based radar and an airborne target. In our case, the radar is airborne and the target is on the surface, but the analysis still applies. The criteria for surface roughness is $h_1/4$ as noted below.

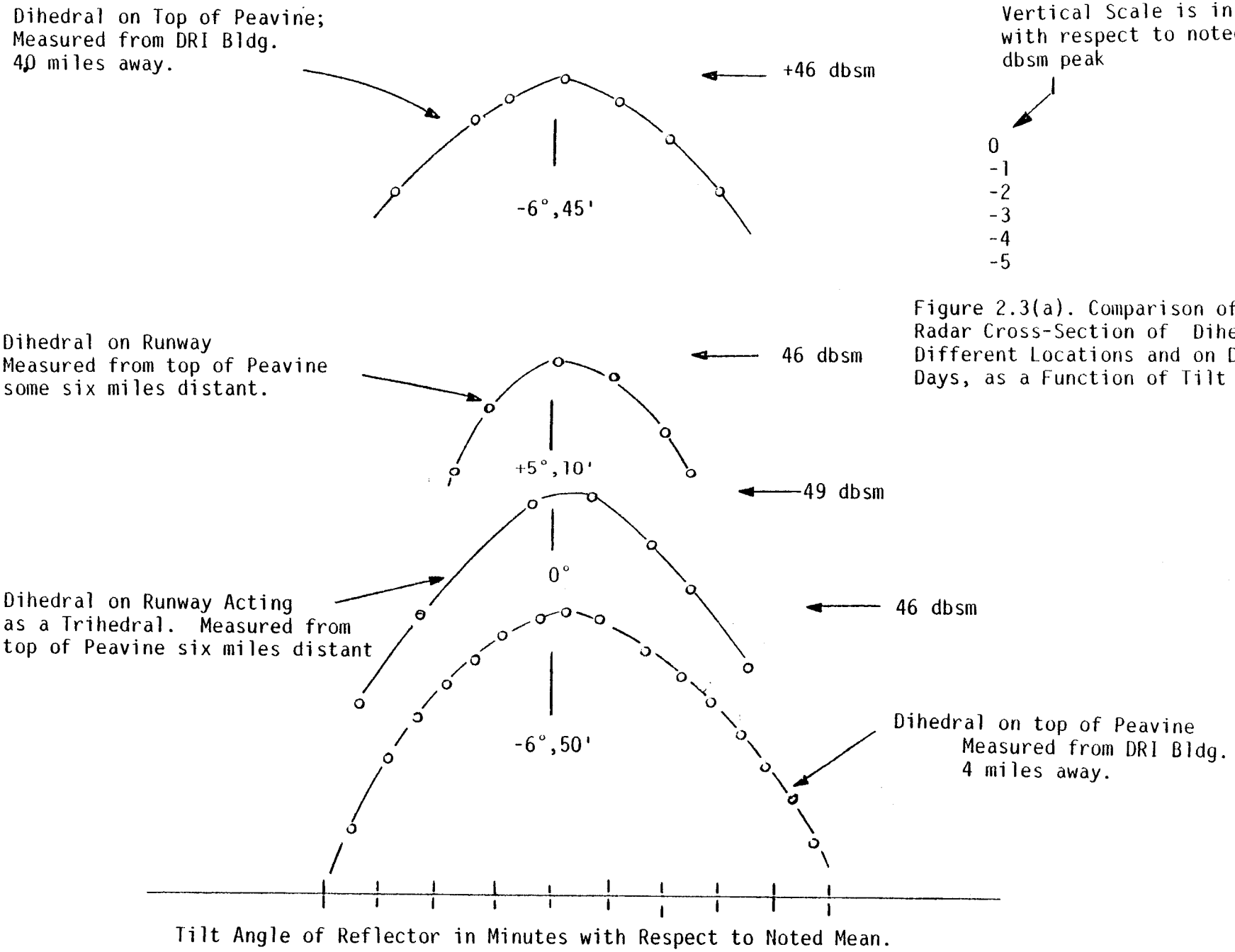

Figure 2.3(a). Comparison of Measured Radar Cross-Section of Dihedral at Different Locations and on Different Days, as a Function of Tilt Angle.

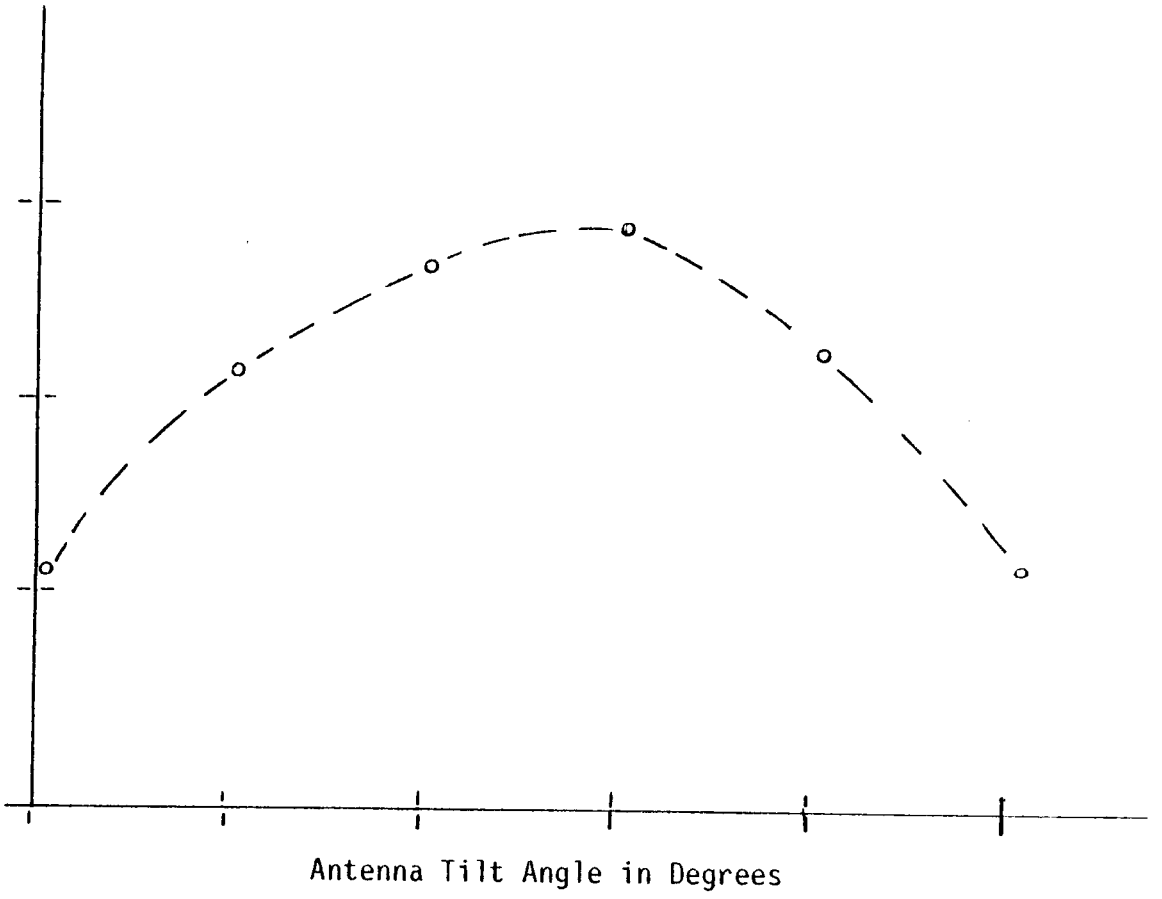

Figure 2.3(b). Antenna Pattern of 18" Flat Plate Antenna

Figure 2.4. Measured Radar Cross-Section of 24" Corner Reflector Raised from Surface to 11" and Back Down. Range 500 yards.

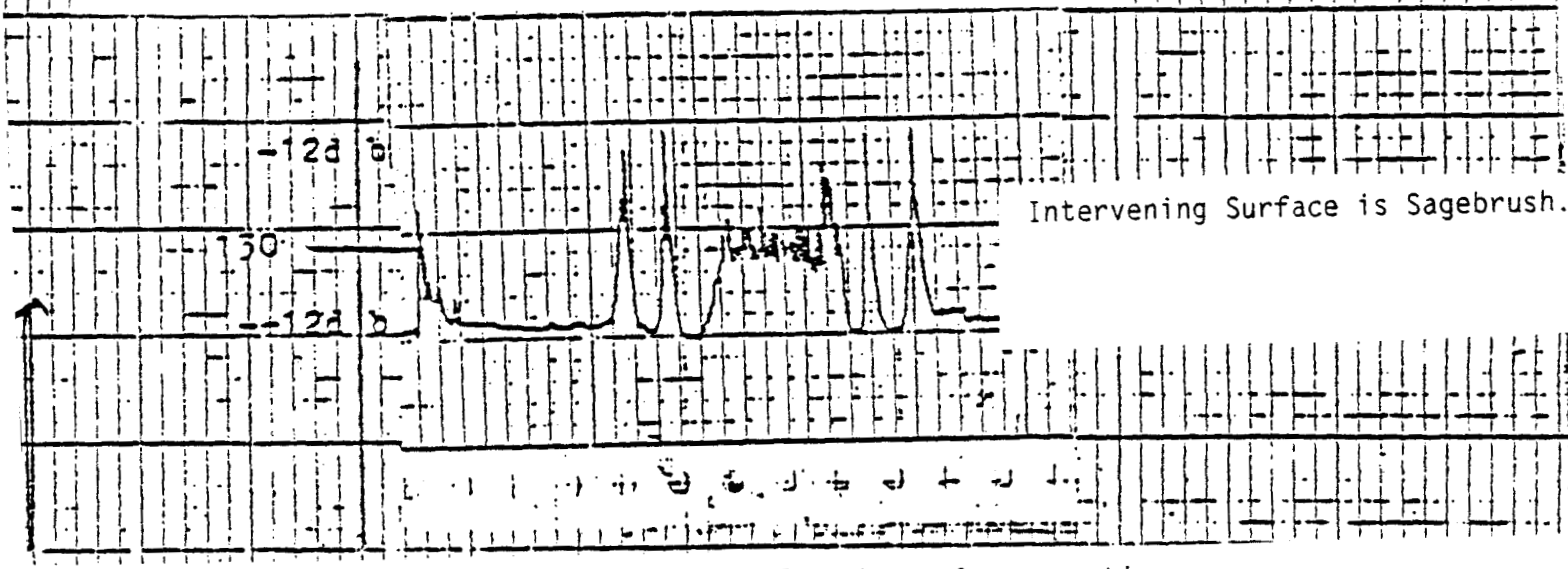

Intervening Surface is Sagebrush.

Radar Cross-Section - 24" Reflector. Free Space Cross-section is in Square Meters - 130 sq. meters.

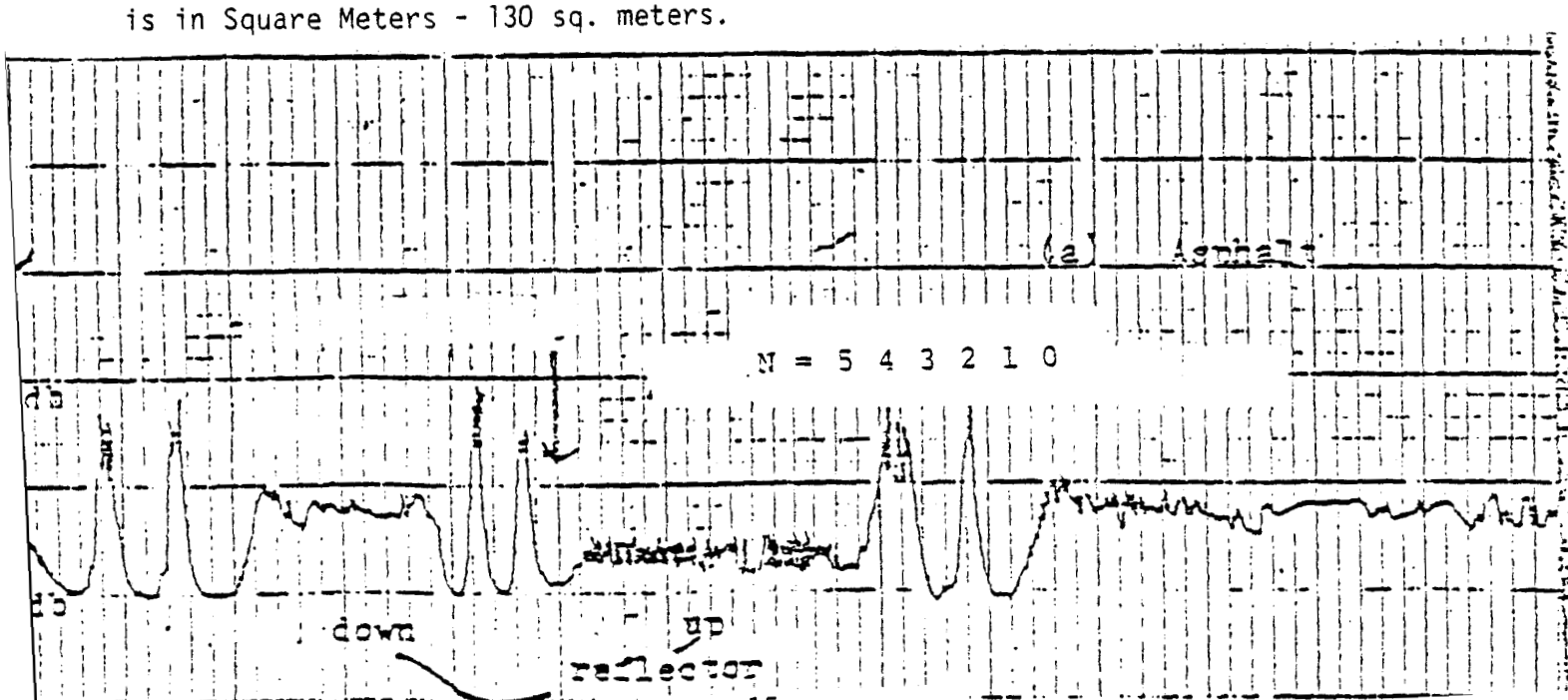

The maximum theoretical free-space range of a radar is often appreciably modified, especially for low-frequency sets, by reflections from the earth's surface. For low angles and a flat earth, the modifying factor is

$$F = 2 \sin \frac{(2\pi h_1 h_2)}{\lambda R}$$

where h_1, h_2, and R are defined in Fig. 2.5 all in the same units as λ. The result-

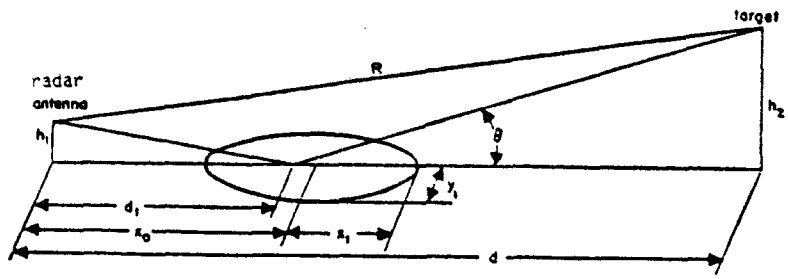

Fig. 2.5 —**Radar geometry, showing reflection from flat earth.**

ing vertical pattern is shown in Fig. 2.6 for a typical case. The angles of the maxima of the lobes and the minima, or nulls, may be found from

$$\theta_m = \frac{h_2}{R} = \frac{n\lambda}{4h_1}$$

where

θ_m = angle of maximum in radians, when $n = 1, 3, 5 \ldots$;

= angle of minimum in radians, when $n = 0, 2, 4 \ldots$.

This expression may be applied to the problem of finding the height of a maximum or null over the curved earth with the following approximate result:

$$H_2 = 44\, n \lambda D / H_1 + D^2/2$$

where

H = feet

λ = centimeters

D = miles

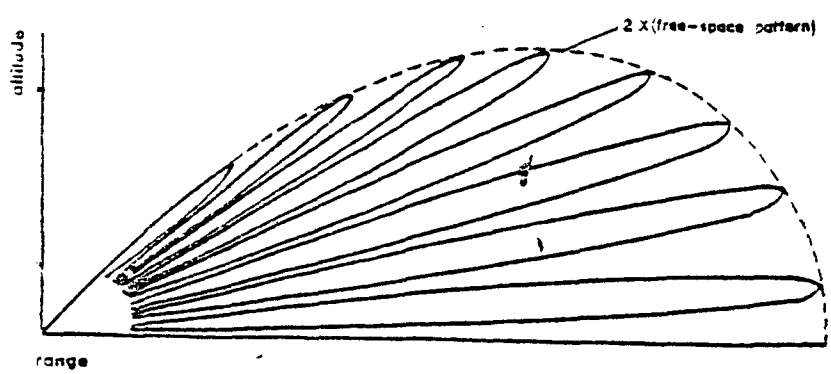

Vertical-lobe pattern resulting from reflections from earth.

Fig. 2.6

The reflection from the ground occurs not at a point, but over an elliptical area, essentially the first Fresnel zone. The center of the ellipse and its dimensions may be found from

$$x_0 = d_1(1 + 2a)$$

$$x_1 = 2d_1\sqrt{a(1 + a)}$$

$$y_1 = 2h_1\sqrt{a(1 + a)}$$

where x_0, x_1, y_1, d, are shown in Fig. 2.3 and

$$d_1 = h_1 d/h_2 = h_1/\sin\theta$$

$$a = \lambda/4h_1 \sin\theta$$

In the maximum of the first lobe, $a = 1$, and the distances to the nearest and farthest points are

$$x_0 - x_1 = 0.7h_1^2/\lambda$$

$$x_0 + x_1 = 23.3h_1^2/\lambda$$

$$y_1 = 2\sqrt{2\,h_1}$$

These dimensions determine the extent of flat ground required to double the free-space range of a radar as above. The height limit of any large irregularity in the area is $h_1/4$. If the same area is available on a sloping site of angle ϕ, double range may be obtained on a target on the horizon. In this case

$$x_0 + x_1 = 1.46\lambda/\sin^2\phi$$

Another rather simplistic way of looking at the situation is to note from Fig. 2.1 that the dihedral can be tipped $\pm$ 0.5° and still behave within a few db of maximum. Translating this to the horizontal surface one can generate Fig. 2.7 which provides an indication of the tolerance on the horizontal surface. Now the area of the horizontal surface that is actually being used, i.e., that reflects rays that, in turn, are reflected from the vertical plates extends out a significant distance in front of the vertical plates. Specifically, the ray that hits the top of the vertical plate, reflects from the ground, for a depression angle of 5°, some 45 ft. in front, (57°/5°x4'), and the

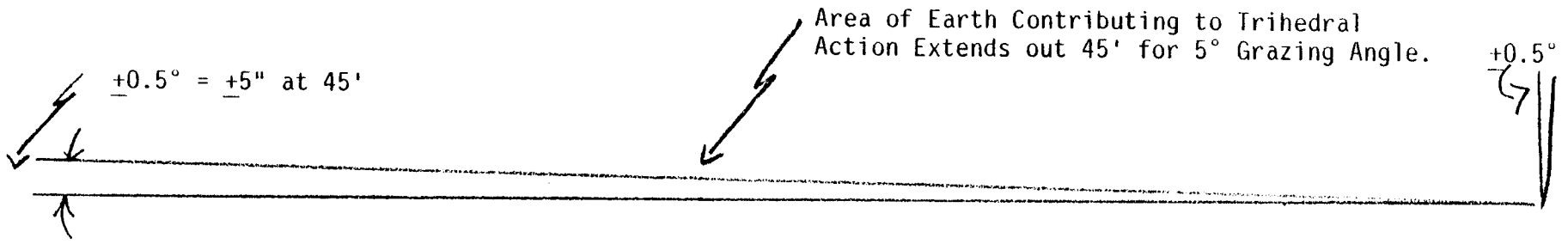

Figure 2.7. Measured Permissible Tilt in Vertical Plates of Dihedral Translated into Possible Permissible Tolerance of the Earth as a Horizontal Plate.

surface tolerance, based on a permissible angular tolerance of $\pm$ 0.5° (from Fig. 2.7) is $\pm$ 5" at that distance.

In any event, the asphalt is satisfactory and probably other surfaces are also very satisfactory.

At some future point in the program, tests should be conducted regarding this matter of acceptable surfaces for MER's. This could be readily done, over elevation angles of about 0° to about 10°, by making measurements at various altitudes on Peavine on reflectors at different locations in Fig. 1.3. The purpose of using different elevation angles is to both verify angular coverage and the effect of the variation of the coefficient of reflection of different surfaces as a function of depression angle.

The radar was next used to scan the area shown in Fig. 1.3 and the display photographed. Four photographs are of particular interest. Fig. 2.8 displays video targets some 14 db below the 46 dbsm reflector, i.e. of the order of 32 dbsm. Fig. 2.9 shows that when the decoder output is displayed, only the coded reflectors are visible.

Figs. 2.10 and 2.11 depict a similar situation except that Fig. 2.10 shows targets of 26 dbsm and greater, i.e., targets 20 db below the reflectors.

In summary,reasonably sized reflectors, when installed with an understanding of the multipath phenomena, and used with a radar employing a pulse width discriminator and pulse pair decoder appear to be quite detectable (subject to flight testing).

It can be further noted that the above test results were obtained with 4'x5' reflectors and hence another 6 db of margin is available with

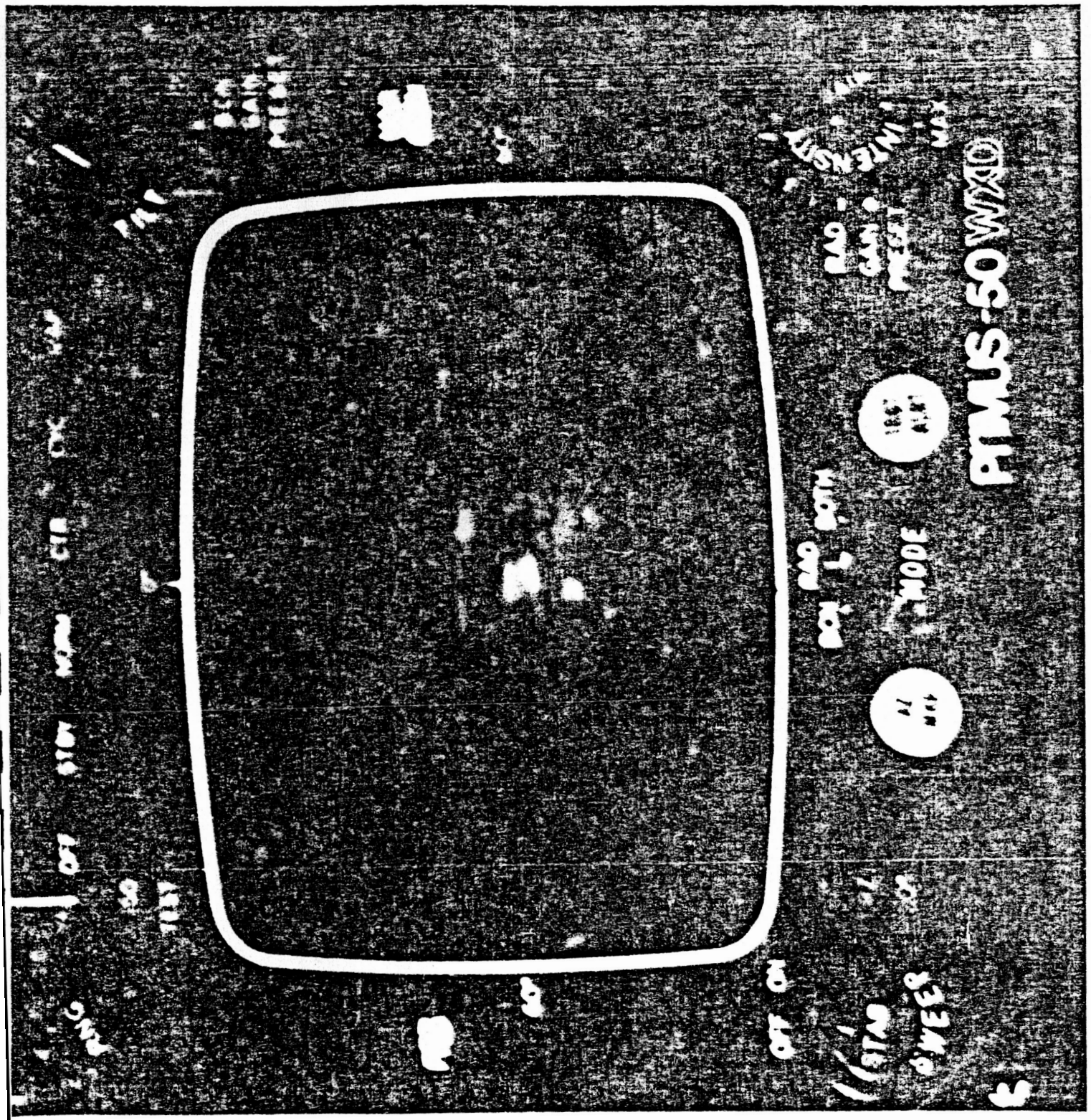

Figure 2.8. Display of raw radar video with gain set to display targets of 32 dbsm or greater. Radar on top of Peavine and reflectors as in Fig. 1.3.

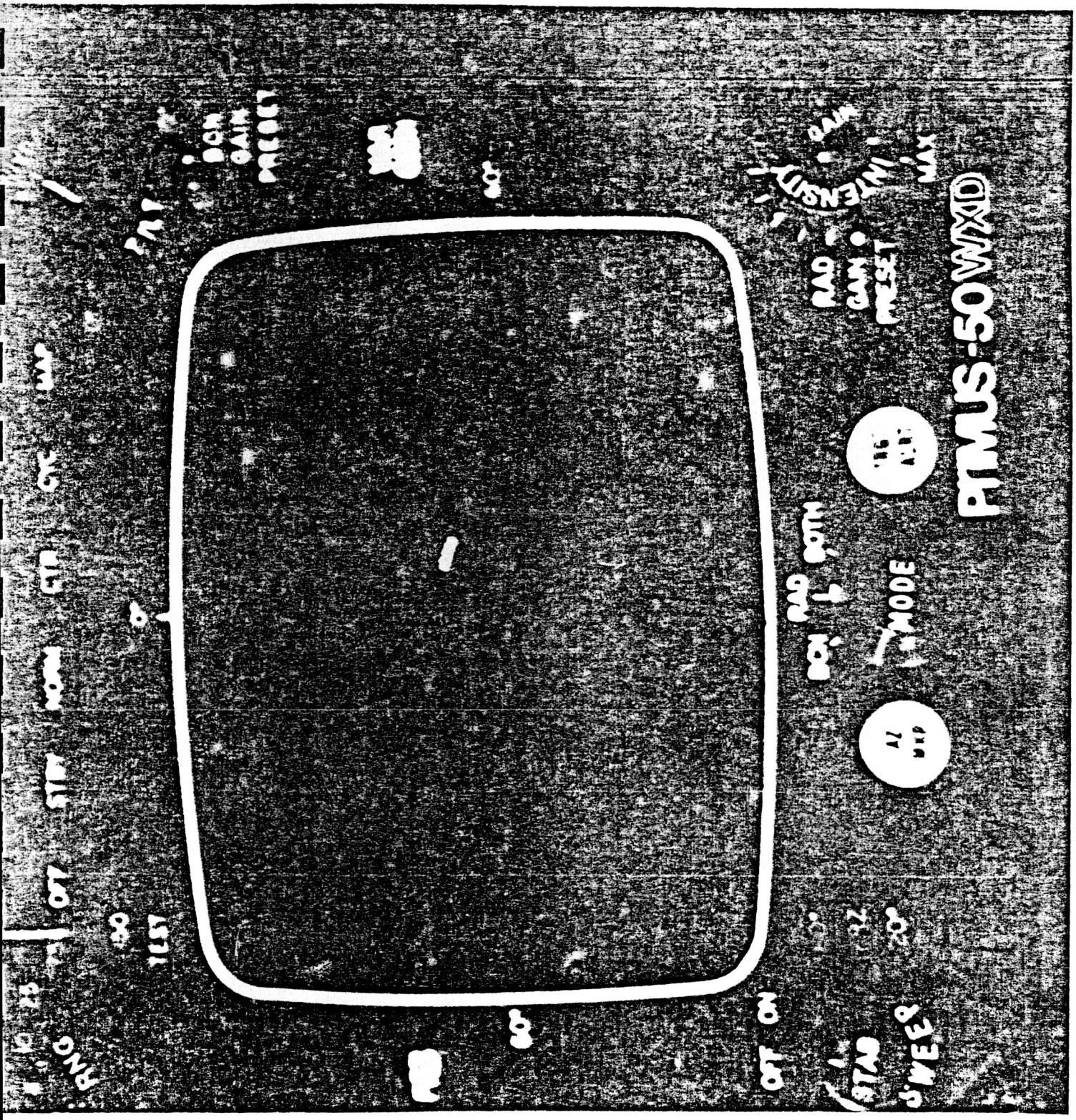

Figure 2.9. Display of output of pulse pair decoder for gain setting of Fig. 2.8. Only target displayed is the pair of coded reflectors.

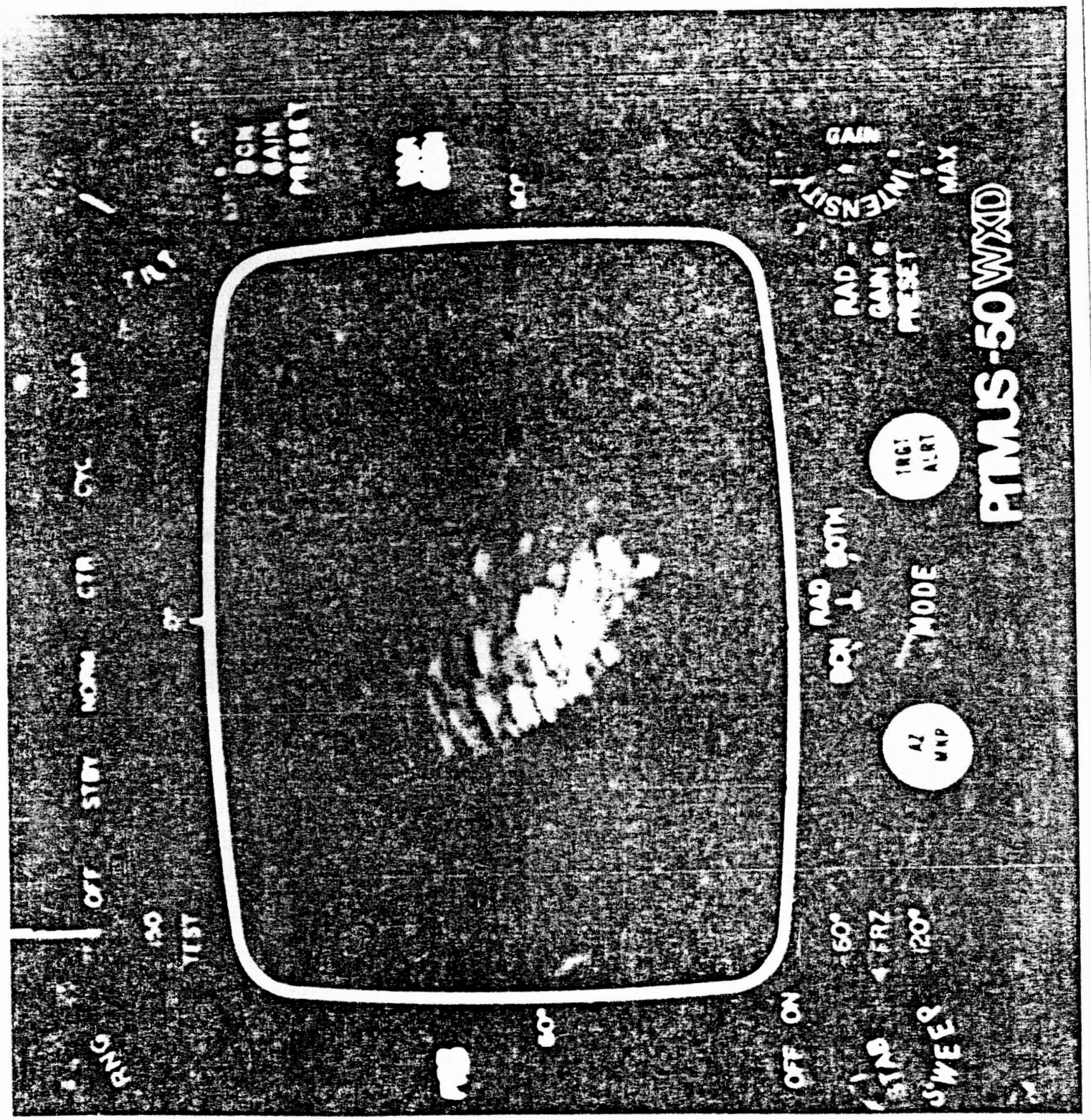

Figure 2.10. Display of raw radar video with gain set to display targets of 24 dbsm or greater. Test configuration as in Fig. 1.3.

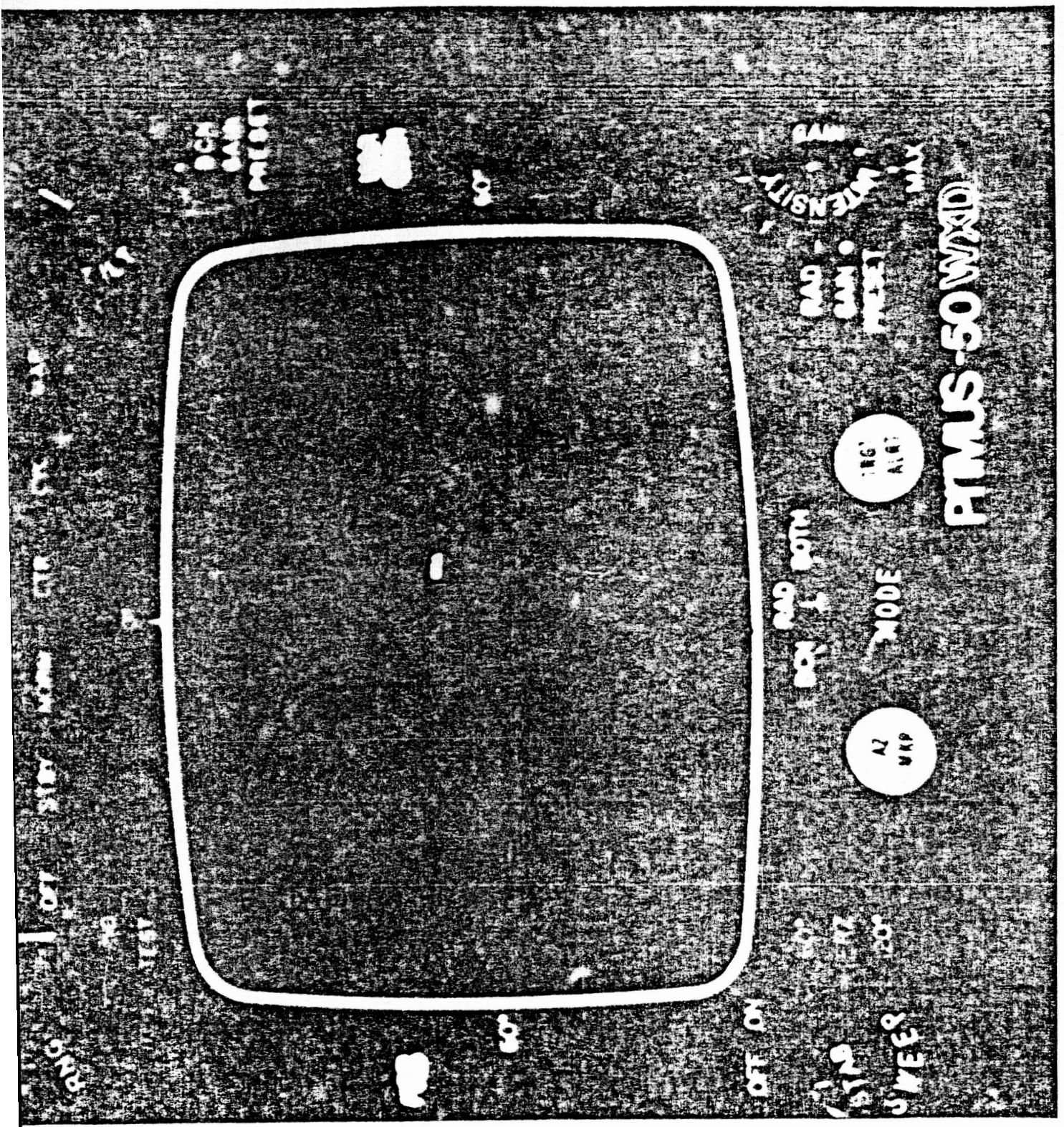

Figure 2.11. Display of output of pulse pair decoder for gain setting of Fig. 2.10. Only target displayed is the pair of coded reflectors.

the 4'x10' reflectors. In addition, another 10 db of margin is probably available with a shorter pulse, i.e., 0.06 microseconds. In other words, the results look promising in terms of building "practical" electronics that can reliably detect practical corner reflectors in clutter.

In effect, while numerous targets get through the pulse width discriminator, i.e., vehicles, small buldings, etc., the decrease in the number of such targets is sufficiently great that the probability of two such targets breaking through the decoder is very low.

It should be noted that this performance was achieved in the presence of several limitations of the present circuitry which limitations are not fundamental, i.e., they can be readily overcome.

One limitation is that the log receiver in the Primus 50 unit has a limited dynamic range and is not too linear (see Fig. 2.12). This performance tends to "squash" strong signals and thus stretch them, thereby limiting either the dynamic range over which the pulse width discriminator will operate on a return from a corner reflector, or requiring that the pulse width "tolerance" be set wider, i.e., more distributed clutter gets through.

This limited dynamic range tends to make it desirable that the area immediately surrounding the targets be reasonably clutter-free, i.e., adjacent targets will produce the same intensity "echo" as the reflectors if limiting occurs, further aggravating the problem. Fig. 2.13 depicts the performance of a state-of-the-art logarithmic receiver.

Another current circuit deficiency is that the comparators used in Fig. 1.2 have a very slow response, i.e., of the order of 0.2 micro-

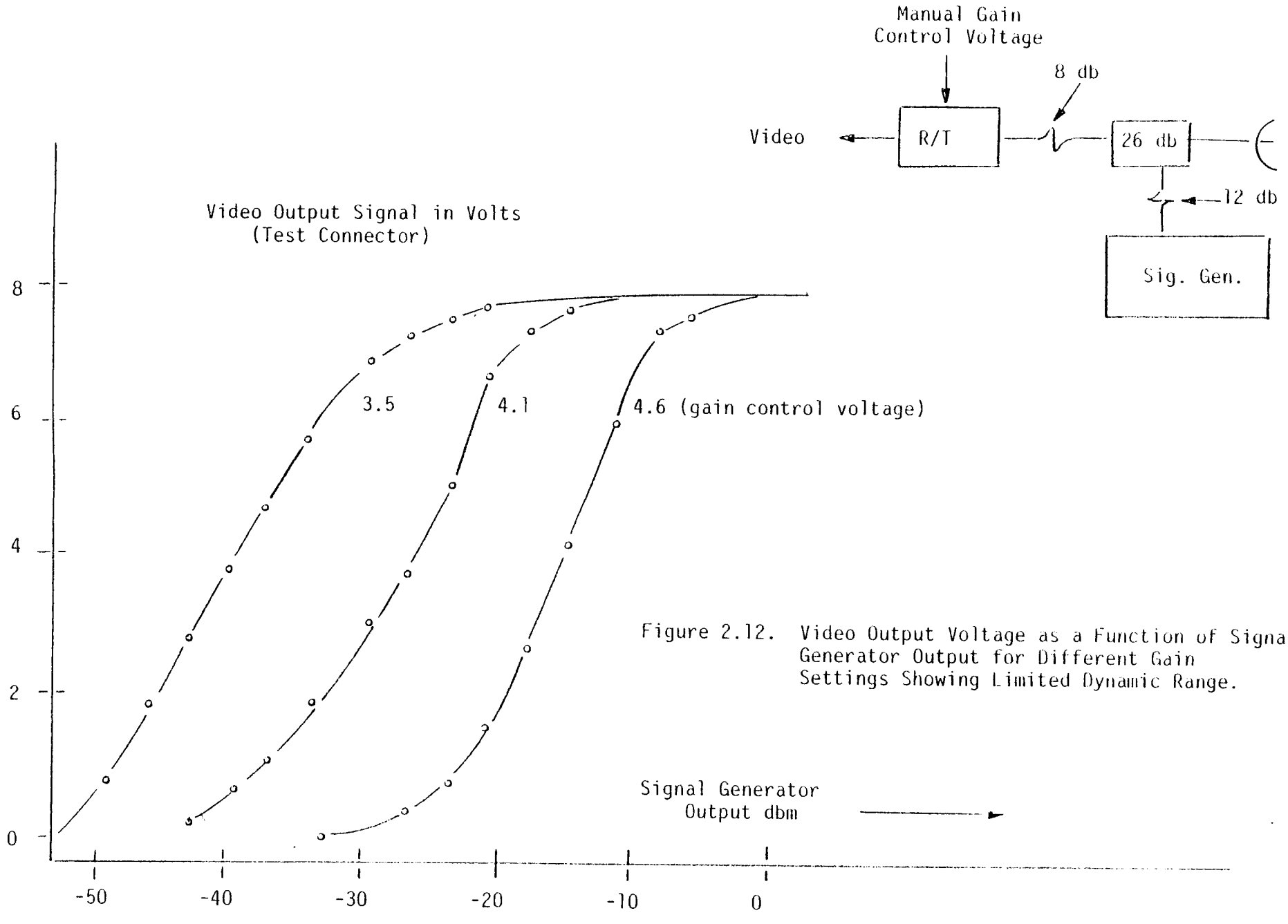

Figure 2.12. Video Output Voltage as a Function of Signal Generator Output for Different Gain Settings Showing Limited Dynamic Range.

LOGARITHMIC IF AMPLIFIERS

Figure 2.13.

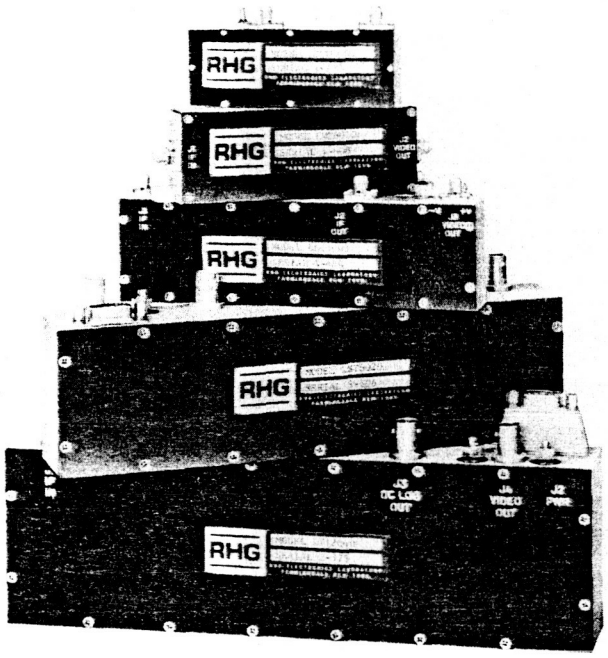

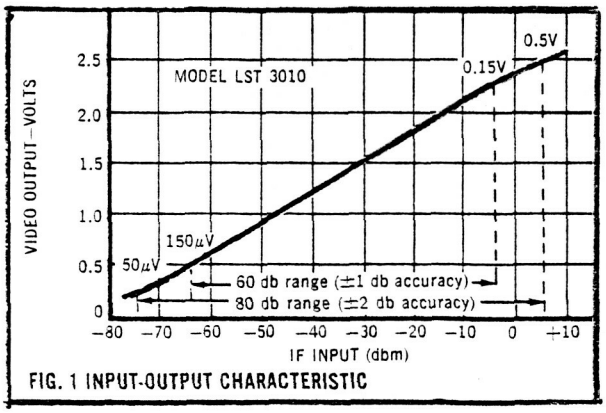

FIG. 1 INPUT-OUTPUT CHARACTERISTIC

Recent developments in radar and communications systems engineering have greatly increased the demand for logarithmic IF amplifiers of all descriptions... and only at RHG is such a wide variety available... with most models "off the shelf." This bulletin lists RHG's line of standard log amplifiers. You will find standard and IC models, center frequencies from 10 to 200 MHz, and bandwidths from 2 to 100 MHz to handle pulse risetimes down to 10 nanoseconds. In short, RHG log amplifiers fill every need, and if the model needed for your application is not there, RHG will design and build it for you. Fully 30% of current orders are for special RHG units built to custom specifications... your special requirements may be on file in our library now.

RHG logarithmic IF amplifiers are compressing type amplifiers whose output is proportional to the logarithm of the input. The successive detection technique utilized is a highly advanced differential amplifier configuration developed by RHG. Each amplifier "stage" consists of two matched high frequency transistors. One of these acts as a saturating IF stage. As it saturates, the current is transferred to the video transistor "half" of the "stage." These video currents are then summed to produce the resultant output.

This technique results in unprecedented stability, accuracy, and pulse fidelity. Units stable and accurate to ±0.25 db have been built and delivered. Direct coupled video to process CW and very long pulses as well as extremely high pulse fidelity is also provided.

The use of the RHG log test set allows accurate alignment and matching on a dynamic basis. Details of this test set, now available to RHG customers, are shown on the following pages.

Figure 1 shows a typical transfer curve of a log amplifier. Note that input signals from –80 to 0 dbm may be accommodated and will provide an output which is compressed so that it varies from 0.25 to 2.5 or 20 db. Note also that ±1 db accuracy is obtained over a 60 db portion of that range and that the average slope of the transfer characteristic is equal to 27 mv per db.

seconds instead of the desired 0.04 microseconds. The 0.2 microsecond units were used becuase they were available. Replacement units have been ordered and will be used in flight.

SECTION III. WORK FOR THE NEXT PERIOD

Based on the results of the tests from the top of Peavine, it has been decided to fly as soon as possible. The following is required in this connection:

A. Fabricate a flyable pulse width discriminator and decoder. This will be done in Reno.

B. Check out the wiring, etc. in the Lear. This will be done at Ames during this period.

C. Finalize the instrumentation system and prepare it for flight.

D. Possibly fabricate eight 2'x5' dihedral reflectors to outline the runway for the flight test program.

PROGRESS REPORT NO. 3
(Summary Report)

Period Covered: October 1 - November 1, 1980

Weather Radar Approach System
(WRAPS)

Prepared by

Dave Anderson/John Bull
Ames Research Center
National Aeronautics and
Space Administration
Moffett Field, CA

John Chisholm
Atmospheric Sciences Center
Desert Research Institute
P.O. Box 60220
Reno, NV

NASA-Ames Cooperative Agreement
No. NCC 2-88

and

DRI ACR No. 1-6-220-6909-001

December 1980

TABLE OF CONTENTS

ABSTRACT

WRAPS is a cooperative program between NASA Ames and the Atmospheric Sciences Center of the DRI, University of Nevada system to determine the utility of the airborne weather radar, operating in conjunction with ground-based radar reflectors, to act as an appraoch aid.

This report covers the fabrication, and airborne installation of the first flight version of WRAPS and the flight test of that equipment. It is also a summary report, including recommendations for future efforts.

The flight test effort can be considered successful. Specifically, on the morning of October 28, 1980, two coded reflectors, that is twoi reflectors spaced a known amount, were installed at the approach end and two coded reflectors were installed at the departure end of Runway 16 at Cannon International Airport, Reno, Nevada.

On the last of the three passes on that morning, the reflector sets continuously generated the only targets visible on the weather radar display from a range of five miles to one mile. A typical display is provided in the frontispiece. The radar controls on this pass were untouched from the previous pass. The radar system was an unmodified RCA Primus 500, except for the insertion of a pulse width discriminator/ pulse pair de3coder int he vidso cable between the R/T and indicator.

It is believed that the WRAPS flight test program has demonstrated that a ground-based reflector system, designed and installed with an understanding of the radar reflectivity environment typical oif airports can be detected by an airborne radar of the weather radar type, and can provide guidance data suitable for approached.

Primus 50 weather radar display on final approach to Cannon International Airport, Reno, NV. Only targets visible are the decoded returns from a pair of coded reflectors at the approach end of the runway and a pair of coded reflectors at the far end of the runway.

Frontespiece

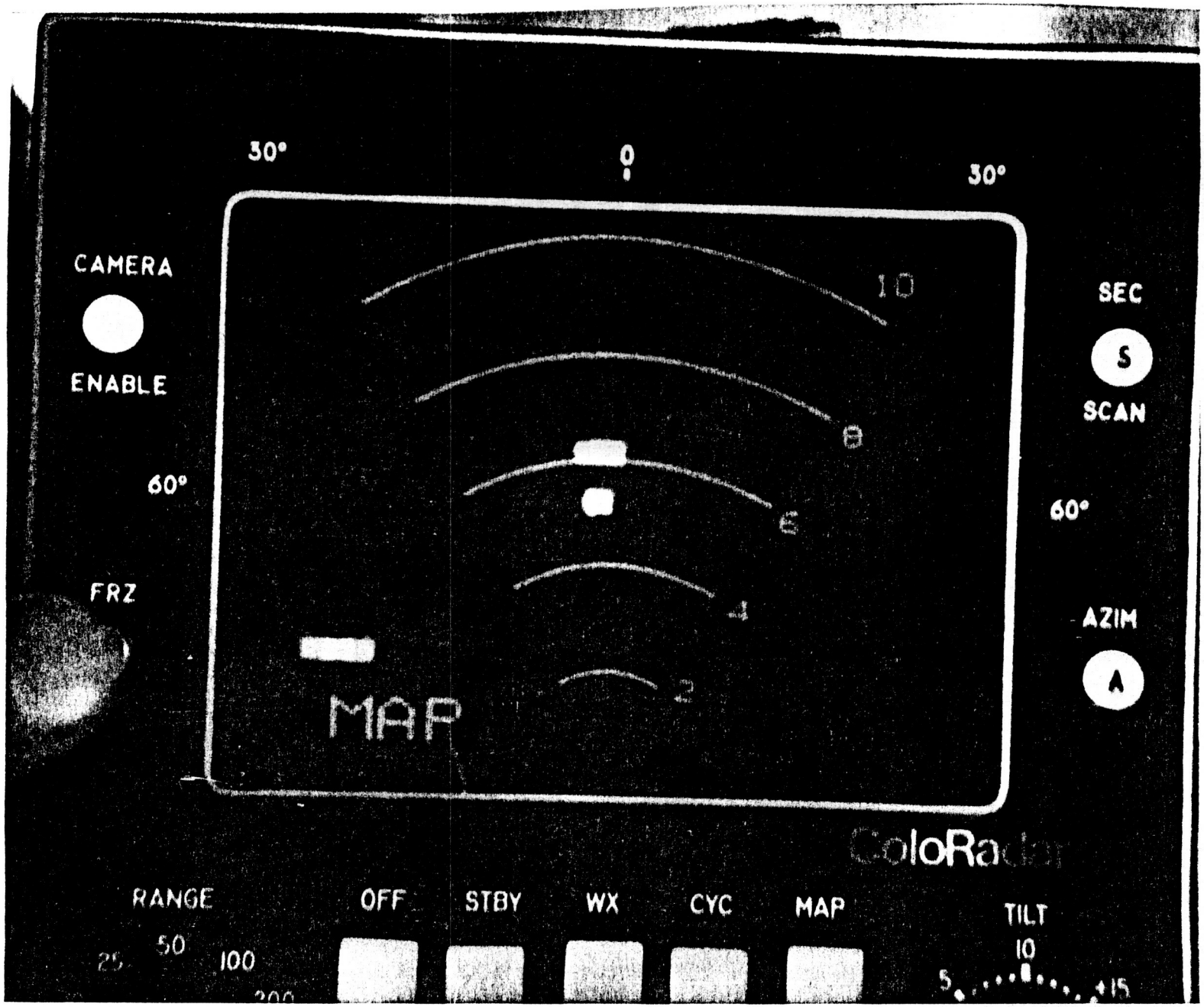

It is further believed that an improved reflector/weather radar system can possibly provide precision approach guidance data comparable to that provided by some existing precision approach landing aids. It is recommended that certain improvements outlined in this report be incorporated into the WRAPS system and that the improved system be flight tested to provide quantitative data on the performance of WRAPS as a non-precision and/or precision approach aid.

SECTION 1. FABRICATION AND INSTALLATION OF WRAPS FLIGHT TEST SYSTEM

(a) General

At the conclusion of successful ground-based testing of the WRAPS concept as discussed in Report No. 2, it was decided to flight test the system.

The flight test program was to utilize a rather elaborate instrumentation system, as described in Progress Reports No. 1 and 2. The instrumentation system was not used for the following reasons.

In early September it was realized that WRAPS system performance would be marginal and flight testing would probably not be justified unless circuitry could be incorporated into the system that distinguished the echo associated with a corner reflector from the echoes associated with distributed clutter. The most promising recognition technique appeared to be the use of a pulsewidth discriminator, based on its performance on other programs. All available personnel therefore focused on the fabrication of such a device since flight testing had to take place within several weeks. This meant that all work on the instrumentation system stopped.

A pulse width discriminator was fabricated and tested from the top of Peavine Mountain in late September. It appeared to solve the distributed clutter problem and hence attention again focused on the flight phase of the program. At this time, the project was notified that the availability of the test aircraft had changed from the last two weeks in October to only the third week in October. On this basis, project personnel had to again concentrate on fabricating a flight version of the pulse width discriminator/pulse pair decoder to the

exclusion of work on the instrumentation system. This decision to forego the instrumentation system was not considered a critical one at this time since the basic purpose of the instrumentation system was to provide data as to why WRAPS did not work and, at this time, there was every indication that WRAPS would work quite well. The subsequent success of the flight test program schedule, indicates that the decision was valid.

(b) Airborne Equipment

The WRAPS flight test equipment is outlined in block diagram form in Figure 1.1.

The system is basically an unmodified RCA Primus 500 radar except for the insertion of a pulse width discriminator/pulse pair decoder (P^3D^2) between the R/T unit and the indicator.

A Primus 500 consists of a standard RCA antenna and pedestal, a standard Primus 50 R/T with 0.6 and 2.35 μsec capability and a Primus 400 color indicator with added short range display capability (2.5 miles). The antenna utilized was a standard 12" flat plate antenna.

(c) Airborne Installation

The test aircraft utilized was a NASA Ames Lear Jet. This NASA aircraft normally carries a Primus 400 weather radar with a 12" antenna.

In the flight test configuration, the 12" antenna installation was left, but the Primus 50 R/T antenna was directly substituted for the 400 R/T unit. In addition, the cabling to the pilots 400 indicator was jumpered to the test rack in the cabin where the 500 indicator was installed. The pulse width discriminator/pulse pair decoder was also installed in this test rack as shown in Figure 1.2(a),(b) and (c). It was inserted in the video cable between the R/T unit and the indicator.

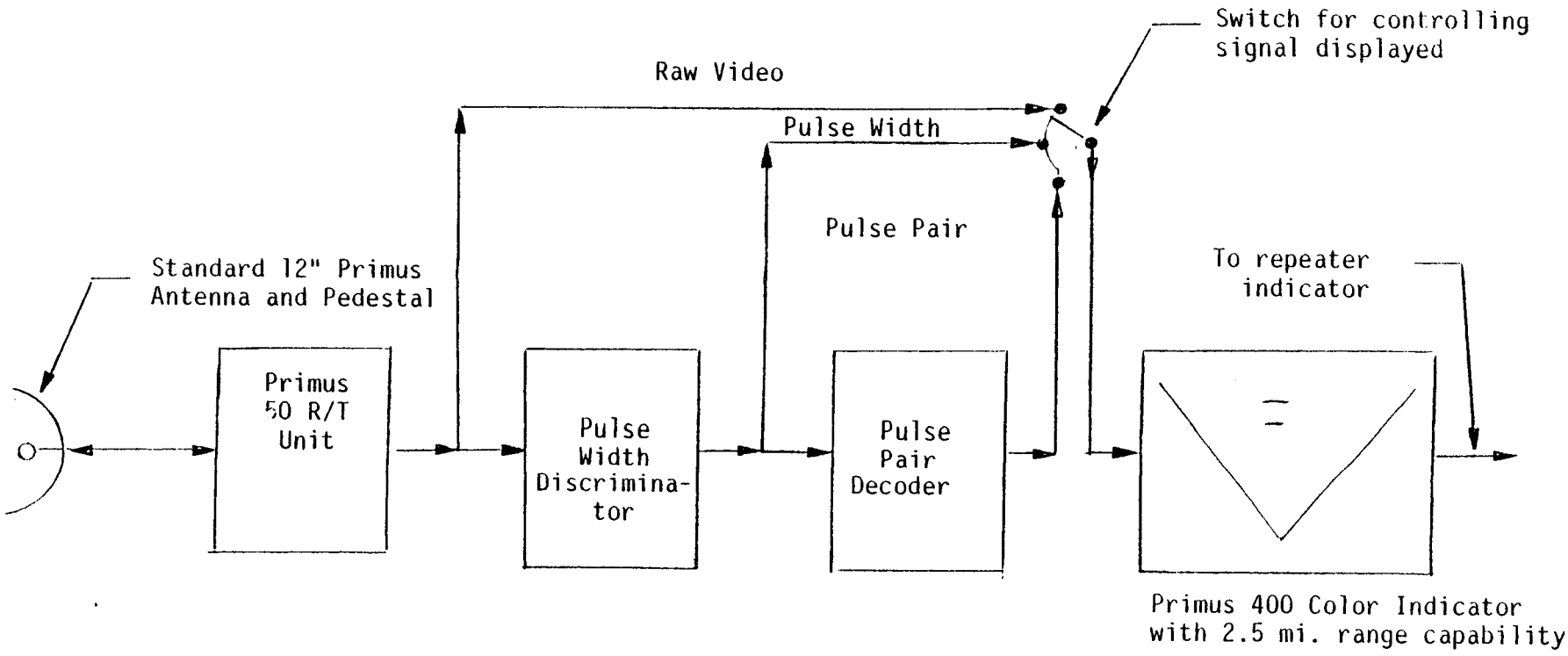

Figure 1.1. Primus 500 Radar System used in Flight Test.

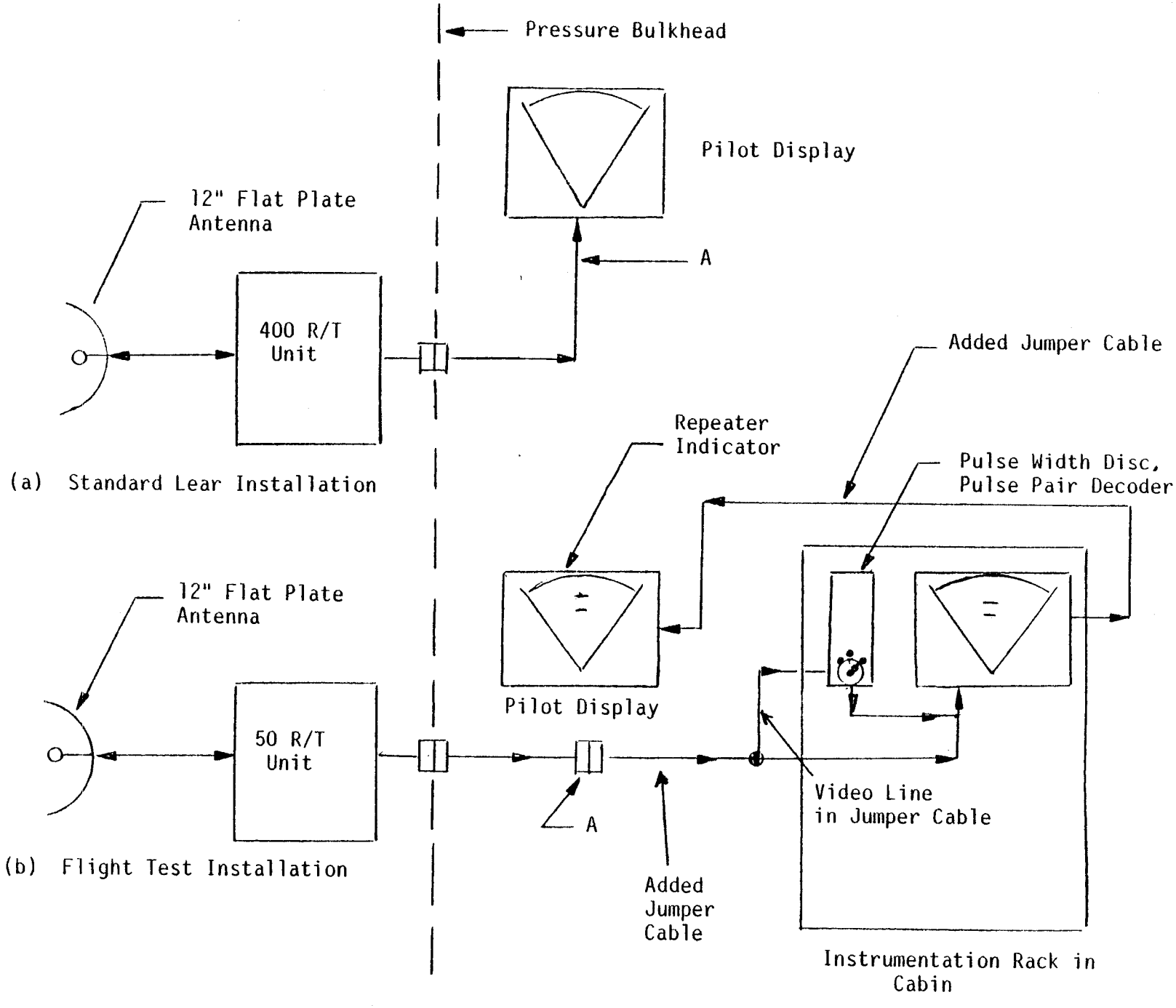

Figure 1.2(a) Block Diagram of Aircraft Installation.

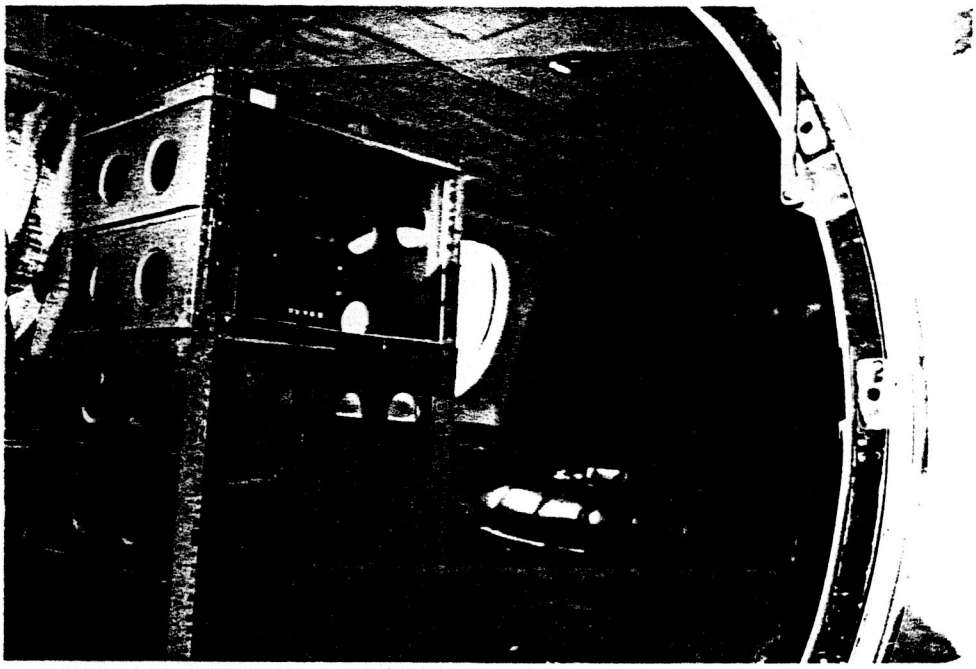

Figure 1.2(b). Installation of instrumentation rack containing indicator and pulse width discriminator/pulse pair decoder in cabin of Lear Jet.

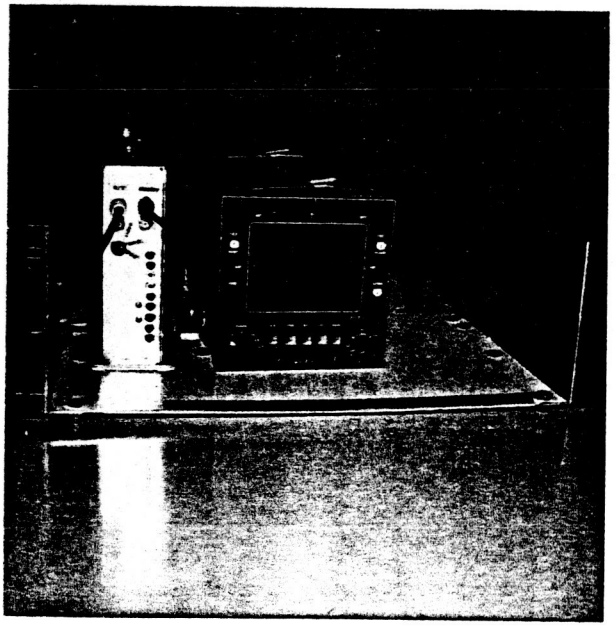

Figure 1.2(c). Installation of pulse width discriminator/pulse pair decoder in instrumentation rack.

A 500 repeater indicator was installed in the pilot's panel in the 400 indicator space. It was connected to the 500 indicator via a jumper cable as shown in Figure 1.2.

A Polaroid SX-70 camera was mounted in front of the rack to obtain data such as that of the frontispiece. The test rack was provided by the Medium Altitude Mission Branch of NASA Ames. All equipment installation was also performed by that Branch in an extremely short period of time.

(d) Pulse Width Discriminator/Pulse Pair Decoder (P^3D^2)

As noted in Progress Report No. 2, the P^3D^2 device effectively eliminated all targets except coded corner reflectors; that is, coded point targets of large radar cross section. It was thus decided to fabricate a flight version of the P^3D^2 unit and then to flight check the WRAPS system in a qualitative way, i.e., would the reflectors be detected and how reliably, etc.

A decision was also made to generate three types of display on the indicator: normal video, pulse width discriminator output, and pulse pair decoder output. In addition, it was decided to stretch the signal output of the pulse width discriminator and pulse pair decoder in order to increase their visibility on the display. The block diagram of this arrangement is shown in Figure 1.1.

The pulse width discriminator, as used, had a discrepancy in that the leading and trailing edge comparators triggered at signal levels differing by 4 dB. Time did not permit this unbalance to be corrected. An additional problem arose in connection with the P^3D^2 unit in that the R^4 correction in the R/T unit was set to operate only from 0.5 to 5

miles (40 dB), since at the beginning of the program, it was not visualized that flight testing on final would extend beyond five miles. Actual flight testing extended from 20 miles to one mile.

This increased range requires an extra 24 dB of receiver dynamic range. This extra 24 dB of required dynamic range, coupled with a probable 10 dB variation in reflector cross-section between the four installed reflectors, as discussed below, coupled with only the 20 dB of dynamic range of the radar receiver (Figure 2.12 of Report No. 2) mandated the use of manual gain control on flights from 20 miles on in. In addition, it dictated that the pulse width discriminator tolerance for target validation be rather wide to preclude invalidation of corner reflector returns under changing flight conditions; that is, under changing signal strength conditions that would exceed the 20 dB dynamic range of the receiver and hence result in stretched echoes. The tolerance was set for 1.2 μsec in contrast to the 0.9 μsec used in ground testing. The radar pulse width was 0.6 μsec.

(e) Ground Based Reflector System

Four reflectors were utilized. They consisted of two trihedral reflectors of Figure 1.3 and two dihedral reflectors of Figure 1.4. Both types of reflectors were utilized as trihedrals (MITS) with the earth as the third side. In this connection it should be noted that the horizontal plate of the trihedral of Fig. 1.3 is not a contributing factor in its reflective action. Rather it is the earth extending some 100 ft. or more in front of the reflector that forms the third plate. The theoretical radar cross-section of the reflectors is about 57 dBsm for the trihedrals and 52 dBsm for the dihedrals based on a perfect

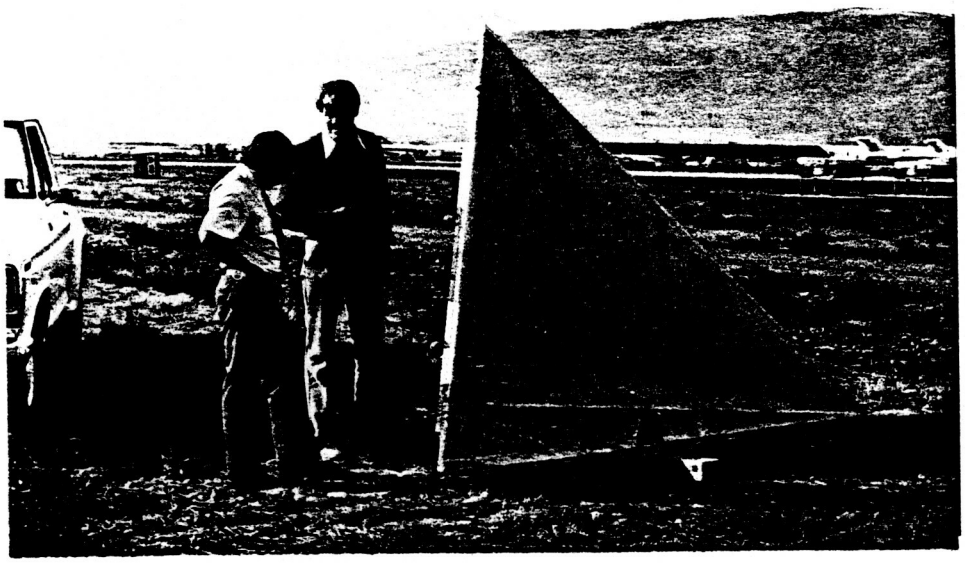

Figure 1.3. Trihedral reflector used as a M.I.T. in flight test. Note inclinometer used to level reflector.

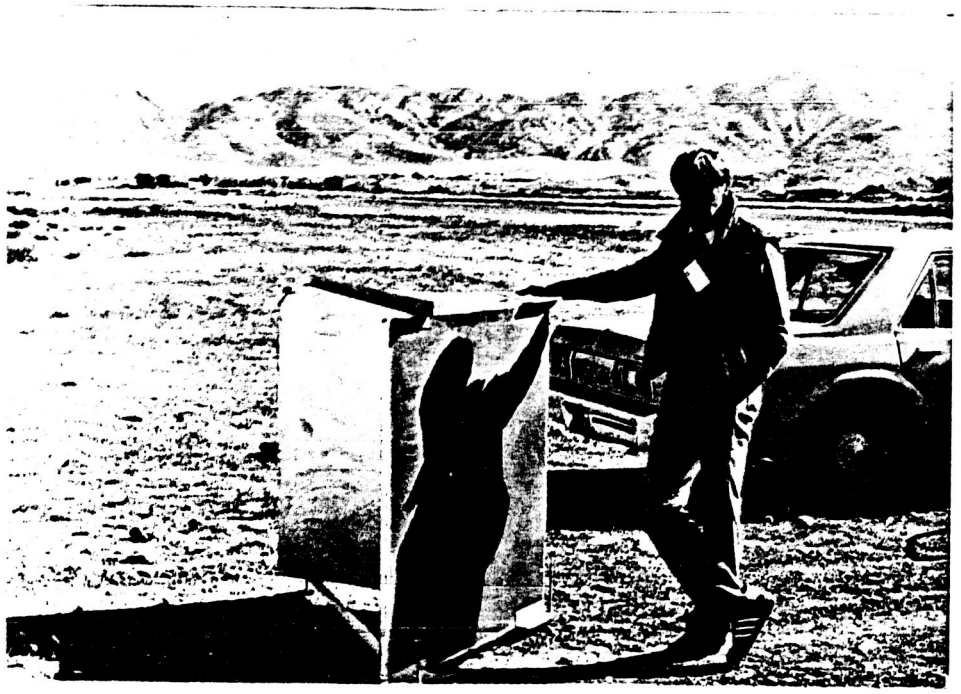

Figure 1.4. Dihedral reflector used as M.I.T. in flight tests.

reflection from the earth. In Progress Report No. 2, it was noted that the dihedrals were some 3 dB below their theoretical maximum, based upon the reflection coefficient of 70% of asphalt runway. It was further noted, and not reported in Progress Report No. 2 that, while one dihedral gave maximum reflectivity at a zero degree angle, the second reflector was several dB off maximum unless tilted somewhat from the vertical. The exact amount of tilt required to maximize the reflectivity was not recorded. The slope of the Stead runway has an average deviation from the horizontal of about 0.25° From Figure 1.2 of Progress Report No. 2 the reflector, when tilted with respect to its fresnel zone by $\pm$0.25°, is down 2 db, and down 6 db when tilted $\pm$0.5°.

It is therefore not unreasonable, based on the fact that one reflector was maximum at 0°, while the other was not, and the fact that the average tilt of the runway is 0.25° to assume that there are short term horizontal perturbations in the runway of 0.25° or greater, which perturbations encompass the fresnel zone in front of the reflectors of 80 to 200 ft. This implies that some of the reflectors, when aligned vertically, were misaligned with respect to their fresnel zone. This could have been checked by use of a transit but time did not permit such tests. This implies that one or more of the reflectors might be down 2-5 db below their possible maximum value due to this phenomena.

In the test program, the reflectors were installed such that the third "plate" was either smooth asphalt , sage brush (Figure 1.5), or dirt (Fig. 1.6). No quantitative data on the actual radar cross-section of these reflectors was obtained but it is not unreasonable to believe that a probable difference of at least 10 dB existed between the

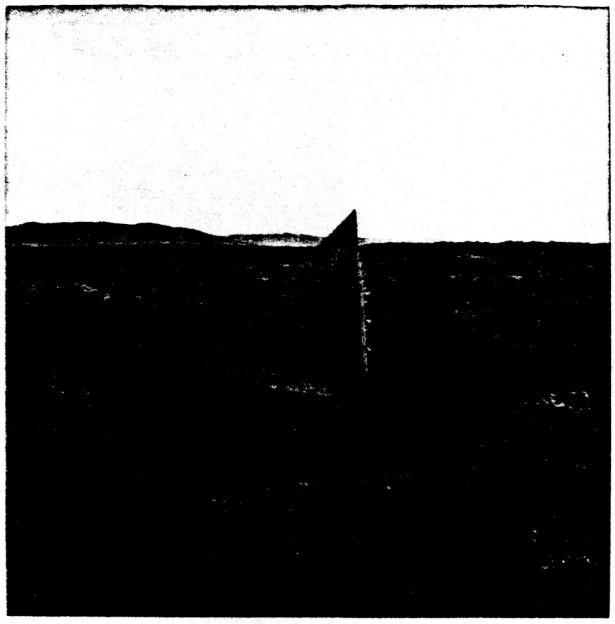

Figure 1.5. Trihedral reflector acting as an M.I.T. installed in sagebrush beside runway at Stead. Fig. 2.5 depicts returns from this installation.

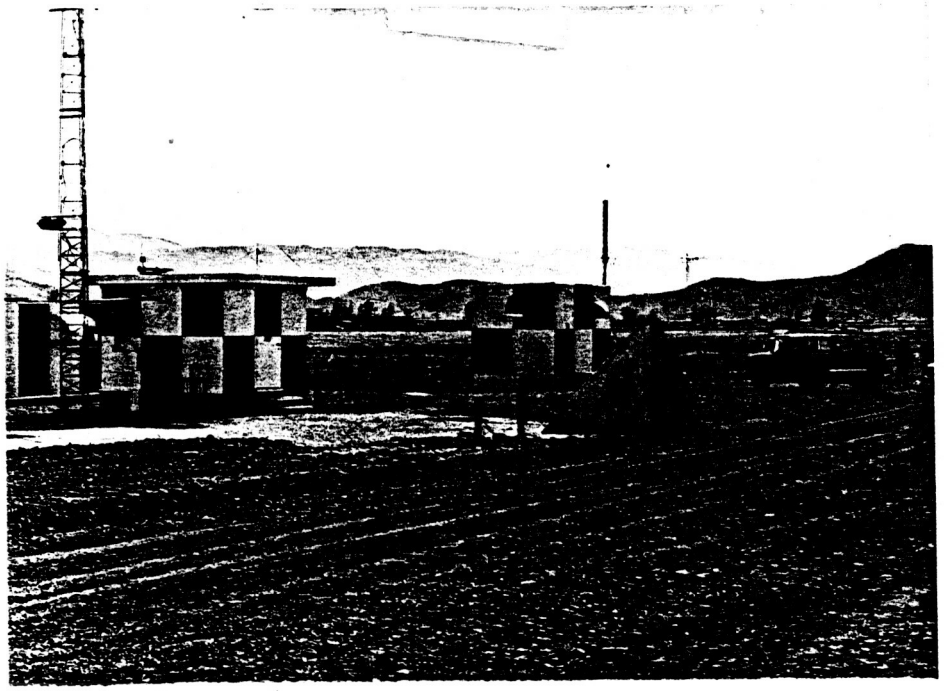

Figure 1.6. Trihedral reflector acting as an M.I.T. installed in dirt beside runway at Reno. This installation generated displays of Figs. 2.8, 2.9 & 2.10.

individual radar cross-sections of the four installed reflectors due to a theoretical radar cross-section variation of at least five dB between the two type of reflectors, the different surfaces that formed the third plate, and the angular orientation; that is, deviation from the horizontal of the fresnel zone in front of the reflectors.

This probable deviation in radar cross-section, coupled with R^4 range correction good only out to five miles, and the limited dynamic range of the receiver, mandated manual gain control and wide tolerance on the pulse width discriminator as discussed above.

SECTION II. FLIGHT TESTING

The first flight was conducted at Stead Airport on the morning of October 22, 1980 in Reno, Nevada using the closed runway of Figure 2.1. The aircrat flew from Moffett to Stead, made several passes and then returned to Moffett. The reflectors were installed on the surface of the runway where noted. Flying was conducted in the presence of cross traffic on the active runway. Because of this limitation, the flights did not descend below 1500 ft.

Four passes were made on this first flight from a range of about 20 miles, with an initial altitude of 6000 ft. descending to 1500 ft. above the 5000 ft. elevation of the runway. On these passes the display was changed from video, to pulse width, to pulse pair. In addition, manual gain and antenna tilt angle were also changed.

These display changes were made as part of an effort to obtain the proper combination of manual gain and tilt angle that would provide a continuous display of the reflectors from 20 miles on in. On the first

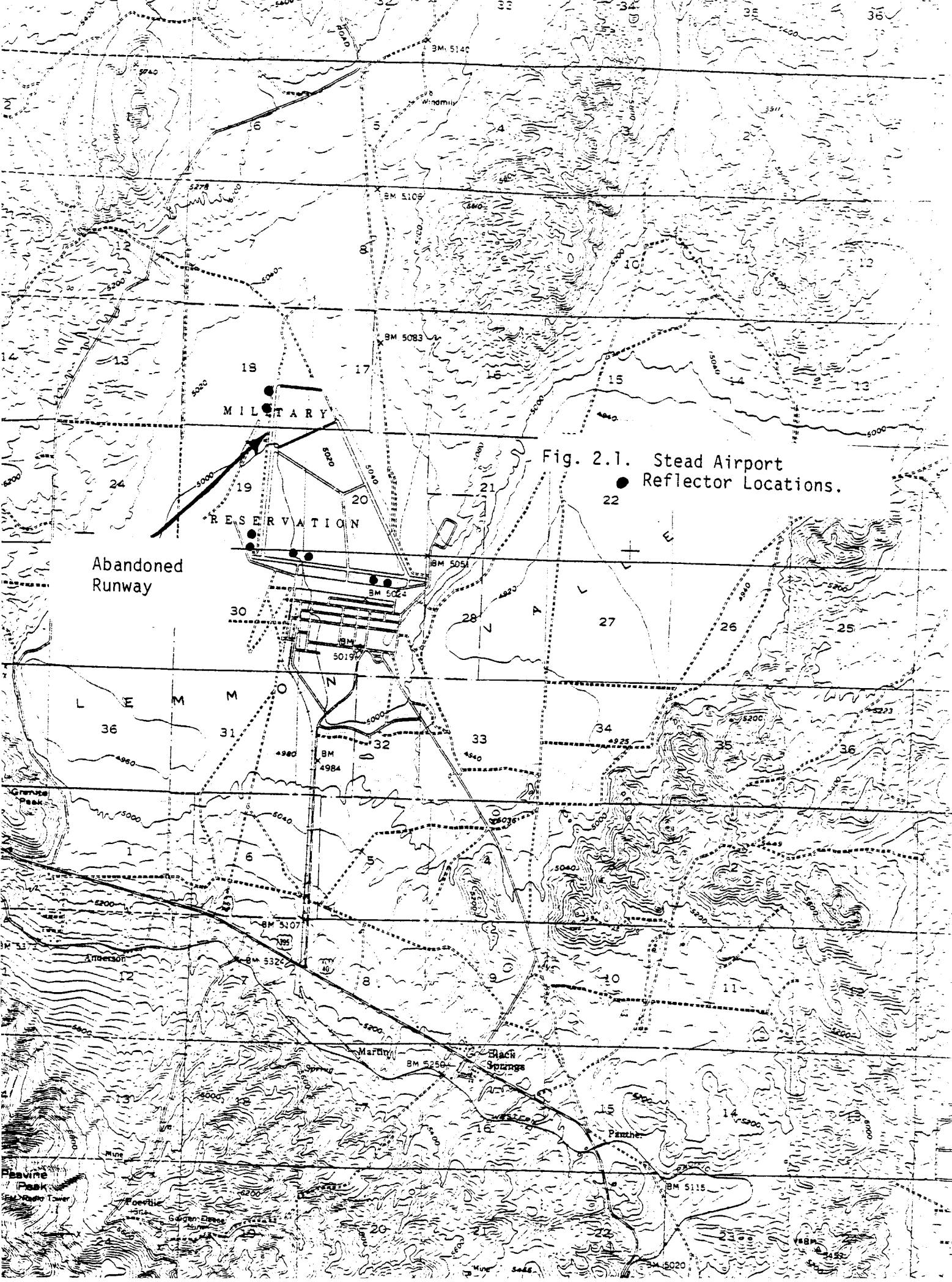

Fig. 2.1. Stead Airport
● Reflector Locations.

several passes, results were sporadic. On the last two passes, results were better but were still not satisfactory.

Fig. 2.2. is a photograph of the display taken on the second pass on October 22. It is interesting in that it is a display of the pulse width discriminator output, showing that all four reflector returns have been validated by the pulse width discriminator. In addition, another target, probably a small building has also passed the pulse width criteria.

It is significant to note that the only area with "natural" targets that generated signals that passed both the pulse width and pulse pair validation criteria was Moffett Field. On take-off at Moffett P^3D^2 targets would sometimes be observed. It is believed that these "natural" targets were the 1000 ft. runway markers. The decoder was set for a 1000 ft. corner reflector spacing. In effect the only targets that were displayed on final on all approaches when the P^3D^2 output was used were those from installed reflectors.

On returning to Moffett Field, the antenna stabilization was checked and found to be inoperative. This meant that as the aircraft changed attitude on final, as for example on leveling to 1500 ft. due to cross traffic, instead of maintaining the constant 3° glideslope, the antenna would be aimed in a different vertical direction, i.e., not at the reflectors. In addition, it was difficult for the pilot to fly a constant glideslope at any time since there was no vertical guidance system, such as ILS, to follow.

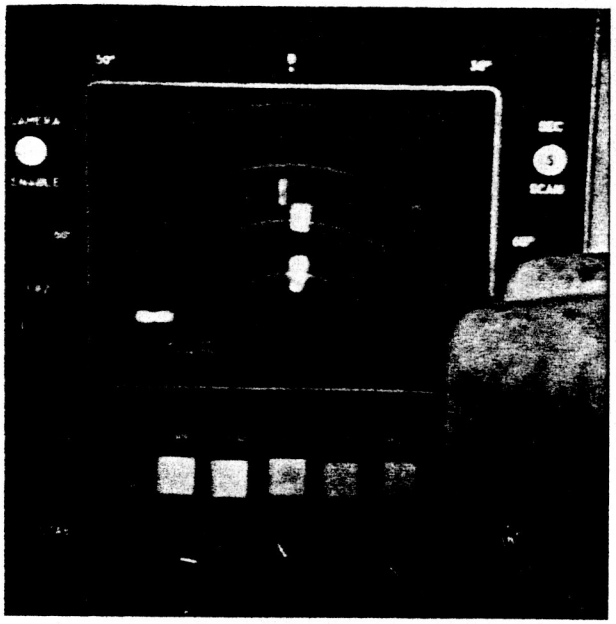

Figure 2.2. Display of pulse width discriminator output on second pass of October 22. All four installed reflectors are validated plus another target.

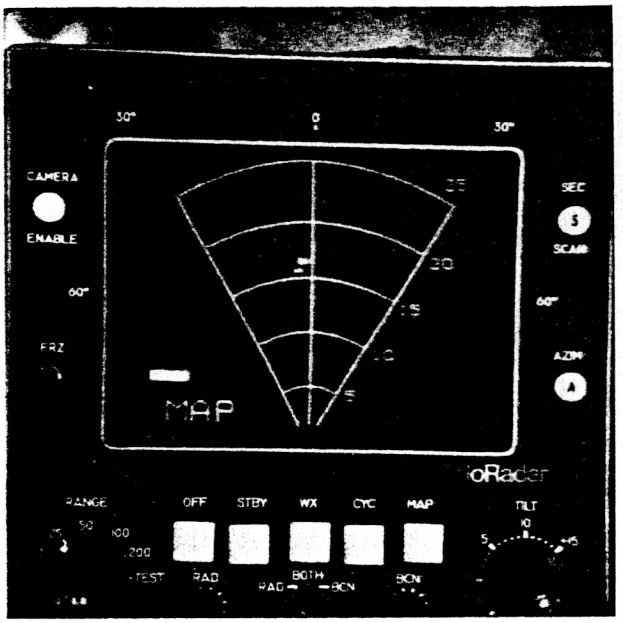

Figure 2.3. Display of P^3D^2 output apparently indicating aircraft far to the right of the extended centerline of the runway. Reflectors on asphalt of closed runway of Fig. 2.1 (10/23/80).

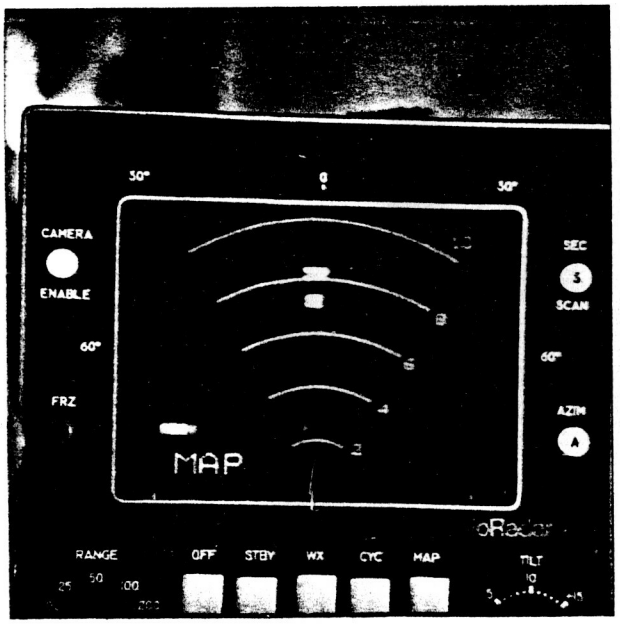

Figure 2.4. Display of P^3D^2 output indicating aircraft aligned with runway. Reflectors on asphalt of closed runway of Fig. 2.1 (10/23/80).

Figure 2.5. Display of one set of two reflectors using the sagebrush of Fig. 1.7 as the third surface of the M.I.T. trihedral. Reflectors installed in sagebrush beside active runway at Stead (10/23/80).

It was determined that the tilt stabilization in the Primus 50 R/T unit was probably set up for use with a different gyro, specifically the one used in the helicopter that the radar had previously flown in. Adjustments were made for the gyro installed in the Lear and tilt stabilization appeared to work much better, at least on the ground. It was then decided to fly again the next day. In addition, it was decided to remove the 16 dB (8 dB one way) attenuator that hade been installed in the antenna waveguide. This had been installed to prevent receiver overloading at shorter ranges by large targets during the ground based tests. This attenuator installation was suitable for short ranges; that is, out to five miles, and the specific P^3D^2 unit used for land based tests. These land tests used an 18" antenna, however, and the Lear has a 12" antenna which results in an additional 6 dB of attenuation (or 6 dB less system performance) for flight tests.

On the second day, two flights were made. The first flight was on the same runway as the day before. It was satisfactory. Fig. 2.3 is a display of the P^3D^2 output at a range of about 16 miles. It can be deduced from this picture that the aircraft is far to the right of the runway, i.e., the two reflectors are not aligned. Fig. 2.4 is a similar display showing the aircraft more aligned with the runway at a range of about seven miles.

Following these tests it was then decided to move the reflectors to the dirt beside the active runway at Stead in order to fly a glideslope to a lower altitude and also to see if the earth instead of asphalt would serve as a suitable third plate of the reflector. Two surfaces were used; one is depicted in Fig. 1.5. The other was a

relatively smooth dirt area. In the half hour intervening between reflector installation and start of flying, the reflectors on the smooth dirt were removed by some glider pilots so they could park their gliders. The only reflectors left installed for the second flight on October 23 were those of Fig. 1.5. They were satisfactorily detected as can be seen from Fig. 2.5 but no data on their actual radar cross-section was obtained, i.e., no quantitative data on just how well the sagebrush/desert soil of Fig. 1.5 acts as a radar reflector was obtained, in contrast to that for asphalt, which apparently has a coefficient of reflectivity of 70% at 5°, as can be noted from Fig. 2.1 and 2.2 of Report No. 2.

It was then decided to install reflectors in the dirt beside the ILS runway at Reno the next day, October 24, so tests could be conducted in a clutter environment more representative of a municipal airport.

On the first flight at Reno, on Friday, October 24, 1980, reflectors were installed 500 ft. in front and 500 ft. behind the ILS glideslope facility of Fig. 2.6 and a flight made. It was not satisfactory in that the reflector returns at ranges greater than 2 miles were very sporadic.

It was postulated that the sporadic performance was probably due to placing the two reflectors 500 ft. in front of, and back of, the ILS glideslope buildings since those buildings, Fig. 2.6, have sides perpendicular to the approach path and so provide a large radar cross-section over the region of the approach path beyond that range at which their angular coverage encompasses the approach path, as can be noted from Fig. 2.7. The echo from the ILS buildings would fall midway between the returns from the two installed reflectors.

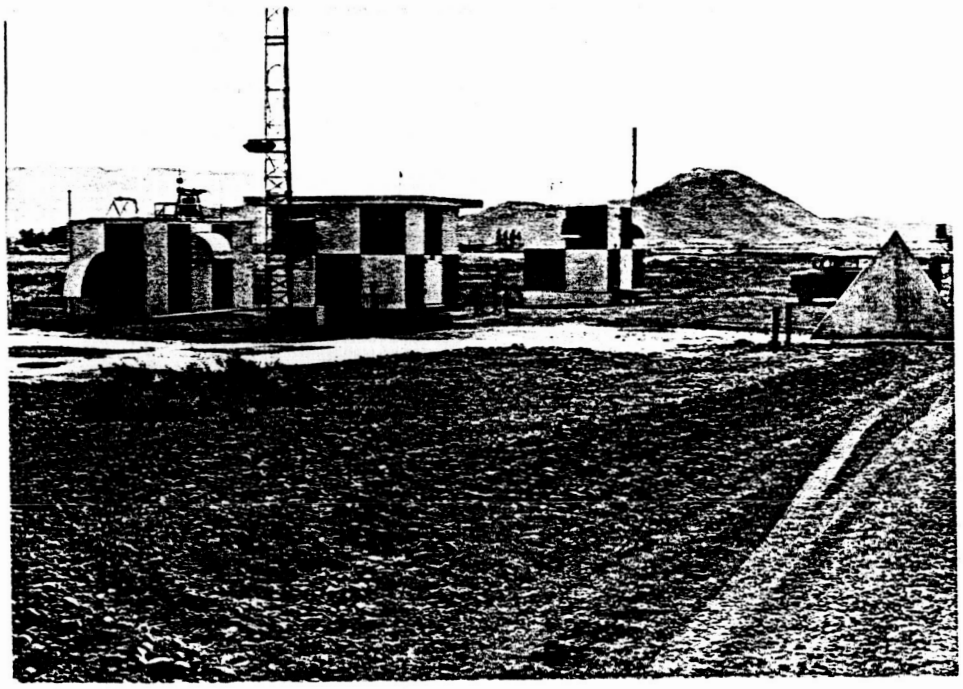

Figure 2.6 ILS glideslope facility buildings at Cannon International Airport, Reno, NV, showing reflector installation used on 10/28/80 flight.

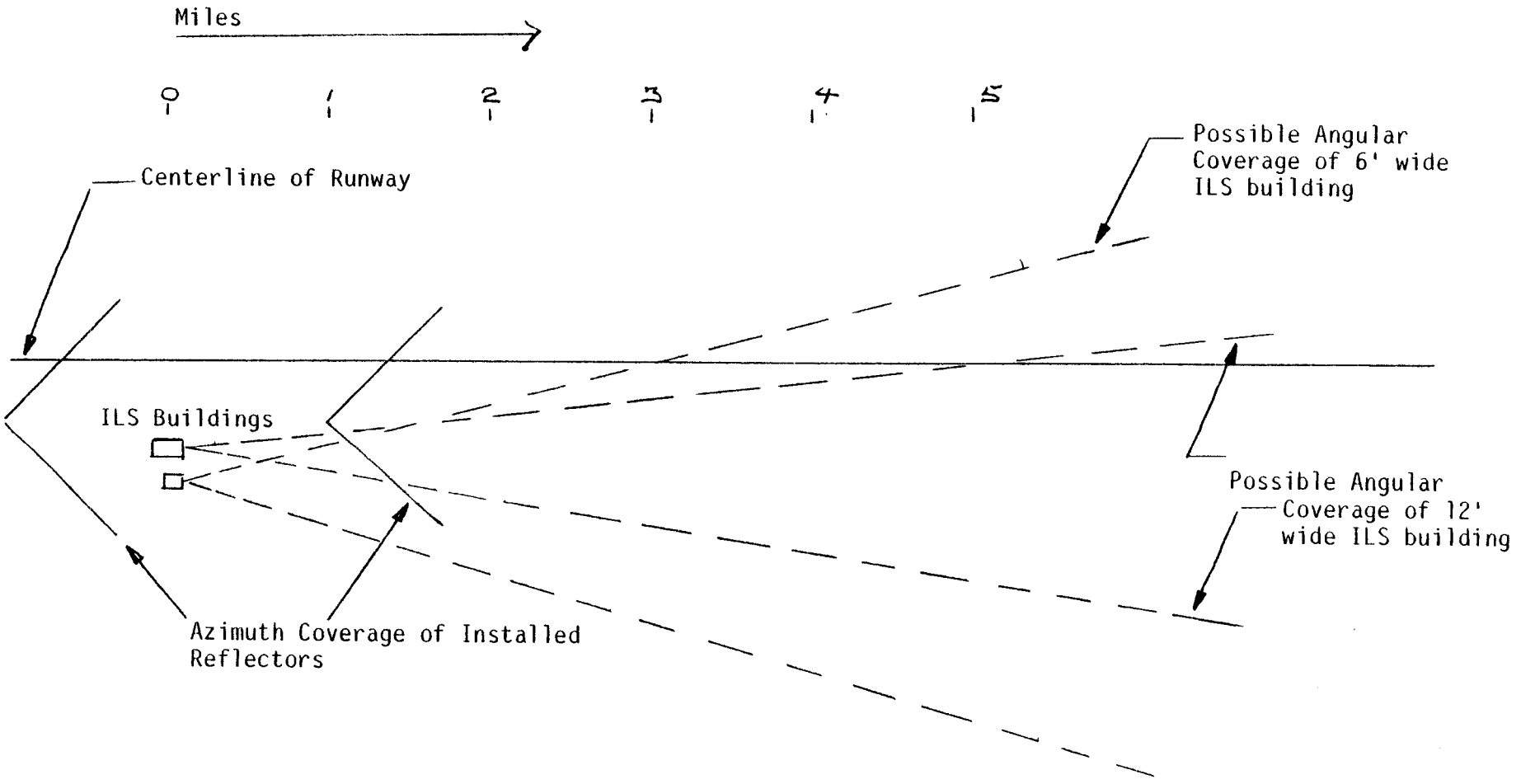

Figure 2.7 Possible Angular Regions over which ILS Buildings can Provide Large RCS.

The ILS building echo could either invalidate the return from the installed reflectors by stretching the return from the first pulse since the pulse width discriminator was set for 600 ft for these tests (1.2 μsec)or invalidate the pulse pair decoder by triggering it falsely.

It was therefore decided to install one of the reflectors at the glideslope building as in Fig. 2.6 and the other reflector 1,000 ft. in front of it so that there would not be a third pulse. In addition, a second set of reflectors was installed towards the other end of the runway. One of the pair of reflectors at the far end of the runway was positioned by the ASR radar building to also minimize the reflections from that building from causing problems.

Another flight was conducted on October 28, 1980 at Reno. Three approaches were made. On the second pass, it was decided, based on satisfactory performance on that pass, to leave the gain setting and antenna tilt angle unchanged from that pass and to make a third pass. This was done and essentially continuous coverage was obtained from 5 miles to 1 mile on both sets of reflectors as discussed in the Abstract. Fig. 2.8,the frontispiece, Fig. 2.9 and 2.10 depict the P^3D^2 display at ranges of 12 mi., 6 mi., 3.5 mi. and 1 mi. on final, the second pass into Reno on October 28. The reflectors had been installed beside the runway an hour previously.

Fig. 2.11 and 2.12 are included for reference. Fig. 2.11 is a display of video output taken on approach into Stead. Fig. 2.12 is a display of pulse width discrminator output taken in the vicinity of Reno.

Figure 2.8. P^3D^2 display on final into Cannon International Airport, Reno, NV, October 28, 1980, second pass.

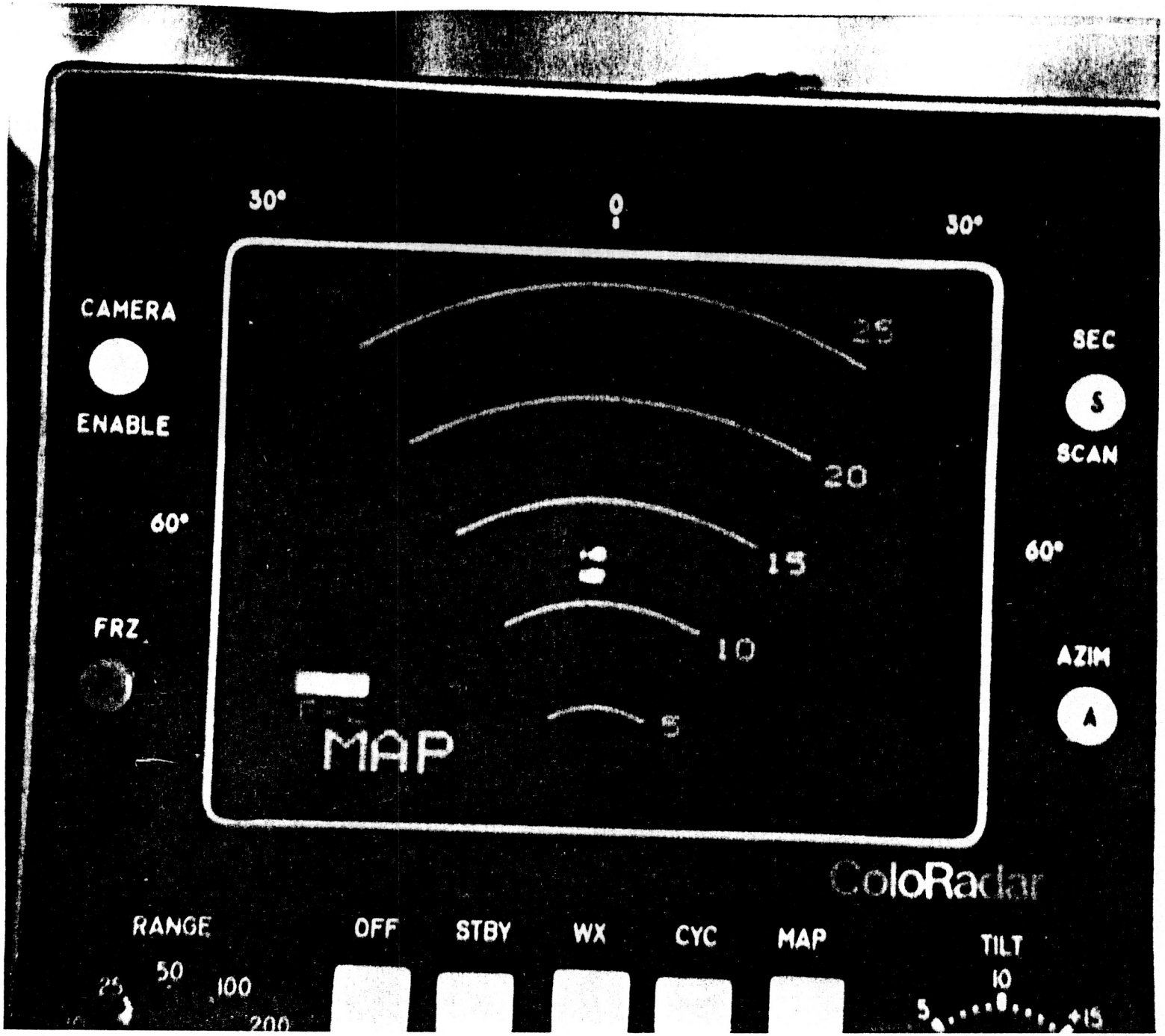

Figure 2.9. P^3D^2 display on final into Cannon International Airport, Reno, NV, October 28, 1980, second pass.

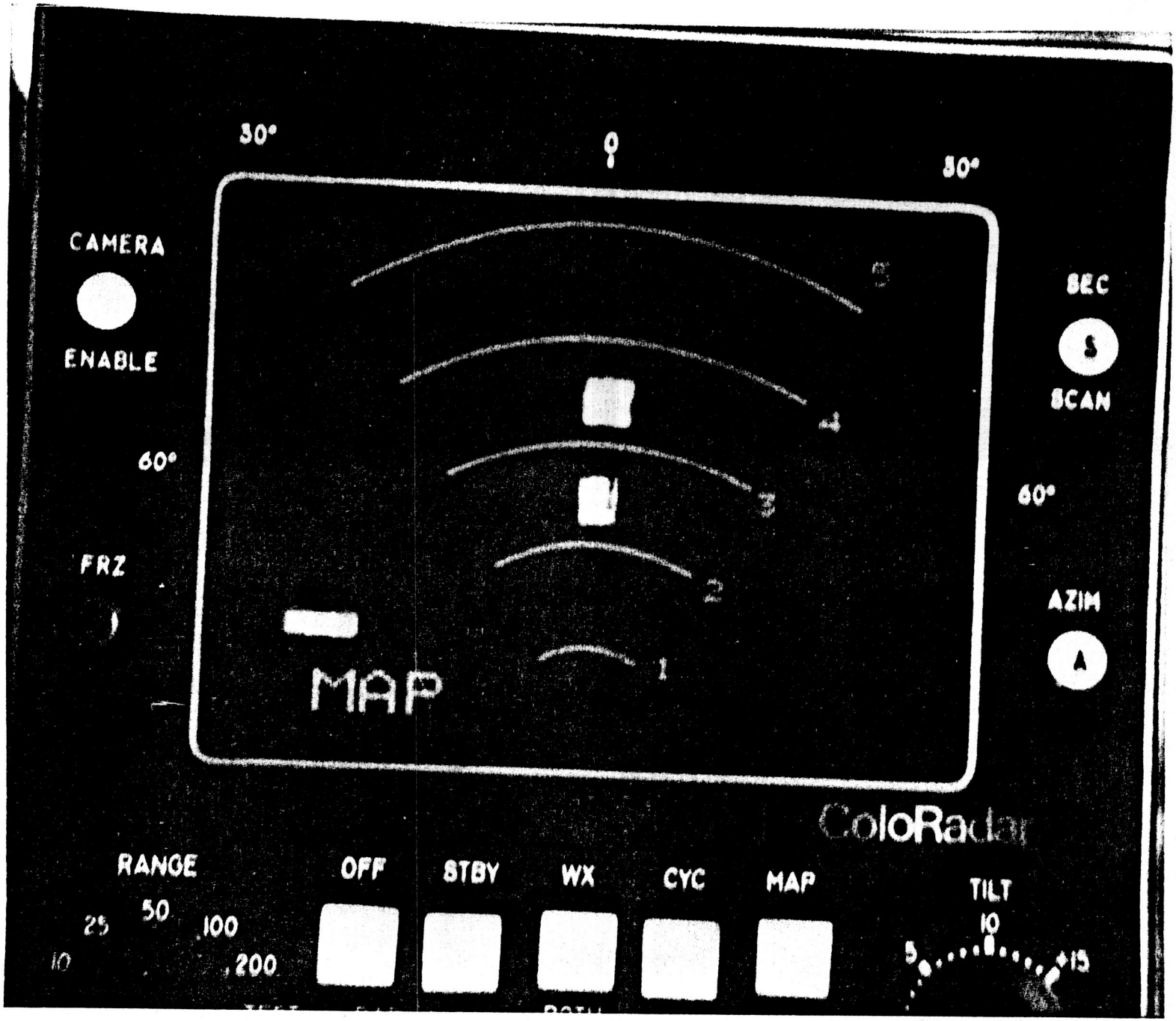

Figure 2.10. P^3D^2 display on final into Cannon International Airport, Reno, NV, October 28, 1980, second pass.

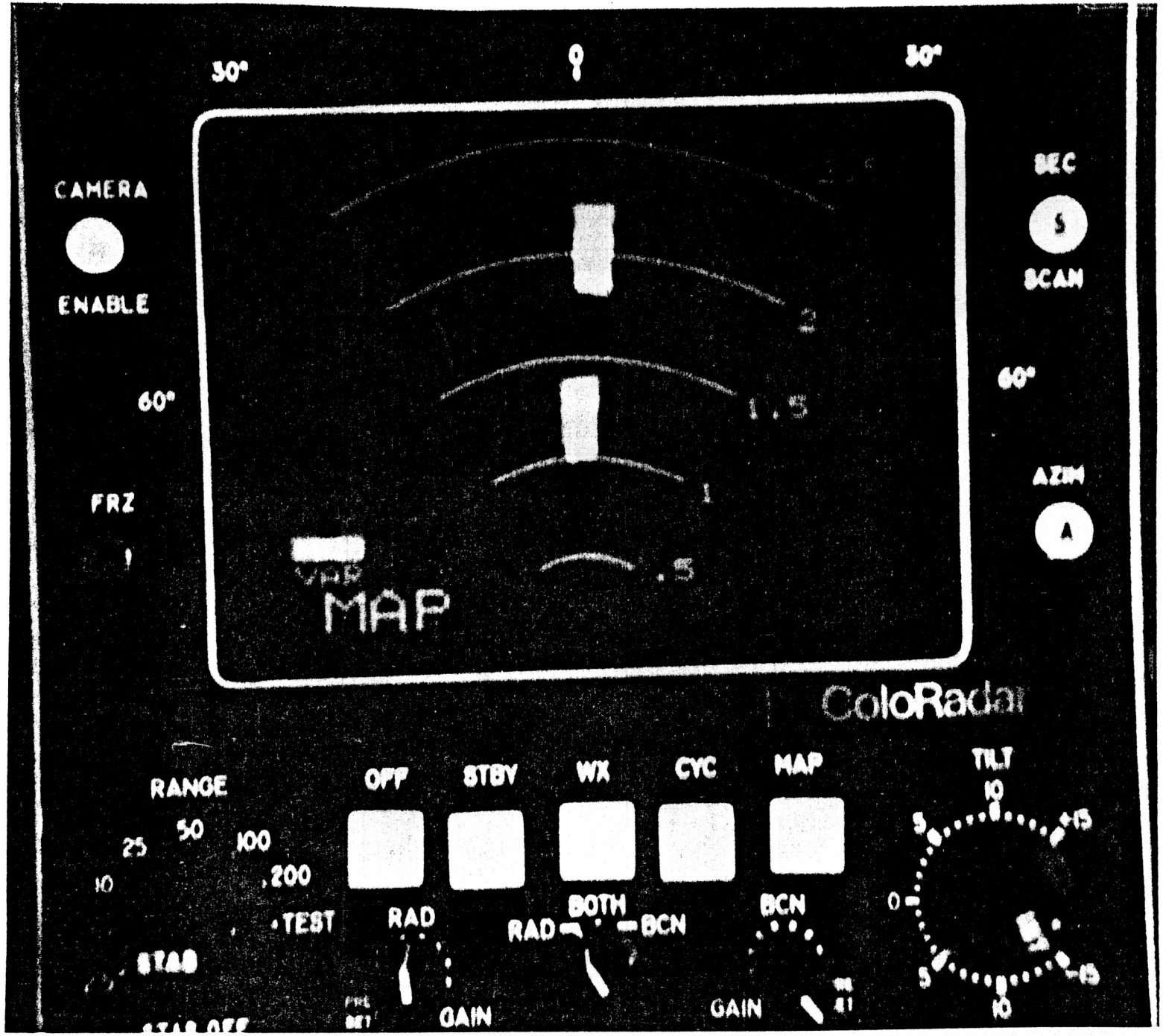

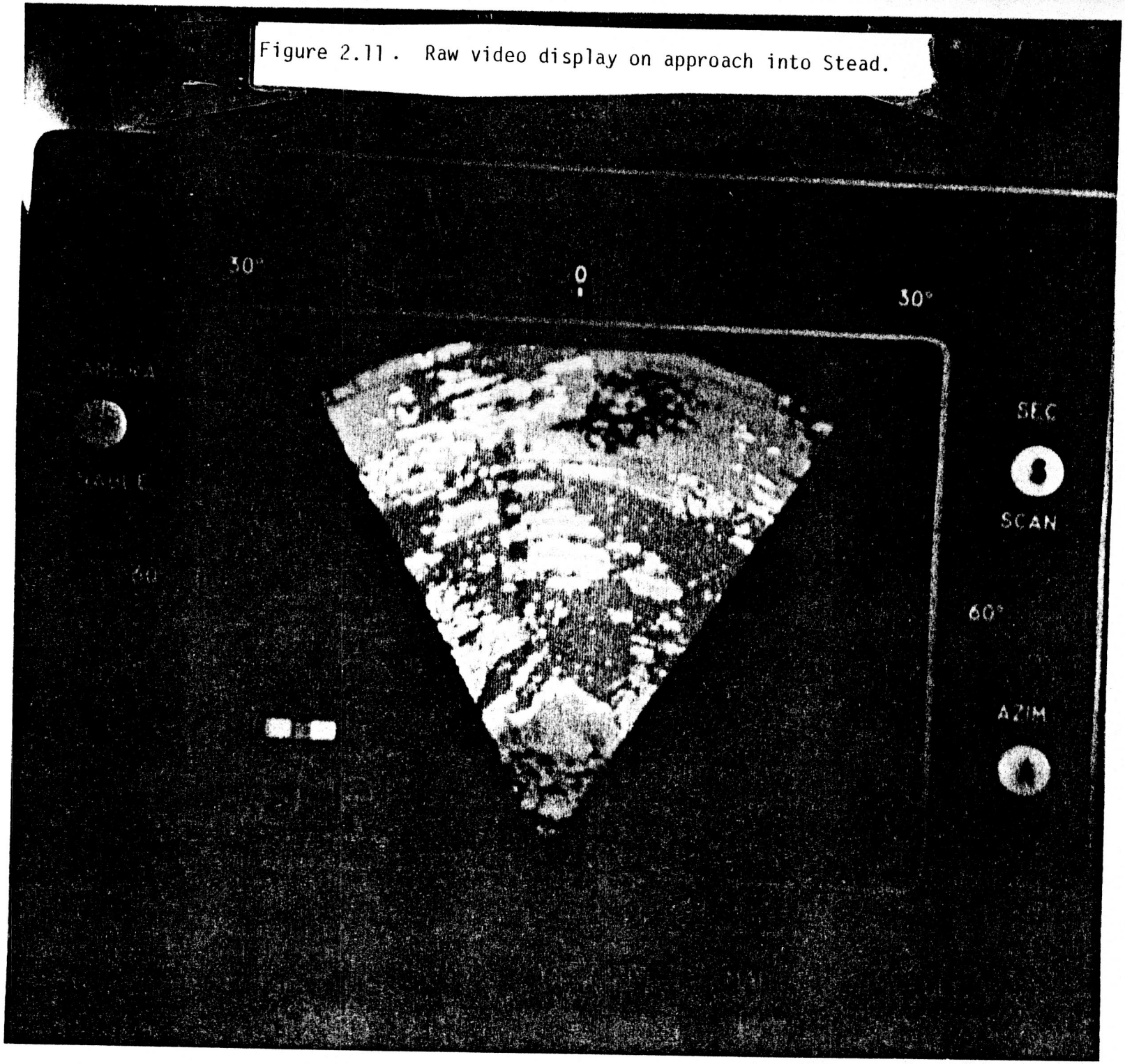

Figure 2.11. Raw video display on approach into Stead.

Figure 2.12. Pulse width discriminator output taken in the vicinity of Reno.

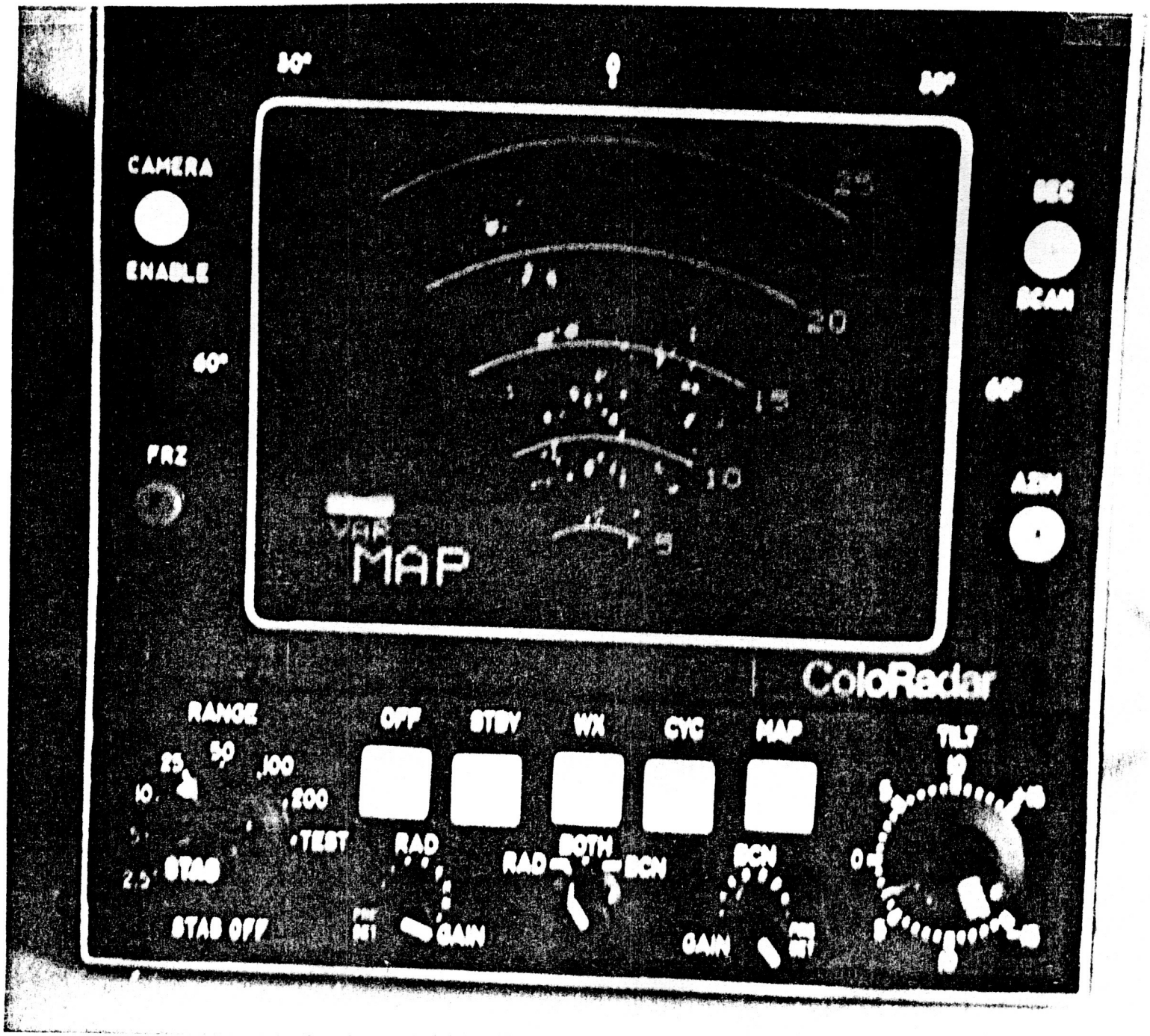

SECTION III. CONCLUSIONS AND RECOMMENDATIONS

(a) Background

The concept of using radar reflectors in conjunction with an airborne radar for navigational purposes is a very old one, essentially dating back to the invention of radar.

The concept of using reflectors to outline a runway is also quite old. Despite this extended interest, a report on a successful demonstration of the concept does not appear to have been published. To the contrary, very recent reports stress that the idea is probably impractical.

In 1977, the concepts outlined in this report were first discussed among participants. They arose in connection with the FAA windshear program. It was desired, on that program, to obtain precision airborne range and range rate for purposes of measuring airborne winds on final for windshear warning purposes. It was reasoned that the airborne radar, ranging on suitable reflectors beside the runway, could provide such data. In addition, it was further reasoned that the reflectors could provide a calibration signal to routinely and properly calibrate the airborne radar and thus further enhance flight safety by perhaps precluding incidents such as the Southern Airways crash in heavy precipitation.

Tests were run in 1977 on the reflector concept at Cannon International airport, Reno, NV. These tests were very instructive in that they delineated the multipath phenomena; that is, the process whereby the reflected path signal cancelled the direct signal, thus making the reflectors invisible. This test demonstrated a sufficient reason for the failure of previous efforts to detect such reflectors. In addition,

once the reason for previous failures was understood, solutions to the problem evolved and the realistic possibility of obtaining precision range, range rate, approach and landing guidance and radar calibration via the use of the weather radar and a reflector system materialized.

A program on this subject was proposed to the FAA on the windshear program. Other solutions appeared more promising to solve the windshear problem and hence the program was not supported within the FAA on that task. Certain FAA personnel, however, believed that the concept had merit for helicopter use and made NASA aware of their beliefs with the result that the cooperative program described in these reports was initiated by NASA Ames.

(b) Conclusions

The land based and flight tests undertaken to date appear to indicate that a standard weather radar, with added simple circuitry, can detect a ground based radar reflector system installed at a municipal type airport and, of course, at more clutter-free areas such as an isolated helipad.

It appears that such detection can offer non-precision approach guidance and possibly precision approach guidance.

In order for such detection to succeed, it appears that perhaps all of the following conditions must be met.

(1) The radar cross-section (RCS) of the reflectors must be of the order of the clutter environment representative of airports, i.e., 45 to 55 dbsm. Reflectors to provide such an RCS are easy to build, relatively low cost and, to date, have met no objection regards their installation adjacent to an active runway.

(2) The RCS of the reflector must be immune from multipath so that they present a stable target over a well-defined angular region.

At least one technique exists for obtaining wide multipath immune angular coverage in both the vertical and the horizontal. Such coverage is desirable for non-precision approach purposes. This technique is based on using an elongated third horizontal plate in a trihedral configuration. The earth appears to offer promise in terms of providing this elongated third plate..

At least one technique exists for obtaining wide horizontal angular coverage and limited vertical angular coverage for precision approach purposes. This technique is to use dihedral reflectors orientated above and below the glideslope and with sufficiently narrow vertical beams so as to exclude multipath signals reflected from the ground, i.e., to have such reflected signals outside their vertical angular coverage.

(3) The reflectors must be placed in a known spacing so that an airborne decoding circuit can utilize knowledge of such spacing to eliminate other non-coded echoes.

(4) Even when the above three conditions are met, it appears that it is also necessary to utilize an additional signature of the echo from a corner reflector in order to distinguish that echo from clutter echoes. An additional signature that appears effective is the fact that the return from a point target such as a corner reflector is of the same pulse length as the transmitted pulse, whereas returns from distributed clutter, and extended buildings, etc. generate echoes longer than the transmitted pulse. An easily implemented pulse width discriminator

circuit appears to eliminate the majority of such clutter targets, allowing the pulse pair decoder to effectively eliminate the remaining clutter targets, leaving only the coded corner reflector returns for display.

Recommendations

It is recommended that hooded and instrumented non-precision and precision WRAPS approaches be made and evaluated using an unmodified and modified radar.

The term instrumented here refers to the use of an independent positioning system that determines how well such approaches are flown. The term unmodified radar here refers to the use of a standard weather radar system of the Primus 500 type or equivalent. No internal circuitry changes are made to such a radar but external circuitry can be added.

The term modified radar here refers to the use of a radar of the above type in which internal circuitry changes have been made, such as changing the pulse length, etc. The details of the recommended program are contained in the proposed Phase II effort.